We thank the reviewers for careful consideration of our article. We have attached a revised version of the manuscript and supplementary document to address the comments made by the reviewer. The reviewer comments are in black text, the authors' responses are in red text and the revised text is in "double quotation marks" (with Line number(s) in updated manuscript).

Response to Reviewer Comment #1 (RC#1):

Specific comments:

• To estimate organic water, it is assumed that "10% of the aerosol water was present in the organic phase, within the range of organic water reported by Pye et al. (2017)." However, Fig 12 of the cited paper shows the fraction of organic water to vary significantly, and even exceed 60% in some areas. With this in mind," within the range" appears to be a massive simplification of expected conditions. How was this 10% number chosen? What could be the expected consequences of a more explicit organic water mechanism (or even simply a greater amount of organic water in the SE)? Another sensitivity case study may be appropriate here.

CMAQ model version 5.2.1 used in this study has a limitation in regards to lack of an explicit representation of aerosol water uptake by organic constituents. In CMAQ v5.2.1, total aerosol water in the model is just the water associated with inorganics calculated with ISORROPIAv2.2 (Fountoukis and Nenes, 2007) without accounting for hygroscopocity of organic constituents at all. We do highlight in Section 4 (Discussions and atmospheric implication- Lines 806-809):
"Organic water uptake, even if higher than the amount assumed here, will still follow the diurnal trend of RH since it is diverted from the aqueous core that is derived from ISORRORPIA-based aerosol water in CMAQ v5.2.1."

Guo et al. (2015) found strong diurnal trends in the fraction of organic water content with the percentage increasing to as much as 50% at night, and reducing much lower during the day (~ 10%). As isoprene chemistry primarily occurs during the day, we selected 10% organic associated water as a model simplification to better predict IEPOX chemistry during the day. Nighttime have higher organic water than the assumed 10% fraction of total aerosol water but it has negligible impact on IEPOX chemistry, which is the primary focus in this work. Furthermore, due to the strong effect of organic water on the viscosity of the organic rich shell in particles with a core-shell morphology, a lower value was selected because instances where diffusion limitations occur are likely to have lower water fractions.

The following text was added in section 2.2 (Lines 217-222) to clarify our assumption:

"Approximately 10% of total aerosol water is associated with the organic phase during daytime when IEPOX chemistry is more prevalent as indicated by the observations collected during the SOAS 2013 campaign (Guo et al., 2015). To best replicate daytime IEPOX chemistry, the 10% value

was chosen under the assumption that the underprediction of nighttime organic water would negligibly impact overall IEPOX-derived SOA. Naturally, this is not applicable for rest of multiphase chemistry and should be addressed accordingly in future work."

Guo, H., Xu, L., Bougiatioti, A., Cerully, K. M., Capps, S. L., Hite, J. R., Carlton, A. G., Lee, S.-H., Bergin, M. H., Ng, N. L., Nenes, A. and Weber, R. J.: Fine-particle water and pH in the southeastern United States, Atmospheric Chemistry and Physics, 15(9), 5211–5228, doi:10.5194/acp-15-5211-2015, 2015.

The most recent release of CMAQ version 5.3 has the explicit organic water mechanism based on κ-Köhler theory as described by Pye et al. (2017) accounting for the hygroscopocity (κ_{org}) of each organic constituent in the total aerosol budget. The proposed 'PhaseSep' algorithms in this study need to be implemented in the updated version of CMAQ (v5.3) to quantify the expected impact of a more dynamic representation of organic water uptake on phase state. This implementation is ongoing and a subject of a future study (subsequent paper), but is beyond the scope of this paper.

• As the authors note in their conclusions, organic hydrophobicity is not considered in this work, including impacts of aging. This seems to me to be a very significant (though understandable) omission, and worthy of more discussion than currently provided.

The following text was added and modified in the conclusions (section 4; Lines 809-819) to address the comment above and add caveats to be addressed in further model development:

"In this work, the O:C ratio of individual organic constituents as listed in Table 1 was used to calculate $T_{g,org}$ based on Shiraiwa et al. (2017). The O:C provides an indication of hygroscopocity of different organic species (Pye et al., 2017), but it is only a surrogate. Lack of explicitly representing hydrophobicity or hygroscopic growth of various organic constituents is a limitation in the CMAQ modeling framework that was used. More recently, degree of diffusivity or uptake of semivolatile organic compounds (SVOCs) such as isoprene oxidation products and ONs in to more viscous or semi-solid particle-phase are found to differ. These changes in η_{org} profoundly impacts both aerosol growth kinetics and their size distribution dynamics (Vander Wall et al., 2020; Zaveri et al., 2020). To assess the actual impacts of aging and hygroscopic growth under varying conditions updates in the CMAQ model are required by adding explicit reactive uptake mechanisms for a wider range of non-IEPOX SOAs."

Following references were added accordingly:

Vander Wall, A. C., Perraud, V., Wingen, L. M., and Finlayson-Pitts, B. J.: Evidence for a kinetically controlled burying mechanism for growth of high viscosity secondary organic aerosol, Environmental Science: Processes & Impacts, 22, 66-83, 10.1039/C9EM00379G, 2020.

Zaveri, R. A., Shilling, J. E., Zelenyuk, A., Zawadowicz, M. A., Suski, K., China, S., Bell, D. M., Veghte, D., and Laskin, A.: Particle-Phase Diffusion Modulates Partitioning of Semivolatile Organic

Compounds to Aged Secondary Organic Aerosol, Environmental Science & Technology, 10.1021/acs.est.9b05514, 2020.

• Page 19: Which species specifically contribute to the modeled change in O:C with elevation?

We added a detailed explanation to address the above comment in Section 3 (Lines 444-454):

"Species with high O:C (> 1.6) parametrized in CMAQ as anthropogenic OA collectively can be used as a surrogate for Highly Oxygenated Organic Aerosol (OOA); specifically low-volatility-LVOOA and semi-volatile-SVOOA oxygenated OA. Table 1 shows the species which are attributed to this specific modeled change in O:C with elevation. The mean mass fraction of anthropogenic OA increased from ~ 40% at surface to ~ 65% at the upper troposphere and eventually ~ 80% at layer 35. Whereas, biogenic OA comprising of isoprene-derived OA drops from ~ 30% at surface to 24% at the upper troposphere and eventually ~ 20% at layer 35. This is in agreement with the findings from airborne measurements in the southeastern United States as part of the Southeast Nexus (SENEX) field campaign that show a sharp drop in isoprene-derived OA and drastic increase in OOA with rising altitude (Xu et al., 2016)."

The following reference was also added:

Xu, L., Middlebrook, A. M., Liao, J., de Gouw, J. A., Guo, H., Weber, R. J., Nenes, A., Lopez-Hilfiker, F. D., Lee, B. H., Thornton, J. A., Brock, C. A., Neuman, J. A., Nowak, J. B., Pollack, I. B., Welti, A., Graus, M., Warneke, C., and Ng, N. L.: Enhanced formation of isoprene-derived organic aerosol in sulfur-rich power plant plumes during Southeast Nexus, *Journal of Geophysical Research: Atmospheres*, 121, 11,137-111,153, 10.1002/2016jd025156, 2016.

• Section 2.7: For the specific locations examined, how well did the modeled O:C values match observations?

In the updated manuscript we added the brief description of recently reported field observations of O:C values at Centreville, AL during Southern Oxidant and Aerosol Study (SOAS) 2013. In section 2.7 (Lines 382-386) the following text has been added:

"We also use observed O:C ratios of various HOMs as reported by Massoli et al. (2018) recorded at Centreville forest site, Alabama during the SOAS 2013 study to compare with the simulations. Massoli et al. (2018) used a high-resolution time-of-flight chemical ionization mass spectrometer with nitrate reagent ion (NO_3^- CIMS) for these observations. More details are provided in the Results section."

More detailed discussion on the modeled O:C values vs O:C observations at Centreville, AL for SOAS 2013 has been added as follows in section 3 (Lines 539-556):

"Massoli et al. (2018) reported the observed O:C at Centreville, AL during SOAS 2013 that ranged between ~ 0.5 to 1.4 and averaging at 0.91. Massoli et al. (2018) presents the first instance of ambient measurements with a NO_3^- CIMS in an isoprene-dominated environment and identified Organic nitrates or Organonitrates (ONs) originating from both isoprene and monoterpene to be a significant component of the NO_3^- CIMS spectra and dominating the observed SOA at Centreville throughout the day, reflecting daytime and nighttime formation pathways. Both isoprene- and monoterpene-derived ONs have very high O:C > 1 and accounting for up to 10% of total oxygen at Centreville site (Xu et al., 2015; Lee et al., 2016), explaining the high overall observed average O:C. Our modeled O:C at the Centerville, Alabama site during SOAS 2013 ranged between ~ 0.5 to 1 and averaging ~ 0.68. CMAQv5.2.1 with carbon bond chemistry (used in this study) uses *aero6* aerosol mechanism, without any explicit representation of formation pathways of isoprene and monoterpene-derived ONs. Specifically CMAQ with *aero6* significantly underestimates monoterpene oxidation that accounts for ~ 50% of organic aerosol in the southeastern United States in summer (Zhang et al. 2018). Consideration of explicit monoterpene organic nitrates and updated monoterpene photoxidation yields in aero7 eliminates the CMAQ model-measurement bias (Xu et al. 2018). The lack of explicit organic nitrates here can explain the lack of high O:C (> 1) predictions in this work for the Centreville, Alabama Forest site during SOAS 2013 possibly leading to the low correlation of model estimated $T_{g,org}$:T with observations."

The following relevant references are now added in the updated manuscript:

Xu, L.; Suresh, S.; Guo, H.; Weber, R. J.; Ng, N. L. Aerosol characterization over the southeastern United States using high-resolution aerosol mass spectrometry: spatial and seasonal variation of aerosol composition and sources with a focus on organic nitrates. *Atmos. Chem. Phys.*, *15*, 7307–7336, 2015. (already in manuscript)

Lee, B. H.; Mohr, C.; Lopez-Hilfiker, F. D.; Lutz, A.; Hallquist, M.; Lee, L.; Romer, P.; Cohen, R. C.; Iyer, S.; Kurtén, T.; Hu, W.; Day, D. A.; Campuzano-Jost, P.; Jimenez, J.-L.; Xu, L.; Ng, N. L.; Guo, H.; Weber, R. J.; Wild, R. J.; Brown, S. S.; Koss, A.; de Gouw, J.; Olson, K.; Goldstein, A. H.; Seco, R.; Kim, S.; McAvey, K.; Shepson, P. B.; Starn, T.; Baumann, K.; Edgerton, E. S.; Liu, J.; Shilling, J. E.; Miller, D. O.; Brune, W. H.; Schobesberger, S.; D'Ambro, E. L.; Thornton, J. A.: Highly functionalized organic nitrates in the southeast United States: Contribution to secondary organic aerosol and reactive nitrogen budgets. *Proc. Natl. Acad. Sci. U. S. A.*, *113* (6), 1516– 1521, 2016. (Lee et al., 2016b in manuscript)

Zhang, H, et al.: Monoterpenes are the largest source of summertime organic aerosol in the southeastern United States, Proceedings of the National Academy of Sciences*, **115**, 2038-2043, https://doi.org/10.1073/pnas.1717513115, 2018. (Zhang et al., 2018b, already in manuscript)*

Massoli, P., Stark, H., Canagaratna, M. R., Krechmer, J. E., Xu, L., Ng, N. L., Mauldin, R. L., Yan, C., Kimmel, J., Misztal, P. K., Jimenez, J. L., Jayne, J. T., and Worsnop, D. R.: Ambient Measurements of Highly Oxidized Gas-Phase Molecules during the Southern Oxidant and Aerosol Study (SOAS) 2013, ACS Earth and Space Chemistry, 2, 653-672, 10.1021/acsearthspacechem.8b00028, 2018.

• Page 27: The authors argue that the worsened NMB of hourly PM2.5 organic car-bon mass vs. observations is likely explained by poorly constrained Henry's law coefficients (and perhaps other parameters). This may be true, but I do not find Figure S6 to be compelling evidence for the argument. Visual and statistical ex-amination of the differences found when using a modified Henry's law coefficient seems to indicate that its importance is actually very low in terms of impacts on overall OC mass. How can such modest "improvements" be considered evidence supporting this explanation for worsened model performance?

We rephrased and added (at end of section 3.3 on sensitivities, Lines 727-739) to explain and resolve the above comment:

"While modest improvement in model performance of $PM_{2.5}$ OC by aforementioned sensitivity simulations (*HighHorg* and *PhaseSep2*- see section 3.2.2.1) occurs, it does not addresses other major issues in the base CMAQ model performance. Firstly, these updates to phase state and phase separation considerations only translate to IEPOX SOA, the only explicit parametrization of multiphase reactive uptake in CMAQ. IEPOX SOA also just makes up approximately 12% of the total $PM_{2.5}$ OC mass simulated by CMAQ on an average for SOAS 2013 period. There are other more important factors introducing major source of uncertainty in models across spatial scales including CMAQ. A very prominent uncertainty being missing representation of species like ONs reported as dominant in SOAS 2013 by new instrumentation providing higher molecular detail (Lee et al., 2016b; Massoli et al., 2018). Furthermore, field or laboratory studies on a wider suit of SOA are needed to explicitly parametrize their multiphase chemistry and are still missing in CMAQ. It is a challenge to implement these mechanistic representations of different SOA holistically, without increased computational cost in CMAQ."

• The authors note that previous work in which phase-separation was included in a box model showed a drastic improvement in NMB (-66.2% to -36.3%). Why would this work not show such improvements? Are there any major differences in the handling of Henry's law coefficients or other parameters that could explain the differences in the performance of the CTM implementation?

Schmeddding et al. (2019), *Atmospheric Environment* uses a 0-D box model that calculated NMB using data from filter samples taken at the Look Rock site in a pristine environment in rural Tennessee (Budisulistiorini et al, 2015). These filter samples only focused on speciated IEPOX-SOA data i.e. reported % NMB was only on IEPOX-SOA. In CTM implementation during this work, % NMB was calculated for the rural Centreville, Alabama, and urban Jefferson Street, Atlanta, Georgia sites, both of which have SEARCH total $PM_{2.5}$ organic carbon measurements. Because these sites use total organic carbon measurements rather than IEPOX-specific measurements, larger changes in IEPOX-SOA due to changes in the Henry's Law constant would still register as smaller changes in total organic carbon once all of the other species are taken into account.

Moreover, the drastic improvement in Box-model study can be attributed to the fact that it assumes core-shell morphology/Phase separation all the time (resulting in drastic reduction in % NMB compared to reactive uptake ignoring impact of organic coating). While in CTM implementation in this work, we clearly have a more refined conditional parametrization on when phase separation does or does not occur. Hence, it is not advisable to compare the model performance of the two approaches.

We also mentioned this point about the 0-D box model study in the manuscript text as (Lines 143-146):
"The aforementioned previous model study (Schmedding et al., 2019) highlighted the significant impact of an organic coating layer on IEPOX-derived SOA formation, but lacked any quantification of conditions that result in phase separation creating such organic coating and its phase state."

• Figures throughout the manuscript and supplementary materials are formatted poorly, overall. Text, colors, positioning, labels, and spacing should all be examined carefully. In particular:

–Fig 2: Panel and colorbar labels are missing completely.

Added Panel and colorbar labels in the updated manuscript.

–Fig 3: This figure is presented as a time series, but the text describes it ex-clusively in terms of the diurnal cycle. I see no benefit to including individual dates, and it's very hard to tell day from night as shown. I suggest a change to diurnal averages.

Figure 3 in the updated manuscript now is in form of diurnal cycle instead of individual dates and shows diurnal averages of $T_{g,org}$ and its dependence on organic aerosol constituents-anthropogenic, biogenic and organic water uptake (Also look at the response to second last major comment by Reviewer 2).

–Fig 7 B and C, and Fig 8: Panel labels for maps needed.

Panel labels added now to Figure 7 (A, B and C) and Figure 8 (Also see response to last Minor Comment by Reviewer 2) in the updated manuscript.

–Fig 9: Statistical information insets are very hard to read. A transpose of the table may help.

Figure 9 updated with statistical information in bigger fonts and other enhancements. Refer to comment on Figure S6 for update on more statistics moved to Table S1 in updated supplementary document now.

–Fig 10: Panel labels are missing. In addition, the colorbar chosen for this map is particularly difficult to interpret. A two-tone version in which zero is white or grey would help.

Panel labels are added and a two-tone color bar with zero represented by white is included to Figure 10 in updated manuscript.

–Figure S6: y-axis is missing label and units.

We have removed older Figure S6 and transposed statistics on model performance with sensitivity simulations in it to Table S1 in supplement to address Reviewer #2's comment.

Response to Reviewer 2:

Major Comments

The authors should clarify the very central assumption in their manuscript that all semisolid particles > 100 Pa s phase separate. What is this assumption based on? A reference is given (Shiraiwa et al. 2017), but I do not see this manuscript making a statement about phase separation dependent on viscosity. All phase-separation percentages given in the text and figures are dominated by this assumption, but how realistic is it and what does it add to our understanding of SOA? The uncertainty of the SSPS assumption strongly diminishes the validity of total fractions of phase-separated particles in the atmosphere that are prominently discussed in this manuscript (l. 659 – 666). Please add sufficient caveats and error estimates in the appropriate places.

The SSPS assumption was chosen as a model simplification to better understand the effects of morphology on the formation of IEPOX-SOA. Schmedding et al (2019) showed that particles with a core-shell morphology and an outer shell that had a liquid like viscosity did not exhibit any diffusive limitations when calculating the reactive uptake of IEPOX. Furthermore, there is little information on the criteria necessary for a particle that is specifically in a semi-solid or glassy state to undergo phase separation. Prior work (Song et al., 2018; Zuend and Seinfeld, 2012) has focused on particles that have a liquid-like viscosity and have highlighted the aerosol and ambient properties that dictate transition from a homogenous mixture of organic and inorganic compounds to a liquid-liquid phase separated particle. The threshold of viscosity > 100 Pa.s, only indicates the transition in phase state of the 'organic coating' from liquid (< 100 Pa.s) to semi-solid or solid (> 100 Pa.s) and should not be confused with dictating phase separation itself.

We edited text in section 2.1 (Lines 178-185) to addresses this comment on the SSPS assumption:

"This simplification is based on recent observations showing higher than anticipated rebound fractions in phase-separated OA that has been attributed to organic aerosol constituents with viscosities > $10^2\ Pa.s$ (Reid et al., 2018). These aerosols were phase-separated with an amorphous solid coating, which, unlike liquid particles, can only dissipate energy by rebounding.

(Bateman et al., 2015a, 2015b, 2017; Reid et al., 2018; Virtanen et al., 2010). A higher bounce factor implies that a particle is more viscous and therefore more likely to exhibit diffusive limitations in reactive uptake."

Whether, this particle viscosity is due to a viscous solid organic coating or a viscous homogenous morphology is a matter of further experimental investigation and the focus of future work. (See response to 'minor comment on 169' as well)

Therefore the 100 Pa.s cut off was chosen as an extreme upper bound scenario for particle morphology to better understand the effects of a core-shell morphology on the heterogeneous chemistry of IEPOX.

To clarify, phase separation and viscosity are expected to follow similar underlying system properties. For example, O:C ratio that drive phase separation (e.g. low O:C ratio organics tend to phase separate from water-rich phases) likely also dictate viscosity. Since low O:C species in ambient aerosols will necessarily have higher molecular weights to have vapor pressures consistent with their presence in the particle phase, given all other factors being equal. In this work, this empirical relationship between viscosity, phase separation, and system properties (O:C, OM to inorganic SO_4^{2-}, RH) has been leveraged to predict viscosity and phase separation simultaneously.

The following text was added in section 2.1 (Lines 185-189) to underline the reasoning of the assumption in question:

"The specific conditions under which a particle will form a glassy rather than liquid-like organic shell are unclear, but thought to be driven by the same underlying physical properties that drive viscosity. This led to the assumption that particles that exhibit a semi-solid or glassy organic shell would inherently adopt a core-shell morphology. This assumption can be thought of as an upper bound on the frequency of particles separating into core-shell morphologies."

And in the discussion emphasis was also added that there is limited information on the internal conditions of a particle that would lead it to adopt a core-shell morphology when in a semi-solid or glassy state (Lines 777-783):

"The conditions under which highly viscous SOA will separate from inorganics in a particle or if the particle will remain homogenously mixed should be further explored as well, given the differences in the frequency of predicted particle-phase separation between the *PhaseSep* and *PhaseSep2* simulations and the implications that this has for the reactive uptake of IEPOX (Table S1). Constraining the viscosity of SOA in low RH (< 30%) conditions is also an area that should be further explored to improve model performance."

The authors show many figures analyzing their model data. However, the manuscript text is widely used to list these numbers, without much interpretation or discussion. Discussion is often

superficial and obvious as indicated in the minor comments below. I would suggest condensing the message of this manuscript to fewer, central figures and discuss them thoroughly.

We have improved on the figures as suggested by both reviewers and we have consistently added more detailed inferences and discussion following the presentation of results in Section 3 of the updated manuscript (Also see the subsequent response to various comments by Reviewer 2 and RC#1).

To avoid confusion, please consider the use of Tg,org instead of Torg for the glass transition temperature of the organic phase throughout the manuscript. In Fig. 2, it would probably be useful if the liquid to glass transition were marked with a distinct change in color. Here, this important transition lies in the middle of the pink/purple color range.

The text was updated to clarify that T_{org} refers to $T_{g,org}$ both in texts and figures. We highlighted in Figure 2 in the updated manuscript, the liquid to glass (semi-solid as well as solid) transition marked with a distinct change in color (next to the color bar).

I do not understand the point of Fig. 3 since it is very hard to see what is going on and do not find it illustrative. It seems that water is the constituent with the highest variability; it is thus very unintuitive to plot it on the base of this plot, especially because a high concentration leads to a low overall value. It would hence be more helpful to not stack these three lines, but just report the diurnal cycle of Tg,org along with the particle composition in a separate panel. A graphical representation like the one shown in Fig. S1 seems better suited to present the data.

Erstwhile Figure 3 has been replaced by updating the previous Figure S1 as both reviewers suggested (also addresses Comment by RC#1).

633 – In the discussion of the PhaseSep2 scenario, it would be very helpful to see how PhaseSep2 compares to NonPhaseSep, i.e. the equivalent of Fig. S7. Please discuss thoroughly which scenario is more likely correct. What effect does the addition of LLPS have on the simulation results?

We added Fig. S6 to discuss more on the comparisons between *PhaseSep2* and *NonPhaseSep*, along with a Table S1 listing comparison among all the simulation cases.

The following text was also added (Lines 717-725):

"Table S1 shows a modest 4% improvement in model performance for total $PM_{2.5}$ OC mass, in the isoprene-abundant southeastern United States with *PhaseSep2*. The range of phase separation frequency in semi-solid particles is still wide when compared to other cases i.e. 29-55.8% SSPS. Increased frequency of bulk phase in semi-solid conditions in *PhaseSep2* relative to *PhaseSep* causes much less resistance to reactive uptake, closer to but still more than in

NonPhaseSep. This is reflected in the similarity of γ_{IEPOX} between *PhaseSep2* and *NonPhaseSep* (Fig. 7C and Fig. S6). Hence, a very marginal difference in IEPOX SOA and biogenic SOA in *PhaseSep2* relative to *NonPhaseSep* occurs (Fig. S6), unlike much higher differences observed in *PhaseSep* (Fig. 8)."

Also, refer to text added for subsequent discussion on model performance and different simulations as part of response to comments by RC#1 on Page 27 (Lines 727-739). Which clarifies more on the fact that more work on including explicit representation of non-IEPOX SOAs consistent with reactive uptake mechanism of IEPOX SOA currently in CMAQ is needed to assess accurate impact of updates to phase state and morphology presented in this work on overall SOA mass.

Minor comments

114-116 – What's the point of this reference in this context? "Low" and "high" are obviously relative. Also, please specify what is meant with "remaining bulk".

The text of the sentence was updated to clarify that remaining bulk refers to the non-IEPOX derived SOA and that there is 2 to 8 order of magnitude difference in volatility between the IEPOX-derived SOA and remaining OA. The low volatility of IEPOX-derived SOA was also clarified by including that the evaporation time of IEPOX-Derived SOA is greater than 100 hours under atmospherically relevant conditions.

See Lines 117-121 for updated text:

"IEPOX-derived SOA in the southeastern United States are found to exhibit higher volatility than the remaining bulk OA with saturation vapor pressures for IEPOX-derived SOA being 2 to 8 orders of magnitude larger than the remaining bulk OA, however IEPOX-derived SOA has a low overall volatility with evaporation time scales >100 hours under atmospherically relevant conditions (Lopez-Hilfiker et al., 2016)."

126 – Where is the amplification? Amplified compared to what?

The text was updated to (Lines 129-133):

"The reduced transport of semi- or low- volatile gas species such as IEPOX on to particles also highlight the effects of phase separation on aerosol formation by decreasing reactive uptake of IEPOX (Gaston et al., 2014). This is due to increased resistance to diffusion of IEPOX through the SOA coating (Zhang et al., 2018a)."

169 – What do you mean with “particles [. . .] can only dissipate energy by rebounding”. Are you talking about particle bounce measurements? How is this connected to the cited “almost full resistance to reactive uptake”? Please fill in the connections between these concepts.

The text was updated to eliminate the parenthesis referring to resistance to reactive uptake. The following clarifying sentence was also added to connect particle bounce measurements to reactive uptake (Lines 183-185):

“A higher bounce factor implies that a particle is more viscous most possibly due to a glassy organic coating and therefore more likely to exhibit diffusive limitations in reactive uptake.”

In equation (3), 205, the sum of wa, wb and ws is not 1. Is this intended?

The text was updated to correct equation (3) so that the 3 terms (w_a, w_b and w_s) sum to 1. The original equation was a typo.

367 – “This indicates that anthropogenic species have a higher range of glass transition temperatures than biogenic species” – The “range” is larger for biogenics, you probably want to point out the overall higher values. Same in 402.

The sentence was changed to (Lines 399-402):

“This indicates that anthropogenic species have a narrower range of glass transition temperatures but overall higher values than biogenic species; however, the maximum values of $T_{g,b}$ and $T_{g,a}$ are more similar than their minimum values.”

399 – How is a bimodal distribution relevant for Fig. 2?

The text was updated to mention that the low peak in Figure 1 occurs over the oceans as shown in Figure 2, and that the cluster of peaks between 0.8 and 0.9 in Figure 1 are caused by the Western US as shown in Figure 2 (Lines 429-437):

“Semi-solid particles with a higher range of T_g values (Fig 2A) were concentrated over areas associated with higher anthropogenic SOA (including anthropogenic POA listed in Table 1) and a low RH, aerosol liquid water content, and biogenic SOA, such as the American southwest and Rocky Mountains. These higher T_g values pulled the net $T_{g,org}$ value up closer to the ambient temperature, and thus, brought the $T_{g,org}$:T ratio closer to 1, which is shown in the cluster of peaks between $T_{g,org}$:T = 0.8 and $T_{g,org}$:T = 0.9. The particles with the lowest $T_{g,org}$:T ratios were located over the Atlantic and Pacific oceans, due to the substantially higher aerosol water content and low levels of anthropogenic and biogenic organics in these environments.”

419 – How is reduction of water connected to disappearance of bimodal Tg,org?

The following sentence was added for clarification (Lines 426-428):

"Particles dominated by w_s had $T_{g,org}$ similar to $T_{g,w}$, with reduced influence from w_a and w_b, which decreased their $T_{g,org}$:T ratio as $T_{g,w}$ is substantially lower than the predicted T_g values for organic species"

Fig. 4A – What is the black line at the bottom of the plot representing? Panels of Fig. 4 do not appear in the order they are presented in the manuscript.

We removed the black line at bottom of curve plot in Fig. 4A to satisfy the reviewer's comment. The text discussing Figure 4 presented Fig. 4F at start, as it is the most dominant factor that affects η_{org}. Figs. 4D and 4E are discussed in subsequent line to put things in perspective to compare the influence of biogenic, anthropogenic and organic water (4F) constituents of organic shell on its viscosity (η_{org}). The rest of Fig. 4 is discussed in order.

474 – "This suggests that anthropogenic aerosol components are likely more water soluble than biogenic components." - Do you have more than statistical evidence for that? Shouldn't that be easy to derive from model input rather than from model output.

Yes, we can easily infer from model inputs as the reviewer suggests. Since, water solubility or hygroscopocity (κ_{org}) has been presented as being linearly proportional to O:C of aerosol components i.e. highly oxygenated species are more water soluble (Pye et al., 2017)- Also refer to response to Specific comment #2 by RC#1.

Average O:C for 26 anthropogenic components is 0.59 as compared to 0.72 for 9 biogenic components used in CMAQv5.2's *aero6* aerosol mechanism as listed in Table 1. Also, w_a and w_b does not indicate the water solubility but just the fraction occupied by anthropogenic and biogenic constituents respectively in total OA.

Hence, we also modified the text in the updated manuscript as (Lines 512-515):

"This suggests that anthropogenic aerosol components are more dominant than the biogenic components. Where biogenic components are likely more water soluble with their average O:C being 0.72 compared to 0.59 for anthropogenic constituents (Table 1)."

486 – "Some mismatch can be attributed to the lack of an explicit mechanism to compute organic aerosol water uptake and some unaccounted SOA formation mechanisms." - Please expand on

this, how would you attribute these to mismatch? Does the data make you recognize this or are these just general shortcomings of the model?

Like the reviewer points out in this comment, both the 'lack of explicit mechanism on organic aerosol water uptake and some unaccounted SOA formation mechanisms' actually refers to a 'general shortcoming of CMAQ model algorithm'. Authors would like to clarify that these are not inherent shortcomings of CMAQ, but rather a limitation of CMAQv5.2 (used in this work). Recently released CMAQv5.3 includes uptake of water onto organic species, updated monoterpene SOA, and explicit SOA from organic nitrates (intended for use in subsequent future work).

We have hence expanded the discussion by presenting the further investigation of modeled O:C ratio with observed O:C ratio data (based on findings from newer instrumentation with higher molecular details) at Centreville, AL forest site to recognize the shortcomings of model in form of unaccounted SOA species (i.e. Organic Nitrates missing in CMAQ v5.2), actually dominant on field.

Updated text as part of this discussion is added in the Section 3.1.2: Lines 539-556 (Refer to response to RC#1 on Section 2.7 for the updated text).

492 – "The difference in observed and model estimated Torg:T range was statistically significant with a P-Value = 0.001" - What does this entail? You are testing the hypothesis that both data sets (model/field) are different. Why?

We agree with the reviewer's comment and remove the ANOVA statistical test, as P-value can be unintuitive and confusing as a form of model validation often, and there is fair evidence based on correlation and mean values that model outputs compared fairly well (although not too high in terms of correlation) to the field data. The text was updated to include the following sentence (Lines 533-535):

"The model estimated $T_{g,org}:T$ range compared to $T_{g,org}:T$ range based on field observations at Centreville, AL for SOAS 2013 give a correlation coefficient of ~ 0.66 between them."

Hence we added the comparison of field observation of O:C ratio at Centreville, AL with modeled estimated O:C ratio, to further explain the cause of not too high of a correlation (or some mismatch) between modeled and observation-derived $T_{g,org}:T$ range for Centreville, AL (as presented in Figure 5). Refer to our response to RC#1 on Section 2.7 for the updated text (Lines 539-556).

500 – "Wider ηorg ranges at higher RH can be explained by increased diffusivity with higher aerosol liquid water in SOA causing quick mixing times often accompanied with drastic differences in composition" – Can you expand on this claim (i.e. drastic differences in

composition) and back it up with data? I would think high variance in ηorg at 80 % RH is simply due to a very steep η(RH) curve in that humidity range.

The text was updated to (Lines 560-565):

"Wider η_{org} ranges in the higher RH bins can be explained by increased diffusivity with higher aerosol liquid water in SOA causing faster mixing times leading to quick changes in composition. Furthermore, these contain the most atmospherically relevant RH ranges for the model simulation period. Therefore, a wide range of particle compositions is expected which also contributes to the wide range of predicted η_{org} values."

508 – "This can be attributed to shattering of highly viscous SOA (ηorg ≥ 10^6 Pa•s) for RH ≤ 30% that inhibits their flow in laboratory measurements of ηorg." - Explain how the shattering of SOA in these studies causes a general overestimation of viscosity. To my knowledge, the authors of these papers tried to account for shattering in their viscosity prediction. Is this really the only source of deviation? This would be a good place to talk about idealized laboratory SOA and field samples

The following text was added to further explore differences between our modeled results and experimentally measured viscosities (Lines 573-581):

"Huang et al. (2018) speculates that differences in physicochemical properties of α-pinene SOA, including viscosity, can exhibit a "memory effect" of the conditions under which the particle formed. This is regardless of the subsequent conditions to which the particle is exposed. This could lead to differences between model-predicted and experimentally measured viscosities, as these memory effects are not well characterized. Grayson et al. (2016) reports that the viscosity of α-pinene SOA may vary as a function of the mass loading conditions with higher mass loading leading to lower viscosity measurements. Unfortunately, there is also a lack of experimental data on viscosity measurements at RH < 60%."

Fig. 8 – Different color scheme for panels a and b is misleading. Caption text denotes that biogenic SOA mass is primarily driven by IEPOX SOA, which according to panel is clearly not the case.

Color scheme for Fig. 8 parts A and B are consistent now in the updated manuscript, in addition to adding panel labels to accommodate comments from both the reviewers.

We removed the 'primarily driven by IEPOX SOA' part from the caption text of Figure 8 to avoid any confusion. Since, we already discuss spatial variability in the proportion of IEPOX SOA making up the total biogenic SOA on average for SOAS 2013 separately through Figure S3 in both *PhaseSep* and *NonPhaseSep* cases.

Technical notes

Plase standardize the use of "O:C". O:C is sometimes in parenthesis, sometimes not. O:Cavg can be misunderstood in way that only the carbon part is averaged.

The text was updated to change any instance referring to the average O:C ratio to $(O:C)_{avg}$.

Math equations in this manuscript appear overall messy, especially due to long italicized words.

Equations are now edited and long words have been removed wherever possible within the scope of manuscript.

Multiple inaccurate multiplication symbols are used: *, •. Please use ·.

All multiplication symbols were changed to "·" throughout the manuscript.

Check use of italic vs. non-italic symbols for variables is not consistent throughout the manuscript (kb and T should be italicized in 1 82, equation numbers are sometimes in italics sometimes not etc.).

The text of equations was updated to ensure accurate *italics* use.

"Tg can determine when aerosols are in a highly viscous glassy state" is a colloquialism.

This was changed to (Lines 174-177):

"Thus T_g can be used to determine when aerosols are in a highly viscous glassy state ($\eta_{org} \geq 10^{12}\ Pa \cdot s$), a semisolid state ($100 \leq \eta_{org} < 10^{12}\ Pa \cdot s$), or in a liquid state ($\eta_{org} < 100\ Pa \cdot s$) (Marcolli et al., 2004; Martin, 2000)."

l. 78-82 – Please revise too long sentence.

The text was updated to (Lines 80-85):

"Pye et al. (2017) used the ratio of organic matter to organic carbon (OM:OC) and the ambient relative humidity (RH) to predict phase separation frequencies. They found that phase separation was common at lower RH in urban areas with low OM:OC, but lower phase separation frequencies in rural areas were attributed to increasing OM:OC except for late mornings when phase separation frequency increased due to low RH."

117 – What does "pathways that typically happen in the ambient conditions" mean? Are there other pathways that happen under other conditions? Please be specific.

For the sake of specificity and clarity, the text in updated manuscript is now (Lines 121-123):

"Specifically, acid-driven multiphase chemistry of IEPOX with inorganic sulfate aerosol results in significant yield of organosulfates that have potentially higher viscosities (Riva et al., 2019)."

120 – Extra white space before comma. Reference missing?

The white space was removed and text was updated: See Lines 123-125.

l.124 – Check subscript of Dorg.

An extra period was removed from the subscript in this instance (See Line 129).

l. 158, 160 and elsewhere – Consider changing the shorthand “phase” to the more proper “phase state” in this manuscript about phase separation.

The text was updated to more accurately describe phase state, phase, and particle morphology.

l. 176 – “Criteria” is plural, so this should be either “criterion” or “were applied”

“was applied” was changed to “were applied”(See Line 191).

l. 202 – superfluous comma

The comma was removed (Lines 223-224).

l. 204 – “adds” should be “add”

The text was changed to replace “adds” with “add” (See Line 225).

l. 215 – There seem to be formatting issues in lines 212 and 215.

The text was updated to more clearly refer which OA species are referenced in the subsequent equations (Refer to Lines 229-235).

l. 295 – Eq. (14) should read Eq. (15).

The text was updated to reflect the correct equations mentioned in each line (See Line 313, Line 316).

l. 308 – I would refrain from using the casual “off of” in a scientific paper.

The text was changed to replace “off of” with “on” (See Line 329, Line 336).

l. 339 – I suppose “chromatogram” should read “chromatography” or “chromatograph” here.

The term “chromatogram” was replaced with “chromatography” (See Line 363).

l. 341f – The term OA (organic aerosol) is misused in this paragraph. It appears you talk about molecules, yet you refer to speciation of particles.

The text in updated manuscript is now modified to clarify the above confusion (Lines 364-367):

“The combined measurements provide comprehensive and quantitative characterization of particle-phase OA composition with over 800 OA components in this data identified as SOA produced predominantly through VOC oxidation, with a time resolution of 4 hours.”

l. 359 – “of” missing?

The text was updated to “calculation of γ_{IEPOX}.” (See Line 391).

l. 522f – Do you really know these numbers to four significant digits?

Three significant digits with scientific notation is used now throughout the text.

Supplementary Material for the ACP manuscript "Predicting Secondary Organic Aerosol Phase State and Viscosity and its Effect on Multiphase Chemistry in a Regional Scale Air Quality Model"

Ryan Schmedding[1,2], Quazi Z. Rasool[1*], Yue Zhang[1,54], Havala O. T. Pye [1,32], Haofei Zhang[4] ~~Zhang[3]~~, Yuzhi Chen[1], Jason D. Surratt[1], Ben H. Lee[6] ~~Lee[5], Claudia Mohr[5,8]~~, Felipe D. Lopez-Hilfiker[6] ~~Hilfiker[5,9]~~, Joel A. Thornton[6] ~~Thornton[5]~~, Allen H. Goldstein[7,8] ~~Goldstein[6,7]~~ and William Vizuete[1€]*

1. *Department of Environmental Science and Engineering, The University of North Carolina at Chapel Hill, Chapel Hill, North Carolina, 27516*

2. *Present Address: Department of Atmospheric and Oceanic Science, McGill University, Montreal, Canada, H3A 2K6*

~~2.~~3. *National Exposure Research Laboratory, Office of Research and Development, Environmental Protection Agency, Research Triangle Park, Durham, North Carolina, 27709*

~~3.~~4. *Department of Chemistry, University of California at Riverside, Riverside, California, 92521*

~~4.~~5. *Aerodyne Research, Inc., Billerica, Massachusetts, 01821*

~~5.~~6. *Department of Atmospheric Sciences, University of Washington, Seattle, WA 98195*

~~6.~~7. *Department of Environmental Science, Policy, and Management, University of California, Berkeley, CA 94720*

~~7.~~8. *Department of Civil and Environmental Engineering, University of California, Berkeley, CA 94720*

~~8. Present address: Department of Environmental Science and Analytical Chemistry, Stockholm University, SE-106 91 Stockholm, Sweden.~~

9. *Present address: Tofwerk AG, CH-3600 Thun, Switzerland.*

** Shared lead authorship*

€ Corresponding author: e-mail: vizuete@unc.edu; Telephone: +1 919-966-0693; Fax: +1 919-966-7911

Formatted: Justified

Formatted: Font: 11 pt

Formatted: Font: 11 pt

Formatted: Font: 11 pt, Not Superscript/ Subscript

Formatted: Font: 11 pt

Formatted: Font: 11 pt

Formatted: Font: 11 pt

Formatted: Font: 11 pt

Formatted: Font: 11 pt

Formatted: Font: 11 pt

Formatted: Font: 11 pt

Formatted: Font: 11 pt

Formatted: Font: 11 pt, Italic

Formatted: Font: 11 pt

Formatted: Font: Italic

Formatted: Normal

Formatted: Font: Italic

Formatted: Normal

Formatted: Font: Italic, Font color: Text 1

Formatted: Font: Italic

Formatted: Font: Italic

Formatted: Normal

Formatted: Font: 11 pt, Italic

Formatted: Normal, Centered, Indent: Left: 0.25", Hanging: 0.5"

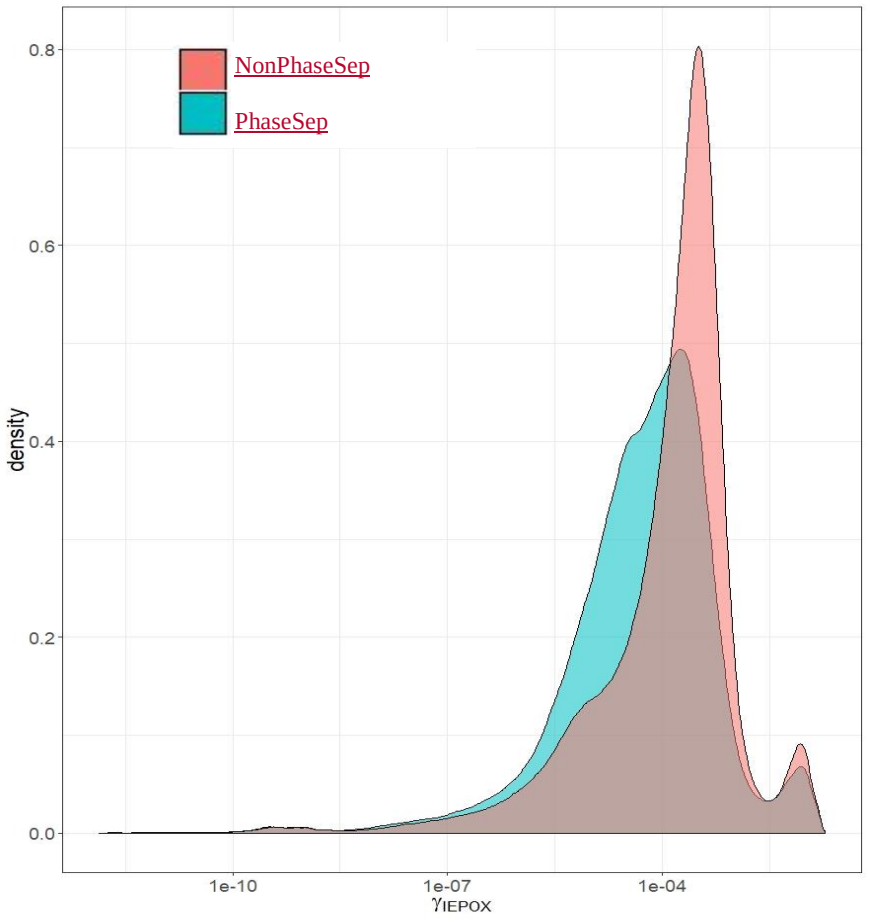
NonPhaseSep
PhaseSep
density
0.8
0.6
0.4
0.2
0.0
1e-10
1e-07
1e-04
γIEPOX

Figure S1

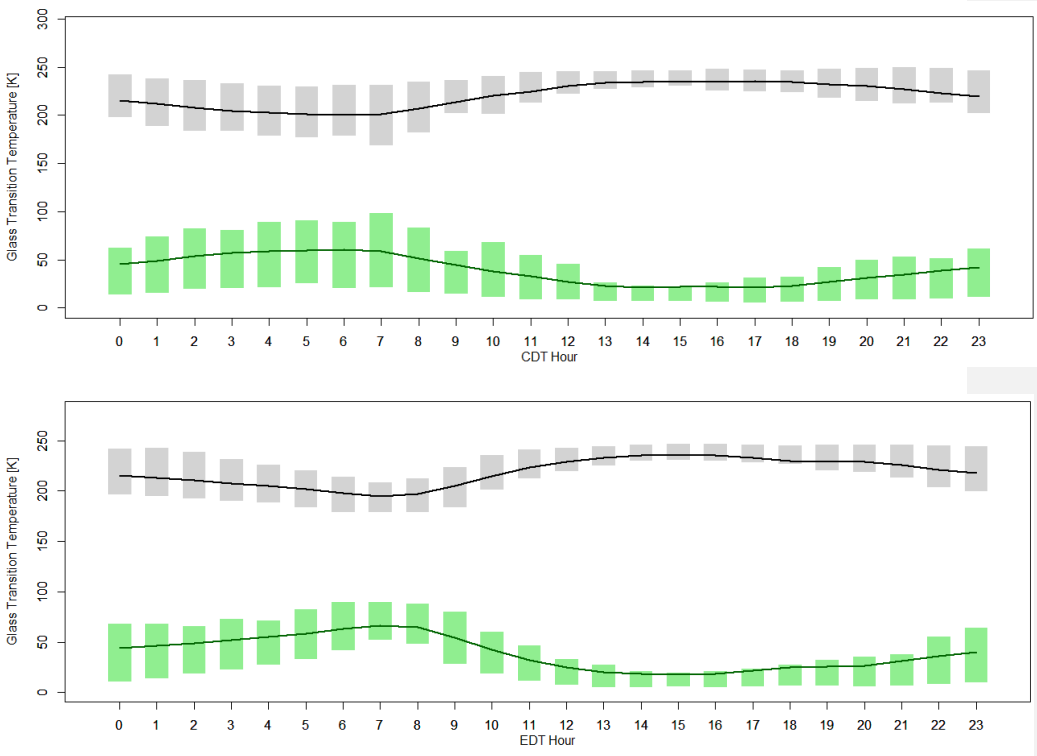

~~**Figure S1** Diurnal pattern for SOAS (June 1- July 15) 2013 of the contributions of aerosol liquid water (green) to Organic glass transition temperature (T_{org}) (gray) at the **(A)** Centreville, AL site and the **(B)** Jefferson Street, Atlanta site. Bars/shading indicate 25th to 75th percentiles. Lines indicate means.~~

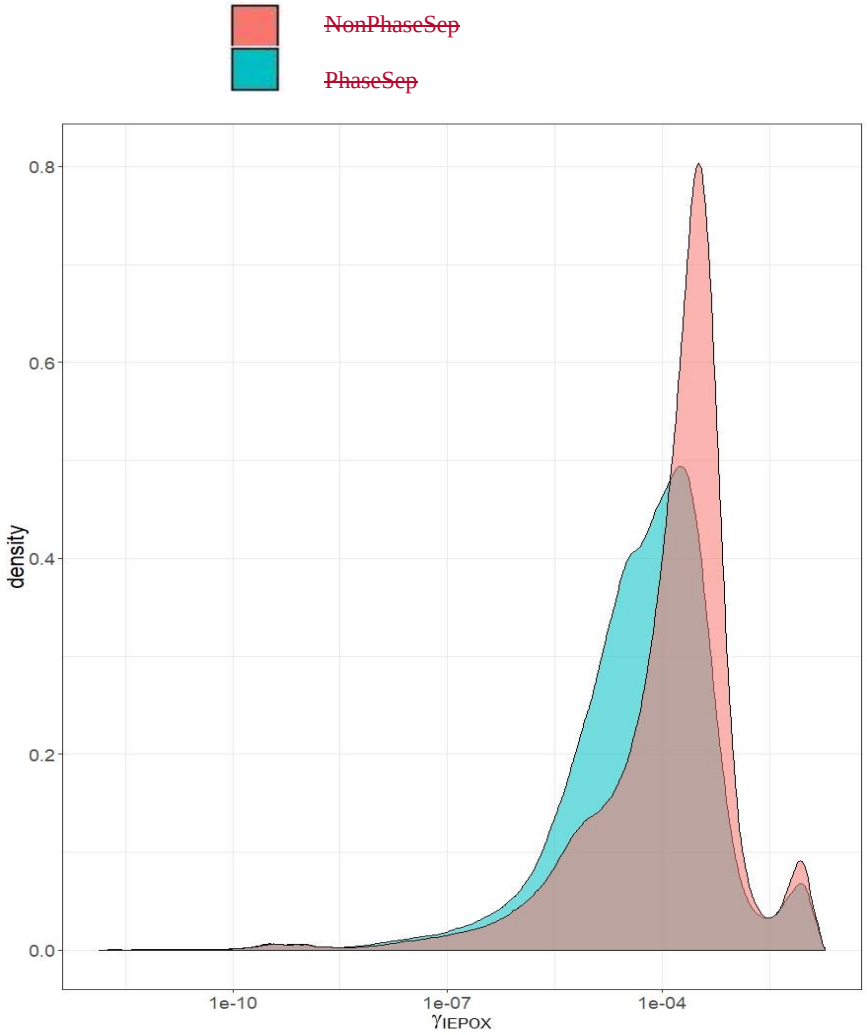

~~**Figure S2**~~ – For Southeastern United States, Probability distribution of γ_{IEPOX} at the surface level for the *NonPhaseSep* (red), *PhaseSep* (green) for SOAS 2013 simulation period.

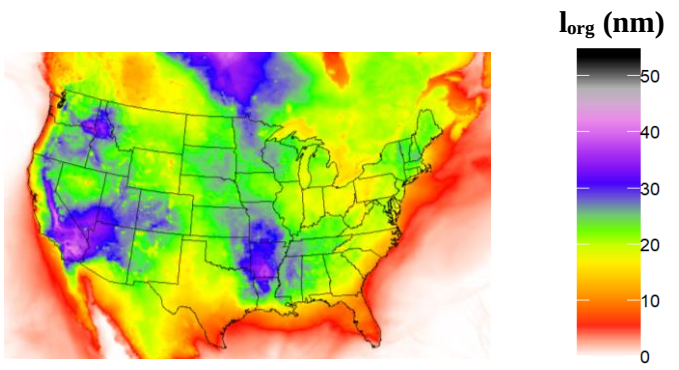

Figure S2~~S3~~ – Average organic coating thickness (l_{org} in nm) at the surface level for *PhaseSep* case for SOAS 2013 simulation period.

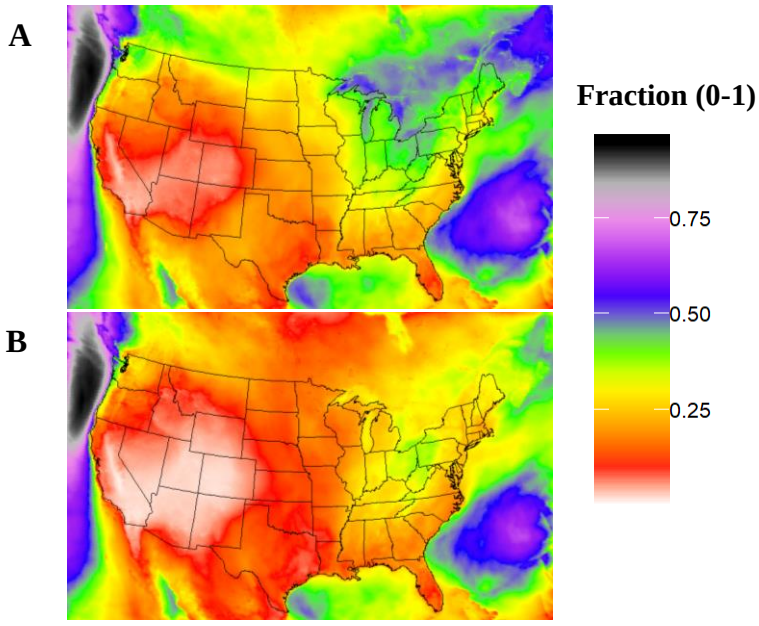

Figure S3~~S4~~ – Average fraction of IEPOX-derived SOA in biogenic SOA mass at the surface level for: **(A)** *NonPhaseSep and* **(B)** *PhaseSep* case for SOAS 2013 simulation period.

Formatted: Indent: Left: 1"

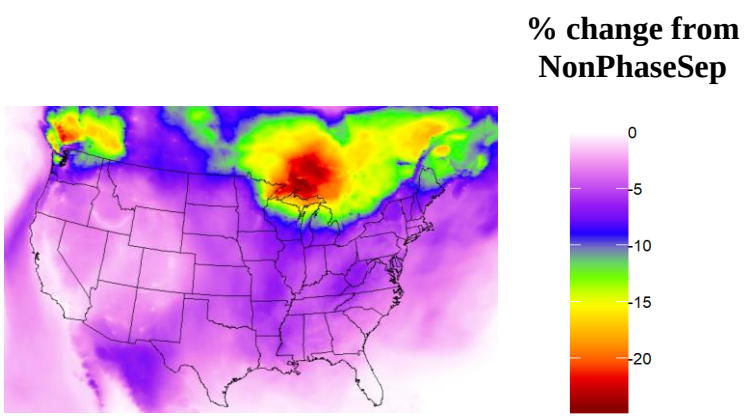

Figure S4~~S5~~ – Spatial map of the mean percent relative change of surface $PM_{2.5}$ organic carbon (OC) mass in *PhaseSep* case relative to the *NonPhaseSep* Simulation.

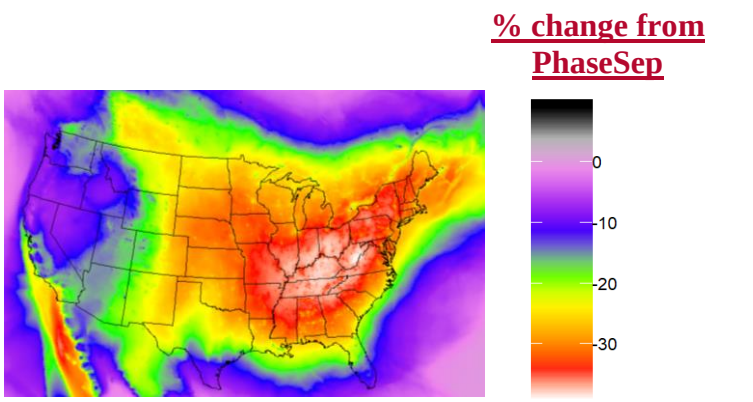

Figure S5 – Spatial map of the mean percent relative change of $PM_{2.5}$

Formatted: Indent: Left: 1"

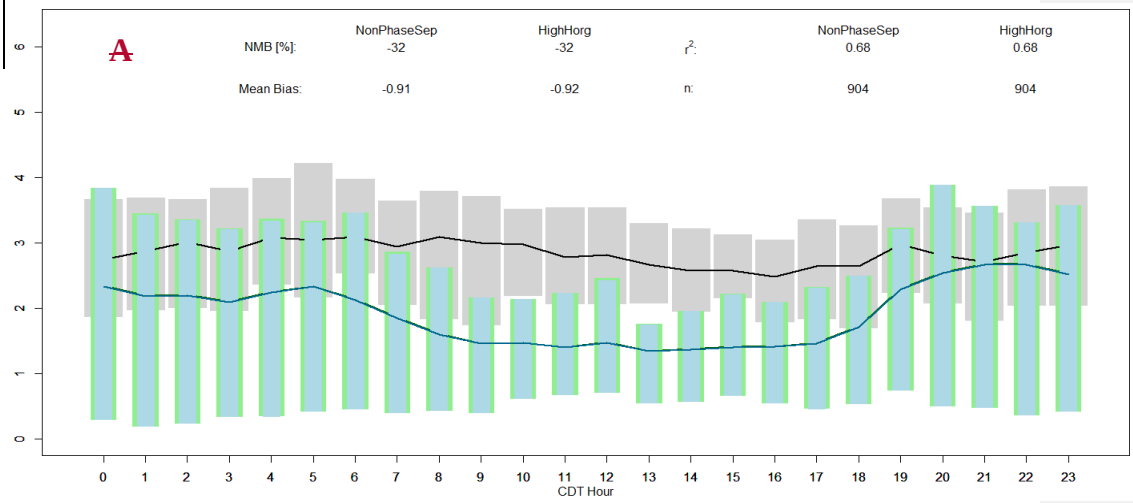
A
NonPhaseSep
HighHorg
NonPhaseSep
HighHorg
NMB [%]:
-32
-32
r2:
0.68
0.68
Mean Bias:
-0.91
-0.92
n:
904
904
0 1 2 3 4 5 6
0 1 2 3 4 5 6 7 8 9 10 11 12 13 14 15 16 17 18 19 20 21 22 23
CDT Hour

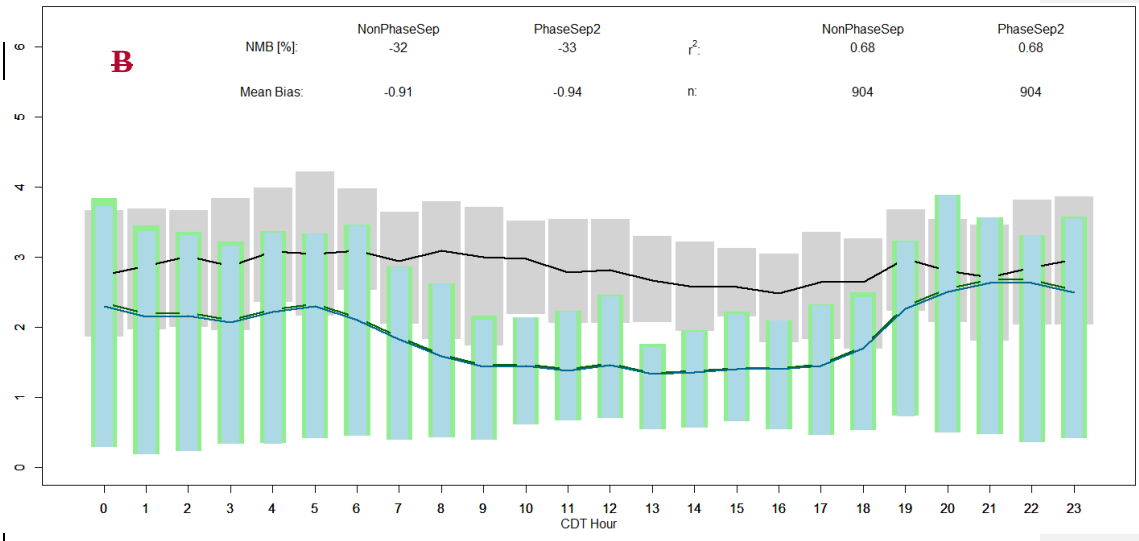
B
NonPhaseSep
PhaseSep2
NonPhaseSep
PhaseSep2
NMB [%]:
-32
-33
r2:
0.68
0.68
Mean Bias:
-0.91
-0.94
n:
904
904
0 1 2 3 4 5 6
0 1 2 3 4 5 6 7 8 9 10 11 12 13 14 15 16 17 18 19 20 21 22 23
CDT Hour

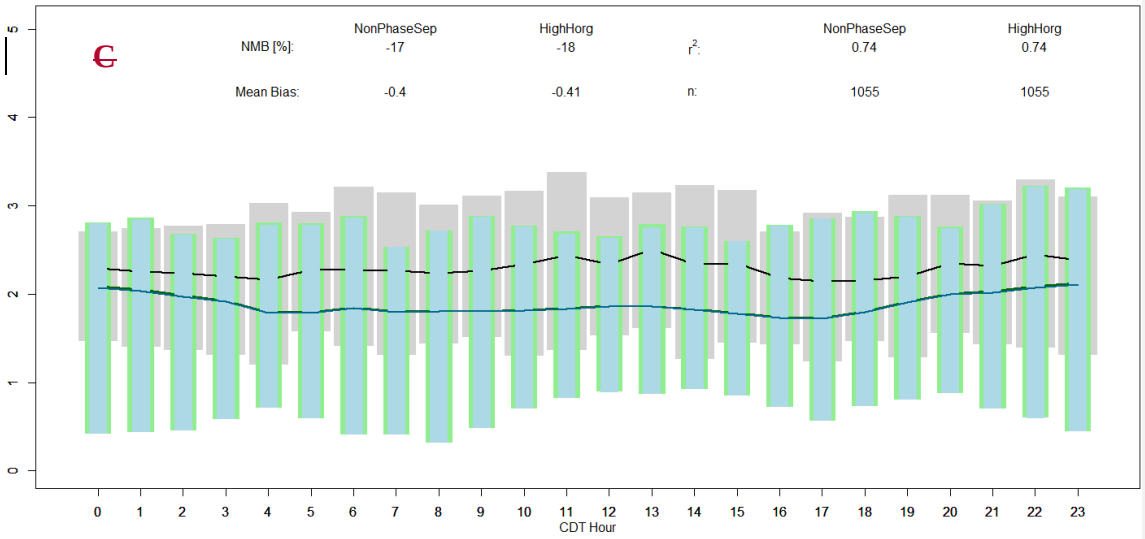

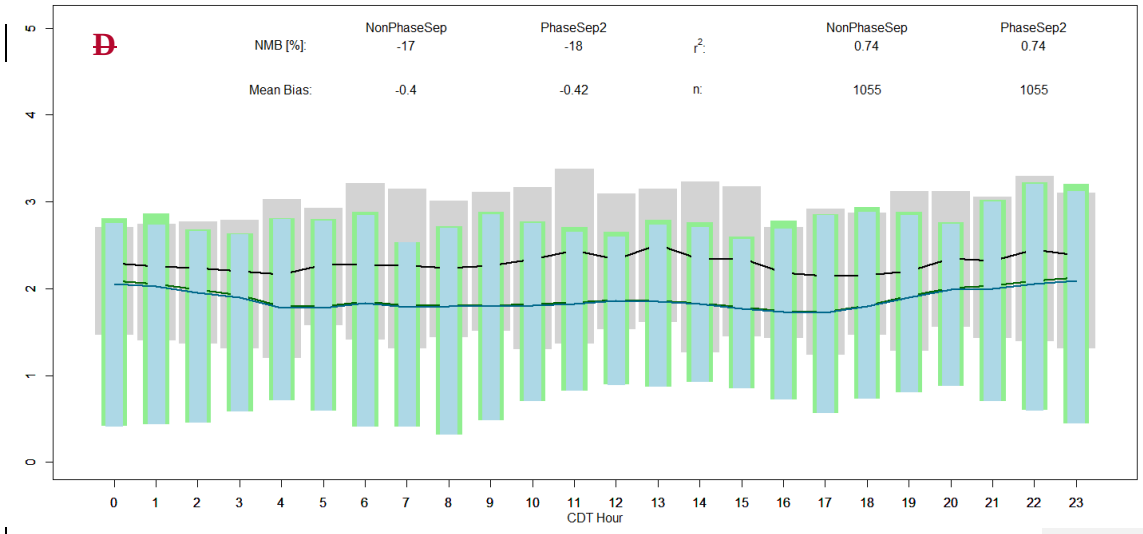

Figure S6 – $PM_{2.5}$ organic carbon (OC) mass (μg/m^3) as a function of hour of the day. Non-aggregated performance statistics- Mean Bias (μg/m^3), % Normalized Mean Bias (NMB) and Spearman's Correlation coefficient (r^2) of *NonPhaseSep* (green) and *HighHorg* (blue) relative to

~~observed (grey) $PM_{2.5}$ OC mass: **A**- for Rural Centreville, Alabama site and, **C**- for Urban Jefferson Street, Atlanta, Georgia site. Non-aggregated performance statistics *NonPhaseSep* (green) and *PhaseSep2* (blue) cases relative to observed (grey) $PM_{2.5}$ OC mass: **B**- for Rural Centreville, Alabama site and, **D**- for Urban Jefferson Street, Atlanta, Georgia site). Bars/shading indicate 25th to 75th percentiles. Lines indicate means. n= number of observation points.~~

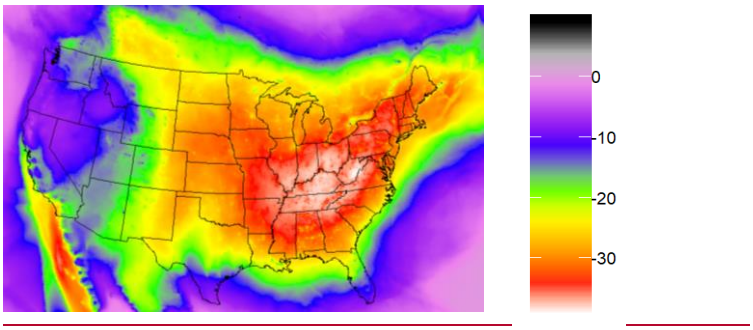

~~**Figure S7** Spatial map of the mean percent relative change of $PM_{2.5}$~~ sulfate mass at surface in *Emission Reduction* sensitivity case relative to the *PhaseSep* Simulation.

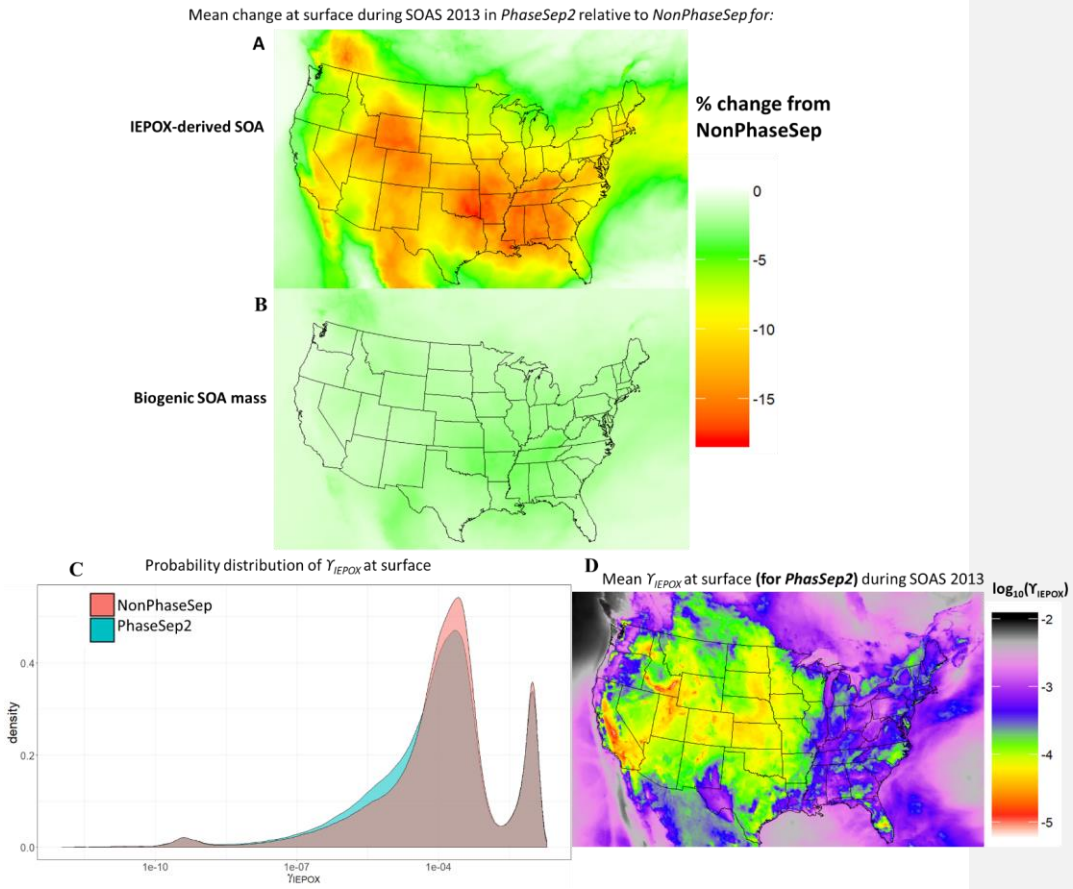

Figure S6 – Spatial map of the mean percent relative change of **(A)** IEPOX SOA and **(B)** biogenic SOA mass in *PhaseSep2* sensitivity case relative to the *NonPhaseSep* Simulation. **(C)** For Continental US, probability distribution of γ_{IEPOX} at the surface level for the *NonPhaseSep* (red), *PhaseSep2* (green) for SOAS 2013 simulation period. **(D)** Mean γ_{IEPOX} at the surface level for the *PhaseSep2* case for SOAS 2013.

Table S1 – Comparison of different simulations on phase separation frequencies and model performance in isoprene-abundant southeastern United States (rural Centreville, AL and urban Atlanta sites).

Parameter (units)		*PhaseSep*	*PhaseSep2*	*Emissions Reductions*	*HighHorg*
LLPS Frequency (%)		13.7	13.7	13.5	12.5
SSPS Frequency (%)		54.8	29	57	55.8
NMB (%, compared to SEARCH PM2.5 OC)	**Rural Centreville, AL forest site**	-36	-33	-44	-32
	Urban Jefferson Street, Atlanta site	-21	-18	-29	-18

Predicting Secondary Organic Aerosol Phase State and Viscosity and its Effect on Multiphase Chemistry in a Regional Scale Air Quality Model

Ryan Schmedding[1,2], Quazi Z. Rasool[1*], Yue Zhang[1,5~~4~~], Havala O. T. Pye [1,3~~2~~], Haofei Zhang[4~~Zhang[3]~~], Yuzhi Chen[1], Jason D. Surratt[1], Ben H. Lee[6~~Lee[5], Claudia Mohr[5,8]~~], Felipe D. Lopez-Hilfiker[6~~Hilfiker[5,9]~~], Joel A. Thornton[6~~Thornton[5]~~], Allen H. Goldstein[7,8~~Goldstein[6,7]~~] and William Vizuete[1€]*

1. Department of Environmental Science and Engineering, The University of North Carolina at Chapel Hill, Chapel Hill, North Carolina, 27516

2. Present Address: Department of Atmospheric and Oceanic Science, McGill University, Montreal, Canada, H3A 2K6

~~2.~~3. National Exposure Research Laboratory, Office of Research and Development, Environmental Protection Agency, Research Triangle Park, Durham, North Carolina, 27709

~~3.~~4. Department of Chemistry, University of California at Riverside, Riverside, California, 92521

~~4.~~5. Aerodyne Research, Inc., Billerica, Massachusetts, 01821

~~5.~~6. Department of Atmospheric Sciences, University of Washington, Seattle, WA 98195

~~6.~~7. Department of Environmental Science, Policy, and Management, University of California, Berkeley, CA 94720

~~7.~~8. Department of Civil and Environmental Engineering, University of California, Berkeley, CA 94720

~~8. Present address: Department of Environmental Science and Analytical Chemistry, Stockholm University, SE-106 91 Stockholm, Sweden.~~

9. Present address: Tofwerk AG, CH-3600 Thun, Switzerland.

* Shared lead authorship

[€] Corresponding author: e-mail: vizuete@unc.edu; Telephone: +1 919-966-0693; Fax: +1 919-966-7911

Abstract

Atmospheric aerosols are a significant public health hazard and have substantial impacts on the climate. Secondary organic aerosols (SOA) have been shown to phase separate into a highly viscous organic outer layer surrounding an aqueous core. This phase separation can decrease the partitioning of semi-volatile and low-volatile species to the organic phase and alter the extent of acid-catalyzed reactions in the aqueous core. A new algorithm that can determine SOA phase separation based on their: glass transition temperature (T_g), Oxygen to Carbon ($O:C$) ratio, concentrations relative to sulfate concentrations; and meteorological conditions were implemented into the Community Multiscale Air Quality Modeling (CMAQ) System version 5.2.1 and was used to simulate the conditions in the continental United States for the summer of 2013. SOA formed at the ground/surface level was predicted to be phase--separated with core-shell morphology i.e. aqueous inorganic core surrounded by organic coating, 68.5% of the time for continental United States. The phase states of organic coatings switched between semi-solid and liquid states, depending on the environmental conditions. The semi-solid shell occurring with lower aerosol liquid water content (western United States and at higher altitudes) has a viscosity that was predicted to be 10^2-10^{12} Pa·s which resulted in organic mass being decreased due to diffusion limitation. Organic aerosol~~The organic phase~~ was primarily liquid where aerosol liquid water was dominant (eastern United States and at surface), with a viscosity < 10^2 Pa·s. Phase separation while in a liquid phase state, i.e. Liquid-Liquid Phase Separation (LLPS), also reduces reactive

uptake rates relative to homogenous internally mixed liquid morphology, but was lower than aerosols with thick viscous organic shell. The implementation of phase separation parameters in CMAQ led to a reduction of fine particulate matter ($PM_{2.5}$) organic mass, with a marginal change in bias and error (< 0.1 $\mu g/m^3$) compared to field data collected during the 2013 Southern Oxidant and Aerosol Study. Sensitivity simulations assuming higher dissolution rate of isoprene epoxydiol (IEPOX) into the particle phase and the treatment of aerosol water content mitigated this worsening in model performance only to revert to original CMAQ bias. This point~~, pointing~~ out the need to better constrain both the parameters that govern phase state and morphology of SOA, as well as expand mechanistic representation of multiphase chemistry for non-IEPOX SOA formation in models aided by novel experimental insights.

1 Introduction

Particulate matter (PM) is one of six criteria pollutants regulated by the United States Environmental Protection Agency's (EPA) National Ambient Air Quality Standards (NAAQS), established by the 1970 Clean Air Act. There are two categories of PM regulated by NAAQS: Fine PM ($PM_{2.5}$), with particle diameter less than 2.5 μm, and coarse PM (PM_{10}), with particle diameter up to 10 μm. PM has adverse effects on the global climate (Carslaw et al., 2013; Grandey et al., 2018; Lee et al., 2016; Regayre et al., 2015). $PM_{2.5}$ also represents a substantial public health risk due to its association with increased overall mortality, due to cardiorespiratory diseases (Hwang et al., 2017; Jaques and Kim, 2000; Zanobetti and Schwartz, 2009). It has been estimated that 20-60% of $PM_{2.5}$ are comprised of organic aerosols (OA) (Docherty et al., 2008). These pollutant species are either directly-emitted primary organic aerosols (POA), or secondary organic aerosols (SOA), which form when volatile organic compounds (VOCs) undergo chemical reactions that reduce their volatility to the point that they either partition into the aerosol phase (Zhang et al.,

2007) or react heterogeneously with the existing particles (Riva et al., 2019). Studies have found that SOA tends to form the bulk of observed OA around the world (Nozière et al., 2015). The VOCs that form SOA may be either from biogenic or anthropogenic sources and can vary both spatially and temporally to areas as confined as the community level (Yu et al., 2014).

Recent studies have shown that SOA may phase-separate under certain atmospherically relevant conditions into different morphologies. These observations have included a "partially-engulfed" organic-inorganic morphology; an "island" morphology, where discrete pockets of SOA dot a larger inorganic particle; and a "core-shell" morphology, characterized by an organic rich outer "shell" and aqueous inorganic "core" (Freedman, 2017; O'Brien et al., 2015; Price et al., 2015; Renbaum-Wolff et al., 2016; Song et al., 2015, 2016; You et al., 2012; Zhang et al., 2015, 2018a). Pye et al. (2018) applied the Aerosol Inorganic-Organic Mixtures Functional groups Activity Coefficients (AIOMFAC) model (Zuend et al., 2008) to predict the thermodynamic favorability of phase separation in SOA using a box model and found that aerosols over the southeastern United States may be phase-separated as frequently as 70% of the time. ~~In other work,~~ Pye et al. (2017) used the ratio of organic matter to organic carbon (OM:OC) and the ambient relative humidity (RH) to predict phase separation frequencies. They found that phase separation was ~~exhibiting a complex behavior, being more~~ common at lower RH in urban areas with low OM:OC ~~at low RH~~, but lower~~higher~~ phase separation frequencies in rural areas were attributed to increasing OM:OC except for late mornings when phase separation frequency increased due to~~at~~ low RH.

When aerosols form a core-shell morphology, experimentally observed viscosities of the outer organic-rich shell and inner electrolyte-rich core have been shown to differ by up to three orders

Field Code Changed

Formatted: French (Canada)

of magnitude resulting in possible diffusion limitations on reactive uptake (Ullmann et al., 2019). It has also been shown that the viscosity and subsequently diffusivity of the organic phase (D_{org}) may vary as a function of SOA composition (Grayson et al., 2017). Laboratory experiments have been conducted to measure the viscosity of SOA using poke-flow and bead mobility techniques (Reid et al., 2018; Renbaum-Wolff et al., 2013; Song et al., 2015, 2016). These studies have found that SOA formed from anthropogenic precursors, such as benzene, toluene, and xylene, have similar D_{org} values in the realm of 10^{-14}-10^{-16} m^2/s (Grayson et al., 2016; Song et al., 2015, 2016, 2018). Similar studies on biogenic SOA comprised of α-pinene oxidation products, however found that its measured viscosities and calculated diffusion coefficients are lower than those of anthropogenic SOA by as much as 2 orders of magnitude at comparable conditions (Song et al., 2016, 2018; Zhang et al., 2015).

The most abundantly emitted biogenic VOC is isoprene (2-methyl-1,3-butadiene) with average annual global emissions totaling to approximately 500-750 Tg-C yr^{-1} (Guenther et al., 2006; Liao et al., 2015). Isoprene is known to react with hydroxyl (OH) radicals under low-NO_x (=$NO+NO_2$) conditions to form isoprene hydroxyhydroperoxides (ISOPOOH) (Jacobs et al., 2014; Krechmer et al., 2015). If the reaction pathway continues with OH, ISOPOOH will react again to form isoprene epoxydiol (IEPOX) (Bates et al., 2014; Paulot et al., 2009; Surratt et al., 2010). It is possible for IEPOX to form products with sufficiently low volatility to form SOA via a reactive uptake pathway onto acidified sulfate seed particles (Bondy et al., 2018; Surratt et al., 2006, 2007, 2010). IEPOX-derived SOA have been observed to account for up to 36% of biogenic SOA in the southeastern United States during the summer (Budisulistiorini et al., 2016). Given the importance

of this pathway there has been increased focus on the phase state of particles and its impact on reactive uptake (Budisulistiorini et al., 2017).

Prior measurements of isoprene-derived SOA suggested that it would not be viscous enough to exhibit diffusion limitations; however, there is much uncertainty with these measurements as those particles mainly formed through nucleation of semi-volatile species (Song et al., 2015). IEPOX-derived SOA that specifically account for up to one-third or more of total organic aerosol mass in the southeastern United States are foundhas shown to exhibit higher volatility than the remaining bulk OA with saturation vapor pressures for , but IEPOX-derived SOA being 2 to 8 orders of magnitude larger than the remaining bulk OA, however IEPOX-derived SOA has does have a low overall volatility with evaporation time scales >100 hours under atmospherically relevant conditions (Lopez-Hilfiker et al., 2016). Specifically, acid-driven multiphase chemistry ofHowever, IEPOX with inorganic sulfate aerosol results in heterogeneous reaction pathways that typically happen insignificantly yield chemical ambient conditions based formation of organosulfates that have potentially higher viscosities (Riva et al., 2019). Furthermore, RH (Huang et al., 2018; Pajunoja et al., 2014; Song et al., 2015, 2016; Zhang et al., 2015, 2018a), temperature (Maclean et al., 2017), degree of oligomerization-, and mass loading (Grayson et al., 2016) also impact particle viscosity. Higher RHs may result in more water to partition into the particle and act as a plasticizer which decreases its viscosity (Song et al., 2015, 2016, 2018; Zhang et al., 2011). Higher temperatures also increase the diffusion coefficient (Chenyakin, 2015). Degree of oligomerization increases the viscosity of SOA and therefore reduce its D_{org} as well (Grayson et al., 2017). The reduced transportThe competing sinks between heterogeneous reactions and losses of semi- or low- volatile gas species such as IEPOX on to particles also highlightamplify the effects of phase separationstate on aerosol formation by decreasing reactive uptake of IEPOX (Gaston et al., 2014). This is due to increased resistance to diffusion of IEPOX through the SOA coating (Zhang

et al., (Zhang et al., 2018a). The experimental data provided from previous studies highlight the urgency of incorporating those results into regional and global models to predict the effects of phase states in aerosol formation in the ambient environment accurately. A recent study by Schmedding et al. (2019) used a dimensionless (0D) box model for phase-separated SOA formation at the Look Rock Site during the 2013 Southern Oxidant and Aerosol Study (SOAS). Our prior work found that the inclusion of a phase-separation parameter could either inhibit SOA due to diffusion limitations in the separated organic phase or increase it by concentrating the electrolytes into the aqueous core leading to faster acid-catalyzed reactions. This resulted in decreasing normalized mean error (NME) of the model from 83.4% to 77.9% and the normalized mean bias (NMB) from -66.2% to -36.3% compared to a previous work simulating the same dataset that assumed homogenous aerosol (Budisulistiorini et al., 2016). The aforementioned Our previous model study (Schmedding et al., 2019) highlighted the significant impact of an organic coating layer on IEPOX-derived SOA formation, but lacked any quantification of conditions that result in phase separation creating such organic coating and its phase state.

The inclusion of an explicit reaction pathway for the reactive uptake of acid-catalyzed IEPOX-derived SOA in both regional and global scale chemical transport models (CTMs), such as the Community Multi-Scale Air Quality Model (CMAQv5.2.1) and the Goddard Earth Observing System (GEOS-Chemv11-02-rc), have substantially improved the performance of predicted SOA yields (Marais et al., 2016; Pye et al., 2013; Pye et al., 2017). These models do not include parameters in their aerosol algorithms that account for aerosol morphology or phase separation and its impact on SOA formation (Marais et al., 2016; Pye et al., 2017, 2018), which can lead to potential deviations of aerosol quantification. This work systematically examines formation

of ~~when~~ coatings comprised of OA derived from a mixture of biogenic and anthropogenic compounds. Besides ~~are formed (i.e.~~ predicting phase separation into core-shell morphology frequencies this work explores ~~and~~ how coatings impacts SOA formation from acid-catalyzed multiphase reactions of IEPOX~~)~~ by implementing parameterizations to determine the viscosity and phase ~~-~~state of particles (liquid or glassy) in CMAQ and simulating for the continental United States.

2 Methods

2.1 Phase state and its impact on reactive uptake: overview

Particles that are in a liquid-like state may either be an internal homogenous mixture, or they can also be phase-separated core shell morphology with both the inorganic-rich core and the organic-rich shell exhibiting liquid-like viscosities, which is also known as liquid-liquid phase separation (LLPS). The occurrence of LLPS depends on the average O:C ratio, organic mass to sulfate ratio, ambient temperature and ambient RH (Song et al., 2018; Zuend and Seinfeld, 2012). Organic constituents of an aerosol may also exhibit a solid-like glassy phase state when the ambient temperature is below the glass transition temperature (T_g), which is a function of RH and the aerosol composition (DeRieux et al., 2018). A liquid phase-state occurs when the T_g is lower than ambient temperature. The difference in viscosity (η_{org}) of the organic-rich coating~~phase of aerosol~~, below and above the T_g, may be as high as 8 orders of magnitude (Marsh et al., 2018). Thus ~~The~~ T_g can be used to determine when aerosols are in a highly viscous glassy state ($\eta_{org} \geq 10^{12}\ Pa \cdot s$), a semisolid state ($100 \leq \eta_{org} < 10^{12}\ Pa \cdot s$), or in a liquid state ($\eta_{org} < 100\ Pa \cdot s$) (Marcolli et al., 2004; Martin, 2000). Aerosols in a highly viscous or a semisolid state are assumed to be phase-~~-~~separated in a core-shell morphology as a model simplification (refer to Section 2.3). This

simplification is based on recent observations showing higher than anticipated rebound fractions in phase-separated OA that has been (i.e., almost full resistance to reactive uptake) attributed to organic aerosol constituents with viscosities > $10^2\ Pa \cdot s$ (Reid et al., 2018)., These aerosols were phase--separated withhaving an amorphous solid coating, which, unlike liquid particles, can only dissipate energy by rebounding. (Bateman et al., 2015; Reid et al., 2018) [illegible] a particle is more viscous and therefore more likely to exhibit diffusive limitations in reactive uptake. The specific conditions under which a particle will form a glassy rather than liquid-like organic shell are unclear, but thought to be driven by the same underlying physical properties that drive viscosity. This led to the assumption that particles that exhibit a semi-solid or glassy organic shell would inherently adopt a core-shell morphology. This assumption can be thought of as an upper bound on the frequency of particles separating into core-shell morphologies. In addition, a sensitivity case was completed where it was not assumed that a semisolid state is always phase-separated [illegible] water content (refer to Section 2.6).

Phase state of an organic shell impacts reactive uptake by affecting the diffusivity of a species through this outer organic shellphase (D_{org}). D_{org} can be related to the viscosity of the organic shellphase (η_{org}) using the Stokes-Einstein Equation, as shown in Eq. (1) (Ullmann et al., 2019):

$$D_{org} = \frac{k_b T}{6\pi \eta_{org} r_{diffusive}} \quad (1)$$

Where k_b is the Boltzmann constant, T is the ambient temperature, η_{org} is the organic shellphase viscosity, and $r_{diffusive}$ is the hydrodynamic radius of the molecule diffusing through the viscous organic shellphase.

Formatted: English (Canada)
Formatted: English (Canada)
Formatted: English (Canada)
Formatted: English (Canada)
Formatted: English (Canada)
Formatted: English (Canada)
Formatted: Font color: Text 1, French (Canada)
Formatted: French (Canada)
Formatted: Indent: Left: 0"
Formatted: Font: Italic
Formatted: Font: Italic

2.2 Determining the Glass Transition Temperature ($T_{g,org}$~~T_{org}~~)

The combined $T_{g,org}$~~T_{org}~~ for anthropogenic and biogenic species and aerosol water associated with them was found using a modified version of the Gordon-Taylor Mixing Rule, as represented in Eq. (2) (DeRieux et al., 2018; Gordon and Taylor, 1952):

$$T_{g,org}\text{~~}T_{org}\text{~~} = \frac{\left(w_s T_{g,w} + \frac{1}{k_{GT}}\left(w_a T_{g,a} + w_b T_{g,b}\right)\right)}{w_s(RH) + \frac{1}{k_{GT}}(w_a + w_b)} \quad (2)$$

where $T_{g,w}$ is the glass transition temperature of water (*137 K*) (Koop et al., 2011). $T_{g,a}$ and $T_{g,b}$ are the respective glass transition temperatures (*K*) for the anthropogenic (also includes all combustion-generated POA in addition to VOC-derived SOA, see Table 1) and biogenic (only includes VOC-derived SOA, see Table 1) fractions of OA. K_{GT} is the Gordon-Taylor constant, which is assumed to be 2.5 based on~~off of~~ Koop et al., (2011). w_a and w_b are the mass fractions of anthropogenic and biogenic OA species, respectively. $w_s(RH)$ or simply w_s is the mass fraction of organic aerosol water.

For this work, it was assumed that 10% of the aerosol water was present in the organic shell, which is a lower bound estimate of~~phase, within~~ the range of organic water reported by Pye et al. (2017). Approximately 10% of total aerosol water is associated with the organic phase during daytime when IEPOX chemistry is more prevalent as indicated by the observations collected during the SOAS 2013 campaign (Guo et al., 2015). To best replicate daytime IEPOX chemistry, the 10% value was chosen under the assumption that the underprediction of nighttime organic water would negligibly impact overall IEPOX-derived SOA. Naturally, this is not applicable for rest of multiphase chemistry and should be addressed accordingly in future work. In CMAQv5.2.1,

the total aerosol water, ~~10% of which is directed to the organic phase,~~ is predicted by ISORROPIA and only associated with inorganic electrolytes such as~~,~~ ammonium bisulfate (Pye et al., 2017). As represented in Eq. (3), the w_s along with the w_a and w_b make up the organic-water component of the aerosol and add~~adds~~ up to 1:

$$w_s = 1 - (w_a + w_b) \qquad \text{~~}(w_a - w_b)\text{~~} \tag{3}$$

Shiraiwa et al. (2017) used 179 organic species to fit a relationship between T_g, the molar mass (M), and O:C ratio (Shiraiwa et al., 2017) . Following the same relationship as in Eq. (4), the respective glass transition temperatures for the anthropogenic and biogenic fractions ($T_{g,a}$ and $T_{g,b}$~~,~~ ~~also referred as, T_{biog} and T_{anth}~~) were calculated using the weighted average molar mass (M_x) and O:C ratio ($(O{:}C)_x$) for all individual anthropogenic and biogenic species addressed in CMAQ (see Table 1). Where, x refers to ~~a~~ anthropogenic (a~~$OA\ (anth$~~) or ~~b~~ biogenic (b) OA and~~$(biog)$~~; i refers to individual species:

$$T_{g,x}\ or\ T_x = -21.57 + 1.51M_x - 0.0017M_x^2 + 131.4(O{:}C)_x - 0.25M_x(O{:}C)_x \tag{4}$$

$$Where,\ M_x \text{~~}M_x = \text{~~}\sum(w_{i,x}M_{i,x})\ ;(O{:}C)_x \text{~~}\sum(w_{i,x} * M_{i,x})\ ;\text{~~}$$

$$\text{~~}O{:}C_x = \text{~~}\sum\left(w_{i,x}(O{:}C)_{i,x}\right);\text{~~}\sum\left(w_{i,x} * O{:}C_{i,x}\right);\ w_{i,x} = \frac{Mass\ Concentration_{i,x}}{Total\ Mass\ Concentraion_x}$$

When the ambient temperature is below the $T_{g,org}$~~T_{org}~~, the viscosity of the coating (η_{org}) is assumed to remain constant at $10^{12}\ Pa \cdot s$. When the ambient temperature is greater than or equal to the calculated $T_{g,org}$~~T_{org}~~, the viscosity of the organic shell~~phase~~ is calculated using a modified Vogel-Tamman-Fulcher Equation (DeRieux et al., 2018; Fulcher, 1925; Tamman and Hesse, 1926; Vogel, 1921) as shown in Eq. (5) with experimentally fitted parameters as shown in Eqs. (6) and (7):

$$log_{10}(\eta_{org}) = -5 + 0.434\frac{T_0 D}{T - T_0} \tag{5}$$

Formatted: Font: Not Italic

Formatted: Font: Not Italic

Formatted: Font: Not Italic

Formatted: Font: Not Italic

Formatted: Font: Not Italic

$$T_0 = \frac{39.17T_{g,org}}{D + 39.17} \quad \frac{39.17T_{org}}{D + 39.17} \tag{6}$$

$$D = 14.4 - 2.3(O:C)_{avg} \tag{7}$$

T is the ambient temperature (K), T_0 is an experimentally fitted parameter of Eq. (5) that varies as a function of $T_{g,org}$ ~~T_{org}~~ and the fragility parameter D, which is a function of the O:C ratio (DeRieux et al., 2018; Zhang et al., In Prep). $(O:C)_{avg}$ ~~C_{avg}~~ refers to the overall OA (including both POA- all anthropogenic and SOA- anthropogenic and biogenic, see Table 1) O:C ratio given by CMAQ.

The effective diffusion coefficient for IEPOX through the organic coating (D_{org}) was then calculated using the Stokes- Einstein Equation (refer to Eq. (1)), assuming that $r_{diffusive} = 1$ nm (Evoy et al., 2019; Ullmann et al., 2019).

2.3 Phase Separation

SOA phase state was determined by multiple criteria. As a model simplification, any SOA was considered to be semisolid –phase- separated (SSPS) when η_{org} > 100 Pa·s ($T_{g,org}$ ~~T_{org}~~$:T \geq$ 0.8) based on Shiraiwa et al., (2017) as shown in Figs. 1 and 4A. LLPS occurs for aerosols with $\eta_{org} \leq$ 100 Pa·s ($T_{g,org}$ ~~T_{org}~~$:T <$ 0.8) when RH ≤ separation relative humidity (SRH_{LLPS}). Song et al. (2018) suggests that LLPS always happens when $(O:C)_{avg} \leq$ ~~$(O:C_{avg}) \leq$~~ 0.56, which we implemented to predict phase separation. When $(O:C)_{avg} > 0.56$, phase separation (or rather LLPS) is predicted based on the ~~along with~~ conditions specified for $(O:C_{avg}) > 0.56$ in Eqs. (8)

Formatted: English (Canada)
Formatted: English (Canada)
Formatted: English (Canada)

and (9). The SRH_{LLPS} is dependent on OA composition as shown in Eqs. (8) and (9) based on Bertram et al. (2011), Zuend and Seinfeld (2012) and Song et al. (2018):

$$SRH_{LLPS} = 35.5 + 339.9(O:C)_{avg} - (O:C_{avg}) - 471.8\,(O:C)_{avg}{}^{2} \quad (O:C_{avg})^{2} \quad (8)$$

$$when\ 0.56 < (O:C)_{avg} \leq (O:C_{avg}) \leq 0.73\ and$$

$$0.1 < (OM : Inorganic\ Sulfate) \leq 15$$

$$SRH_{LLPS} = 0 \quad \text{——————} i.e.\ no\ LLPS \quad (9)$$

$$when\ (O:C)_{avg} > (O:C_{avg}) > 0.73\ and$$

$$0.1 < (OM : Inorganic\ Sulfate) \leq 15$$

2.4 Model description and implementation

All simulations were completed in CMAQv5.2.1 for the SOAS campaign from June 1 - July 15, 2013, with ten days of spin-up time starting on May 21, 2013. Model inputs are described in Xu et al. (2018). The horizontal resolution of the simulation was 12km x 12km. Model vertical extent between the surface and 50 hPa (representing possible stratospheric influences) consisted of 35 layers of variable thickness. Weather Research and Forecasting model (WRF) Advanced Research WRF (ARW) version 3.8 with lightning assimilation was used to generate the meteorological inputs for the simulations (Appel et al., 2017; Heath et al., 2016). The National Emission Inventory (NEI) 2011 v2 produced by the EPA was used to generate anthropogenic emissions. Biogenic emissions were determined using the Biogenic Emission Inventory System (BEIS) v3.6.1 (Bash et al., 2016). BEIS predicts lower emissions amounts for isoprene than the Model of Emissions of Gases and Aerosols from Nature (MEGAN) (Carlton and Baker, 2011). Therefore, emissions of isoprene were increased in this work to 1.5x their original levels based on Pye et al. (2017) who found that this increase led to better agreement with field measurements of

isoprene and OH at the Centreville site during the 2013 SOAS. Carbon Bond v6.3 (CB6r3) was used for the gas-phase chemistry in the model (Emery et al., 2015; Hildebrant Ruiz and Yarwood, 2013; Yarwood et al., 2010).

2.5 Reactive Uptake

IEPOX-derived SOA is modeled with a first-order heterogeneous uptake reaction that includes a new term that accounts for diffusion limitations due to an organic coating when the aerosol phase state demands it, as described below in Eqs. (10)-(13) (Anttila et al., 2006; Gaston et al., 2014; Ryder et al., 2014; Budisulistiorini et al., 2017). The impact of organic coating was not considered in the original IEPOX reactive uptake algorithm in CMAQ (Pye et al., 2013):

$$IEPOX_{(g)} \rightarrow IEPOXSOA_{(aerosol)} \quad (10)$$

This first-order heterogeneous-reaction rate constant (k_{het}) is defined as:

$$k_{het} = \frac{SA}{\frac{r_p}{D_g} + \frac{4}{\nu\gamma}} \quad (11)$$

Where SA is the aerosol surface area ($\mu m^2/m^3$), ν is the mean molecular speed (m/s) of gas phase IEPOX estimated by Eq. (12):

$$\nu = \sqrt{\frac{8RT}{\pi MW_{IEPOX}}} \quad (12)$$

r_p is the effective molecular particle radius including both the inorganic core and organic shell (m), D_g is IEPOX diffusivity in the gas phase ($1.9 \cdot (MW_{IEPOX})^{-\frac{2}{3}} * (MW_{IEPOX})^{-\frac{2}{3}} \frac{m^2}{s}$), MW_{IEPOX} = 118 g mol^{-1} is the molecular weight of IEPOX and γ is the reactive uptake coefficient:

Field Code Changed

Formatted: French (Canada)

Formatted: Font: Not Italic

Formatted: Font: Not Italic

$$\frac{1}{\gamma} = \frac{1}{\alpha} + \frac{vr_p^2}{4H_{inorg}RTD_a r_{core}} \frac{1}{q\coth(q) - \frac{1}{q}} + \frac{vl_{org}r_p}{4H_{org}RTD_{org,eff}r_{core}} \quad (13)$$

D_a is the IEPOX diffusivity in the aerosol core ($10^{-9}\frac{m^2}{s}$) and q is the diffuso-reactive parameter as defined in Eq. (14~~13~~):

$$q = \mathrm{r_p}\sqrt{\frac{\mathrm{k_{particle}}}{\mathrm{D_a}}} \quad (14)$$

$k_{particle}$ is the pseudo-first order rate constant (s^{-1}) defined in Eq. (15~~14~~) (Pye et al., 2013), with parameters defined in Table 2:

$$k_{particle} = \sum_{i=1}^{N}\sum_{j=1}^{M} k_{i,j}\,[nuc_i][acid_j] \quad (15)$$

Formatted: Font: Not Italic

$D_{org,eff}$ ($\frac{m^2}{s}$) is the effective diffusivity of IEPOX through an organic coating compromised of the species given in Table 1 and 10% of the total aerosol liquid water.

The contribution of organic species to the volume of the core is assumed negligible and water moves freely between the inorganic core and the organic shell, leading to approximately 90% aerosol water in inorganic core and 10% in the organic shell for this work as described by Pye et al. (2017). An extension of this assumption is that the inorganic ion species are concentrated entirely within the aqueous core when calculating $k_{particle}$. H_{org} ($2 * 10^5\ M/atm$) is the effective

Henry's Law constant for the organic coating and l_{org} is the organic shell~~phase~~ thickness given by Eq. (16) calculated at each time step based on~~off of~~ Riemer et al. (2009). r_p is the surface-area weighted median particle radius based on surface area distribution of different species and β is the ratio of inorganic particle volume (90% of the particle water and inorganic species) to the total particle volume (all organic species, water, and inorganic species):

$$l_{org} = r_p(1 - \beta^{\frac{1}{3}}) \quad (16)$$

r_p is the effective aerosol radius (m) same as in Eqs. (11), (13) and (14), and r_{core} is the aerosol inorganic core radius (m). r_{core} is defined based on~~off of~~ Riemer et al. (2009) below:

$$r_{core} = r_p\beta^{\frac{1}{3}} \quad (17)$$

Particles that did not have LLPS or SSPS morphology were assumed to form a homogenous mixture of organics and inorganics (i.e. $l_{org} = 0$), reducing Eq. (13) to the standard CMAQ treatment.

2.6 Sensitivity simulations

Three Sensitivity simulations were performed over the updated CMAQ with phase state and phase separation prediction mechanism as detailed out between sections 2.1-2.5 (*PhaseSep*). A sensitivity simulation (*Emission Reduction*) was conducted using the EPA's emission reductions estimates of 34% and 48% for NO_x and SO_2, respectively, from 2013 to 2025 (Marais et al., 2016; Eyth et al., 2014). A second sensitivity (*HighHorg*) was conducted that used the same upper bound of H_{org} as reported by Schmedding et al. (2019) increasing the value from $2 \cdot$~~$*$~~10^5 M/atm to $3 \cdot$~~$*$~~10^8 M/atm. To better understand the effects of viscosity on particle morphology and phase separation,

a third sensitivity simulation (*PhaseSep2*) was conducted where phase separation of particles was determined solely by Eqs (8) and (9). This simulation excluded the rest while criterion criteria that particles with η_{org} > 100 Pa·s were automatically phase-separated with a semi-solid outer core, also referred as SSPS morphology. In *PhaseSep2*, guidelines laid down in section 2.3 only for LLPS in *PhaseSep* (Eqs. (8) and (9) along with phase separation always happening at $(O:C)_{avg} \leq 0.56$) are now expanded to predict SSPS frequency as well. Table 3 gives a brief description of the *NonPhaseSep* simulation (base CMAQ without phase state and organic coating impacts), the new *PhaseSep* proposed in this work, and the three sensitivity simulations: *Emissions Reductions*, *HighHorg*, and *PhaseSep2*.

2.7 Measurement Comparisons

Field data were collected using a high-resolution time-of-flight chemical ion mass-spectrometer (HTOF-CIMS) coupled with a filter inlet for gases and aerosols (FIGAERO) and a two-dimensional gas chromatography chromatogram time-of-flight mass spectrometer (GC×GC-TOFMS) at the Centreville, AL site during the 2013 SOAS campaign (Zhang et al., 2018b). The combined measurements provide comprehensive and quantitative characterization molecular compositions of particle-phase OA composition with over 800 OA components in this data identified as SOA produced predominantly through VOC oxidation, species with a time resolution of 4 hours. Chemical formulas were assigned to all the species based on high-resolution peak fitting and hence their O:C ratios and molecular weights are known, which were then used to empirically calculate the average $T_{g,org}$ T_{org} of the OA at the site for the duration of the entire SOAS campaign (June 1- July 15, 2013). The speciated OA were estimated to account for 74% of total fine OA mass during SOAS. The uncharacterized fraction of fine OA (e.g., organosulfur compounds, highly oxidized multifunctional molecules (HOMs), etc.)) will likely have some influence on the estimated $T_{g,org}$ T_{org}.

Also note that both techniques use thermal desorption approach to analyze OA composition which was recently shown to cause thermal decomposition for certain species (Lopez-Hilfiker et al., 2016; Cui et al., 2018). Thus, some interferences in $T_{g,org}$~~T_{org}~~ estimation could be expected by thermal decomposition; however, at this time it remains unclear how substantial these interferences could be due to lack of understanding of the degree of decomposition that occurs in these analytical methods. Nevertheless, to our knowledge, this is the most comprehensive molecular-level OA speciation data set, and thus, is appropriate to use for comparison with modeled $T_{g,org}$~~T_{org}~~ in this work.

We also use observed O:C ratios of various HOMs as reported by Massoli et al. (2018) recorded at Centreville forest site, Alabama during the SOAS 2013 study to compare with the simulations. Massoli et al. (2018) used a high-resolution time-of-flight chemical ionization mass spectrometer with nitrate reagent ion (NO_3^- CIMS) for these observations. More details are provided in the Results section.

Model simulation results (*PhaseSep*, *HighHorg* and *PhaseSep2*) were compared to recorded values for $PM_{2.5}$ organic carbon mass concentration at monitoring stations that are a part of the South Eastern Aerosol Research Characterization study (SEARCH) (Hansen et al., 2003) to better constrain the parameters used in the calculation of γ_{IEPOX}.

3 Results

3.1 Predicted Aerosol Phase State

The ratio of $T_{g,org}$~~T_{org}~~ to the ambient T is the strongest indicator of the phase state of the aerosol. The mean value for $T_{g,org}$~~T_{org}~~ for all grid cells on the surface level and for all time steps was 207 K with a

maximum value of 284 K, and a minimum value of 137 K, which suggested that particles would be in ~~and~~ a semi-solid or liquid-like because~~median~~ of the similarity to the ambient temperature.~~223 K.~~ The values of $T_{g,b}$~~T_{biog}~~ and $T_{g,a}$~~T_{anth}~~ ranged from 160-301 K and 230-311 K, respectively. This indicates that anthropogenic species have a narrower~~higher~~ range of glass transition temperatures but overall higher values than biogenic species; however, the maximum values of $T_{g,b}$~~T_{biog}~~ and $T_{g,a}$~~T_{anth}~~ are more similar~~relatively closer~~ than their minimum values. This is attributed to the abundant biogenic acid-catalyzed IEPOX-derived SOA species, such as organosulfates and 2-methyltetrols, having a high T_g of 301 K and a viscosity of 10[illegible] Pa s [illegible]

For the simulation period, the diurnal variability (i.e., between day and night) in the ambient T at any site was ~10 K, while $T_{g,org}$~~T_{org}~~ varied by as much as 75 K within a 24-hour period. This indicates that changes in the $T_{g,org}$~~T_{org}~~$:T$ ratio (i.e. Phase state) were driven by $T_{g,org}$~~T_{org}~~ (i.e., composition of the organics-water system) rather than T.

Figure 1 gives the predicted probability density distribution of the $T_{g,org}$~~T_{org}~~$:T$ ratio at the surface level of CMAQ for all grid cells and time steps. At the surface the minimum $T_{g,org}$~~range of T_{org}~~$:T$ ratio~~ratios~~ was ~~from~~ 0.46~~455 to 0.987~~ with a maximum~~median value~~ of 0.99~~763 and a mean value of 0.703~~. In the surface layer over 63.5% of the $T_{g,org}$~~T_{org}~~$:T$ ratios were less than 0.8, a value which is given as the transition point from a semi-solid viscosity to a liquid-like viscosity (Shiraiwa et al., 2017), with~~while~~ the remainder in a ~~other 36.5% of the condition that the $T_{org}:T$ were more than 0.8, indicating the aerosols were in~~ semi-solid phase state. Also shown in Figure 1 are the $T_{g,org}$~~T_{org}~~$:T$ ratio at the 18th layer (~ 1.8 km above ground level), 28th layer (~ 8 km above ground level) and the 35th layer (~ 17 km above ground level). For 18th layer (i.e., lower troposphere), the

majority of particles had *a* $T_{g,org}$:T ratios between 0.8 and 1.0, indicating a semi-solid state with few solid particles having $T_{g,org}$$T_{org}$:$T$ ratios >1 ranged from 0.464 to 1.022 with a median value of 0.807 and mean value of 0.772. For 28th layer (i.e., upper troposphere), 84.8% particle had a $T_{g,org}$:T ratio in the semi-solid regime between 0.8 and 1.0. At the T_{org}:T ratios ranged from 0.523 to 1.201, with a median value of 0.890 and mean value of 0.892. For 35th level nearly all of the [illegible]

Figure 2A shows a map of the average surface layer $T_{g,org}$$T_{org}$:$T$ ratio across the Continental United States for the duration of the simulation. The $T_{g,org}$$T_{org}$:$T$ ratios exhibited a bimodal distribution both at the surface (Fig. 1 and Fig. 2A) and in the lower troposphere (Fig. 12B), where particles over the oceans had substantially higher w_s. Particles dominated by w_s had $T_{g,org}$ similar to $T_{g,w}$, with reduced influence from w_a and w_b , which decreased, driving down their $T_{g,org}$$T_{org}$:$T$ ratio as $T_{g,w}$ is substantially lower than the predicted T_g values for organic species. These particles correspond to the peak at $T_{g,org}$:T located over approximately 0.45 (Fig. 1).. Semi-solid particles with a higher range of T_g values (Fig 2A) were concentrated over areas associated with higher anthropogenic SOA (including anthropogenic POA listed in Table 1) and a low RH, aerosol liquid water content, and biogenic SOA, such as (i.e., the American southwest and Rocky Mountains.). These higher T_g values pulled the net $T_{g,org}$$T_{org}$ value up closer to the ambient temperature, and thus, brought the $T_{g,org}$$T_{org}$:$T$ ratio closer to 1, which is shown in the cluster of peaks between $T_{g,org}$:T = 0.8 and $T_{g,org}$:T = 0.9.. The particles with the lowest $T_{g,org}$$T_{org}$:$T$ ratios were located over the Atlantic and Pacific oceans, due to the substantially higher aerosol water content and low levels, or even lack of anthropogenic and biogenic organics in these environments.

Figures 2B, 2C and 2D show the spatial profiles of the mean $T_{g,org}$$T_{org}$:$T$ ratio for each grid cell at the 18th layer of CMAQ (lower troposphere), 28th layer of CMAQ (upper troposphere) and the

35th layer of CMAQ (stratosphere). The value of T drops with the decreasing pressure. The O:C ratio of the particles are predicted to increase when compared to the surface due to atmospheric oxidation. The mean O:C ratio of all particles at the surface was 0.73, while across the troposphere (at layers 18 and 28) it increased slightly to~~was~~ 0.75, and at layer 35 it was 0.77. Species with high O:C (> 1.6) parametrized in CMAQ as anthropogenic OA collectively can be used as a surrogate for Highly Oxygenated Organic Aerosol (OOA); specifically low-volatility- LVOOA and semi-volatile-SVOOA oxygenated OA. Table 1 shows the species which are attributed to this specific modeled change in O:C with elevation. The mean mass fraction of anthropogenic OA increased from ~ 40% at surface to ~ 65% at the upper troposphere and eventually ~ 80% at layer 35. Whereas, biogenic OA comprising of isoprene-derived OA drops from ~ 30% at surface to 24% at the upper troposphere and eventually ~ 20% at layer 35. This is in agreement with the findings from airborne measurements in the southeastern United States as part of the Southeast Nexus (SENEX) field campaign that show a sharp drop in isoprene-derived OA and drastic increase in OOA with rising altitude (Xu et al., 2016). The mean ~~The mean~~ value of $T_{g,org}$~~T_{org}~~ also increased from 207 K at the surface to 219 K at layer 18, 223.5 K at layer 28 and 239 K at layer 35. This change in $T_{g,org}$~~T_{org}~~ was primarily driven by decreases in organic water in the aerosol, which gradually decreased from [illegible] led to the disappearance of the bimodal $T_{g,org}$~~T_{org}~~$:T$ ratio beyond the 28th layer (upper troposphere). The mean $T_{g,org}$~~T_{org}~~$:T$ ratio was less than 1 for all grid cells at the 18th layer (lower troposphere), and 59.7% of particles were likely to be liquid based on the $T_{g,org}$~~T_{org}~~$:T$ ratio < 0.8 with the remainder in the ~~. The remaining 40.3% of particles were~~ semi-solid regime. These semi~~because their $T_{org}:T$ values were between 0.8 and 1. Semi~~-solid particles were still concentrated over the American southwest and Rocky Mountains. At the 18th layer (upper troposphere), 69.35% of the

particles were semi-solid with $T_{g,org}$~~T_{org}~~:T ratio between 0.8 and 1, with 15.61% and 15.03% of particles likely to be liquid ($T_{g,org}$~~T_{org}~~:T ratio < 0.8) and solid ($T_{g,org}$~~T_{org}~~:T ratio > 1). At the 35th layer of CMAQ, all particles had a $T_{g,org}$~~T_{org}~~:T ratio-> 1, indicating that the organic phases of all of the particles had glassy viscosities. By layer 35 (stratosphere), the particles mostly exhibit a solid-like behavior across the Continental United States. Particles with the highest $T_{g,org}$~~T_{org}~~:T ratio at this altitude were located over the southern half of the simulation area, with $T_{g,org}$~~T_{org}~~:T ratios approaching ~1 in the northern half of the simulation. Particles in the Northern half of the Continental United States domain had higher concentrations of biogenic and anthropogenic SOA in comparison to those in the southern half of the domain and therefore had higher $T_{g,org}$~~T_{org}~~ values than their southern counterparts had.

Figure 3 is an illustrative example through model data extracted for June 1 - July~~June~~ 15, 2013, at two SEARCH monitoring sites. Figure 3 shows the diurnal profile and relative contributions of the model predicted anthropogenic, biogenic and water fractions to $T_{g,org}$~~T_{org}~~ for a rural site in Centreville, Alabama (Fig. 3A) and at an urban site at the Jefferson Street, Atlanta, Georgia (Fig. 3B). Both Centreville and Atlanta sites (Fig. 3) had $T_{g,org}$~~T_{org}~~ values that ranged from 150~~175~~-250 K (Fig. 3~~S1~~). The Centreville site, however, is rural and the $T_{g,org}$~~T_{org}~~ is more dominated by biogenic emissions (Fig. 3A). Whereas, the Jefferson Street site has a significant contribution by both anthropogenic and biogenic emissions, but anthropogenic dominating slightly (Fig. 3B). Fig. 3 also~~S1~~ gives the diurnal pattern of relative contribution of aerosol liquid water (associated with organics) to $T_{g,org}$~~to T_{org}~~. The peaks in $T_{g,org}$~~T_{org}~~ coincided with the daytime period of high emissions of VOCs and lower contribution of aerosol liquid water (Fig~~Figs~~. 3~~and S1~~). At night and early morning, due to higher contribution of aerosol liquid water, $T_{g,org}$~~T_{org}~~ is lower than daytime for both the sites (Fig. 3~~S1~~). Figure 3B shows

that $T_{g,org}$ ~~T_{org}~~ at the Jefferson Street, Atlanta, Georgia has similar peaks, but a higher minimum value during the night, due to the higher budgets of anthropogenic VOCs or combustion-generated anthropogenic POA as compared to biogenic. Both sites have a relatively high contribution of aerosol water (generally true for eastern United States, see Fig. 2A) to the organic phase, especially at night and early morning for 18:00-8:00 local day hours (Fig. 3~~S1~~).

3.1.1 Predicted Viscosity

The abundance of water relative to organics (Fig. 4F) drives the model predicted variability in viscosity and phase separation. Whether a particle is semi-solid, or liquid, and whether it is in a LLPS state is influenced by the proportion of SOA constituents, including uptake of water by them and has implications for the organic shell ~~phase~~ viscosity. Figures 4D-F show that, w_s (i.e., water related to organic shell~~phase~~) had the strongest correlation with η_{org} (r = 0.92~~919~~) followed by w_b (r = 0.74~~736~~) and w_a (r = 0.62).~~620) (i.e., biogenic and anthropogenic constituents in the organic phase, respectively).~~ Figure 4A gives the probability density distribution of η_{org} at the surface level for all grid cells and time steps. The predicted viscosity for *PhaseSep* simulation spanned 14 orders of magnitude~~ranged from 5.94*10^{-3} Pa•s to 5.31*10^{11} Pa•s~~ with a mean value of 8.45·*10^5 Pa·s (median of 343 Pa·s). Due to this large difference in the mean and median of the predicted viscosities, we chose to use the median value as a more robust measure of the central tendency of the predicted viscosities for inter and intra-simulation comparisons.~~•s).~~ As shown in Figure 4A, the overall phase separation frequency was 68.5%, where 54.8% of predicted viscosities were greater than 100 Pa·s, indicating that they exhibited SSPS morphology. The median viscosity ~~mean of η_{org}~~ of SSPS particles was on~~1.54*10^6 Pa•s, and~~ the order of ~~median was 7.79*~~10^3 Pa·s, just above the threshold where particles start exhibiting a glassy state.~~•s.~~ The remaining 13.7% of

Formatted: Superscript

the phase-separated particles exhibited a LLPS morphology. The median viscosity of LLPS particles was on the order of 10^0 Pa·s, indicating a very liquid-like state.1.14 Pa•s with a mean of 14.2 Pa•s with a range of $7.86*10^{-3}$ to 99.99 Pa•s. Ambient RH was also more strongly correlated with η_{org} (r = 0.68677) than O:C ratio (r = 0.62) (Fig. 4B-C). $D_{org,eff}$, which is inversely related to η_{org} as derived from Eq. (1), had a range 1.20 $*10^{-24}$ m²/s to $3.58*10^{-11}$ m²/s and a mean and median of 3.40·$*10^{-12}$ m²/s and 3.94·$*10^{-11}$ m²/s, respectively. The mean O:C ratio of LLPS particles was 0.65 [illegible] 0.70 [illegible] (w_s) was 42.4% [illegible] 99.9% The mean values of w_a and w_b in LLPS were 37% and 19% [illegible] contributions [illegible] % and 37.7%, respectively, with ranges of w_a and w_b to the total organic mass were 9.69 $1.76*10^{-5}$ to 82.1% and 8.21% $2.15*10^{-5}$ to 96.9%. This suggests that anthropogenic aerosol components are more dominant than the biogenic components. Where biogenic components are likely more water soluble with their average O:C being 0.72 compared to 0.59 for anthropogenic constituents (Table 1). The mean fraction of the organic shell composed of water (w_s) was 42.4% and a maximum of 99.9%. than biogenic components.

3.1.2 Comparison to Observed data

Figure 5 shows the $T_{g,org}$ T_{org}:T ratio calculated from speciated organic aerosol composition field data at the Centreville, Alabama field site (Zhang et al., 2018b) during the 2013 SOAS period. $T_{g,org}$ T_{org}:T ratio derived from data collected by Zhang et al. (2018b) ranged from ~ 0.63630 to 0.88881. Also shown in Fig. 5 are the predicted $T_{g,org}$ T_{org}:T ratios using the phase separation (*PhaseSep*) parameterization. CMAQ modeled $T_{g,org}$ T_{org}:T ratio using *PhaseSep* simulation ranged from ~ 0.53531 to 0.9902, slightly exceeding the range predicted from observations. It should be noted that the Zhang et al. (2018b) observations were recorded every four hours for ~ 60% of the 2013 SOAS time period. Modeled $T_{g,org}$ T_{org}:T mostly captures the peaks and drops, which the field observation--derived $T_{g,org}$ T_{org}:T shows (Fig. 5). Some mismatch can be attributed to the lack of an

explicit mechanism to compute organic aerosol water uptake in CMAQ and some unaccounted SOA formation mechanisms. Further, Zhang et al. (2018b) only accounted for ~ 70% of SOA species listed in Table 1. During this time period the model had a normalized mean bias (NMB) of 2.37% when compared to observationally calculated values. The Median and mean $T_{g,org}$ T_{org}:T ratio ratios predicted from the 2013 SOAS field observations was of 0.799 and 0.773 and was, respectively, were quite close to the corresponding value values of 0.784 and 0.769 predicted by *PhaseSep* simulation in CMAQ. The The difference in observed and model estimated $T_{g,org}$ T_{org}:T range compared to $T_{g,org}$:T range based on field observations at Centreville, AL for SOAS 2013 give was statistically significant with a P-Value = 0.001, and a correlation coefficient of ~ 0.66 between them. There is also a discernable consistent diurnal trend across the 2013 SOAS period for $T_{g,org}$ T_{org}:T, such as stronger contribution of aerosol liquid water for 18:00-08:00 hours and a lowering of the $T_{g,org}$ T_{org}:T during those hours (Fig. 3A and S1).

Massoli et al. (2018) reported the observed O:C at Centreville, AL during SOAS 2013 that ranged between ~ 0.5 to 1.4 and averaging at 0.91. Massoli et al. (2018) presents the first instance of ambient measurements with a NO_3^- CIMS in an isoprene-dominated environment and identified Organic nitrates or Organonitrates (ONs) originating from both isoprene and monoterpene to be a significant component of the NO_3^- CIMS spectra and dominating the observed SOA at Centreville throughout the day, reflecting daytime and nighttime formation pathways. Both isoprene- and monoterpene-derived ONs have very high O:C > 1 and accounting for up to 10% of total oxygen at Centreville site (Xu et al., 2015; Lee et al., 2016), explaining the high overall observed average O:C. Our modeled O:C at the Centerville, Alabama site during SOAS 2013 ranged between ~ 0.5 to 1 and averaging ~ 0.68. CMAQv5.2.1 with carbon bond chemistry (used in this study) uses *aero6* aerosol mechanism, without any explicit representation of formation pathways of isoprene and monoterpene-derived ONs. Specifically CMAQ with *aero6* significantly underestimates

monoterpene oxidation that accounts for ~ 50% of organic aerosol in the southeastern United States in summer (Zhang et al. 2018). Consideration of explicit monoterpene organic nitrates and updated monoterpene photoxidation yields in aero7 eliminates the CMAQ model-measurement bias (Xu et al. 2018). The lack of explicit organic nitrates here can explain the lack of high O:C (> 1) predictions in this work for the Centreville, Alabama Forest site during SOAS 2013 possibly leading to the low correlation of model estimated $T_{g,org}$:T with observations.

Figure 6 shows the predicted viscosity of our phase separation implementation for all days, grid cells and layers sorted into 10% RH bins. The trends in range of modeled η_{org} are the same as in Fig. 4B, with narrower ranges at lower RH and wider ranges with increasing RH. Wider η_{org} ranges in the~~at~~ higher RH bins can be explained by increased diffusivity with higher aerosol liquid water in SOA causing faster~~quick~~ mixing times leading to quick changes in composition. Furthermore, these contain the most atmospherically relevant RH ranges for the model simulation period. Therefore, a wide range of particle compositions is expected which also contributes to the wide range of predicted η_{org} values.~~often accompanied with drastic differences in composition.~~ Also, shown in Fig. 6 are viscosities of aerosols made in the laboratory. The red dots represent the viscosities of α-pinene SOA measured by Zhang et al. (2018a), and the blue box plots represent the range of viscosities of toluene SOA measured by Song et al. (2016). Both laboratory-based experimental studies show good agreement at atmospherically-relevant RH ranges with the viscosities predicted by our implementation. At lower RH ranges (~ 30%), the experimentally measured viscosities are slightly higher than those predicted by our study. This could~~can~~ be attributed to shattering of highly viscous SOA ($\eta_{org} \geq 10^6$ Pa·~~s~~s) for RH ≤ 30% that inhibits their flow in laboratory measurements of η_{org} (Renbaum-Wolff et al., 2013; Zhang et al., 2015; Zhang

et al., 2018a). Huang et al. (2018) speculates that differences in physicochemical properties of α-pinene SOA, including viscosity, can exhibit a "memory effect" of the conditions under which the particle formed. This is regardless of the subsequent conditions to which the particle is exposed. This could lead to differences between model-predicted and experimentally measured viscosities, as these memory effects are not well characterized. Grayson et al. (2016) reports that the viscosity of α-pinene SOA may vary as a function of the mass loading conditions with higher mass loading leading to lower viscosity measurements. Unfortunately, there is also a lack of experimental data on viscosity measurements at RH < 60%.

3.2 Impact on Model predictions

3.2.1 Reactive uptake coefficient of IEPOX (γ_{IEPOX})

Previous experimental studies show that phase separation forming semi-solid organic aerosol coatings is expected to decrease IEPOX reactive uptake (γ_{IEPOX}), and thus, the resulting SOA (Zhang et al., 2018a). Figure 7A shows reductions in γ_{IEPOX} with *Emission Reduction* sensitivity case subsequently reducing SOA (Fig. 10A), in agreement with recent modeling predictions that show emission reductions expected by 2025 lead to reductions in IEPOX SOA (Marais et al., 2016). This study implemented the phase separation and the phase separation parameters into CMAQ (*PhaseSep*), showing agreement with the previous experimental work (Zhang et al., 2018a), with the mean value of γ_{IEPOX} decreasing by~~to $1.141*10^{-3}$ or a~~ 18.3% decrease at the surface level, compared to the~~$1.397*10^{-3}$ in~~ original CMAQ with no phase separation considered (*NonPhaseSep*) (Fig. 7A).~~7A). Similarly, the median value of γ_{IEPOX} for the *PhaseSep* case reduced to $4.454*10^{-5}$ from $1.479*10^{-4}$ for *NonPhaseSep* simulation.~~ For southeastern United States, it is clear that an overall shift of higher γ_{IEPOX} values > 10^{-3} to lower

values ranging between 10^{-4} to 10^{-6} occurs with introduction of phase separation and phase state parameters in CMAQ (Fig. S1~~S2~~). For continental United States, there is a similar trend with the shift in highest peak of the probability distribution of γ_{IEPOX} with *PhaseSep* case relative to *NonPhaseSep* case (Fig. 7A).

Figures 7B and 7C show the mean value of γ_{IEPOX} for each grid cell across the continental United States during the *PhaseSep* and *NonPhaseSep* simulations, respectively, for the 2013 SOAS period. The plot shows an overall reduction in γ_{IEPOX} when phase separation was introduced. There was high variability in the value of γ_{IEPOX} between regions; specifically, between the eastern and western United States. To understand the drivers that influence changes in γ_{IEPOX} with the new *PhaseSep* simulation, grid cells that exhibited the maximum increase and decrease relative to the *NonPhaseSep* were analyzed. When phase separation was included, particles in grid cell and time-step with maximum reduction in γ_{IEPOX} were the result of a low $D_{org,eff}$ ~~-~~of 5.83·~~*~~10^{-19} m^2/s and an l_{org} as high as 100 nm resulting in a relatively thick organic coating with diffusion limitations. Particles in the grid cell and time-step with the highest increases in γ_{IEPOX} had a $D_{org,eff}$ value of 7.34·~~*~~10^{-16} m^2/s and l_{org} of 0.67~~668~~ nm, and were located over oceans with an abundant amount of aerosol liquid water that were in close proximity to biogenic isoprene emission sources (Fig. S2~~S3~~). These large increases in γ_{IEPOX} were primarily caused by increases in $k_{particle}$ due to added nucleophiles (i.e. abundant aerosol liquid water) and a lack of diffusive limitations through the organic shell. Mean γ_{IEPOX} for the 2013 SOAS period across the continental United States shows a higher reduction in the *PhaseSep* (Fig. 7B) relative to *NonPhaseSep* (Fig. 7C), in regions such as the southwest US and southern Canada, with higher l_{org} (Fig. S2~~S3~~). To summarize, phase (which influences $D_{org,eff}$) and thickness (l_{org}) of the organic coating are the main drivers of change in

γ_{IEPOX}. A recent study by Riva et al. (2019) demonstrated that the formation of organosulfates during the IEPOX reactive uptake process leads to an organic coating, and thus, a reduced γ_{IEPOX}. This manifests as a self-limiting effect during the IEPOX-derived SOA formation. Atmospheric models, including this work, do not consider this recently observed self-limiting process yet, but accounting for it may lead to a further reduction of the γ_{IEPOX}.~~,~~

3.2.2 Predicted SOA mass

Variability in the values of γ_{IEPOX}, as calculated in the *PhaseSep* simulation (Fig. 7B) relative to the *NonPhaseSep* simulation (Fig. 7C), were also reflected in the large geospatial variations in the concentrations of IEPOX-derived SOA (i.e., organosulfates and tetrols (Fig. 8A)). Higher reduction in the IEPOX-derived SOA for *PhaseSep* relative to *NonPhaseSep* were also in regions such as the southwest United States and southern Canada (more pronounced near the Great Lakes), with higher reductions to γ_{IEPOX} owing to thick organic coatings (Fig. S2~~S3~~). Figure 8B shows the average relative change in predicted biogenic SOA mass. Although, the southwest United States shows high reduction in IEPOX-derived SOA (Fig. 8A), it is not reflected for changes in biogenic SOA (Fig. 8B). While the high reduction in IEPOX-derived SOA (Fig. 8A) in southern Canada is reflected in reductions in biogenic SOA in that region (Fig. 8B). This spatial variability can be explained by the lower fraction of IEPOX-derived SOA in total biogenic SOA on average in southwest United States compared to their higher fraction in southern Canada near Great Lakes (Fig. S3A~~S4A~~), which are further reduced to be negligible in the southwest US in the *PhaseSep* case (Fig. S3B~~S4B~~). Hence, magnitude of changes in biogenic SOA (Fig. 8B) and eventually $PM_{2.5}$ organic carbon mass (Fig. S4~~S5~~) are dampened as compared to changes in IEPOX-derived SOA mass with introduction of phase separation parameters (Fig. 8A). On average, the largest reduction

659 in biogenic SOA mass at any one grid cell was 40.9% and occurred over forested region in Ontario,
660 Canada near Lake Superior (Fig. 8B) which also exhibits high IEPOX-derived SOA contribution
661 to total biogenic SOA (Fig. S3~~S4~~). For southeastern United States, modeled average reductions for
662 2013 SOAS period in IEPOX-derived SOA ranged between 25-30%, which translated to 10-15%
663 reduction in total biogenic SOA (Fig. 8). Whereas, the highest average reduction in IEPOX-
664 derived SOA was 74.06% that occurred over Colorado (Fig. 8A), which eventually matters less in
665 terms of overall biogenic SOA reduction (Fig. 8B) owing to negligible contribution of IEPOX-
666 derived SOA to total biogenic SOA in the American southwest (Fig. S3~~S4~~). In the southern
667 Canadian region near the Great Lakes where the maximum biogenic SOA reduction in *PhaseSep*
668 occurred, the average reductions in IEPOX-derived SOA ranged from 63% to 66%. The southern
669 Canadian region with maximum biogenic SOA reduction had average particle viscosities in the
670 range of $1.3 \cdot * 10^3$ to $8.36 \cdot * 10^5$ Pa·s. The phase separation frequency of particles for southern
671 Canada region was 86.3% of all time steps and was SSPS 62.04% of the time and LLPS 24.26%
672 of the time. The combination of these factors led to a 52.64% average reduction in γ_{IEPOX}.

673 **3.2.2.1 Comparison to Observed Data**

674 Figure 9 shows that consideration of phase state and separation in CMAQ slightly worsened
675 the NMB based on comparison with hourly $PM_{2.5}$ organic carbon mass SEARCH observations at
676 both the Centreville rural site and Jefferson street, Atlanta urban site by ~ -4%. However, this
677 change was marginal in terms of mean bias change in *PhaseSep* relative to *NonPhaseSep* case
678 being < 0.1 μg/m^3. The sensitivity cases that assumed a higher H_{org} (*HighHorg*) and considered
679 LLPS in predicting SSPS (*PhaseSep2*) resulted in correcting the worsening of model performance
680 observed with *PhaseSep* case (Fig~~Figs~~. 9 and Table S1~~S6~~). This highlights the importance of

poorly constrained parameters in models like H_{org} assumed as a constant and factors that might govern phase separation under low RH or low aerosol water at different O:C ratios.

3.3 Sensitivities

The reduction in emission sources of NO_x and SO_2 impacted aerosol composition, and thus, the $T_{g,org}$~~T_{org}~~. The average $T_{g,org}$~~T_{org}~~ for the emissions reduction simulation predicted a small but statistically significant (p-value = $2 \cdot 10^{-16}$) increase of 1.5 K from the *PhaseSep* simulation, indicating the future emission reductions could result in minor increases~~an increase~~ in viscosity and frequency of phase separation. The overall phase separation frequency for this sensitivity was 70.5% (57.0% SSPS, 13.5% LLPS) with predicted viscosities ranging from $6.13 \cdot 10^{-3}$ to $1.73 \cdot 10^{11}$ Pa·s, which was slightly narrower as compared to η_{org} range from *PhaseSep* simulation (refer to section 3.1.1). With the implementation of the future NO_x and SO_2 emissions reductions, overall there was a mean 7.85% reduction in biogenic SOA at the surface level from the *PhaseSep* simulation for Continental United States. As shown in Figure 10A the areas with the largest reductions in SOA mass occurred in American southeast, while a marginal increase in SOA mass that occurred over the Atlantic Ocean and in some sparse areas in Northern Canada and Western United States. The American southeast was highly sensitive to the Emissions Reductions sensitivity due to the high concentrations of SO_2 from coal-fired power plants and the high concentrations of IEPOX-derived SOA, whose chemistry is driven by particulate sulfate. Fig. S5~~S7~~ shows that highest reductions in particulate sulfate occurs in the American southeast, which would be accompanied by the reduction in aerosol liquid water, driving the reductions in IEPOX-derived SOA as shown in recent literature (Pye et al., 2017), and hence the large reductions in biogenic SOA mass. Also, NO_x reductions in the NO_x-limited southeastern United States region essentially

results in stronger decrease in biogenic SOA as shown by Fig. 10A, which is consistent with findings from SENEX aircraft (Edwards et al., 2017) and SOAS ground measurements (Xu et al., 2015) in the southeastern United States.

When increases in H_{org} were simulated in scenario *HighHorg* it had impacts in opposite directions compared to changes in the emission reduction scenario. This increase in biogenic SOA can simply be attributed to the increased dissolution of IEPOX into the particle phase through the organic coating with a three order of magnitude higher H_{org} relative to that in *PhaseSep* simulation. The average $T_{g,org}$~~T_{org}~~ in the *HighHorg* simulation had a similarly small but also statistically significant increase of 1.4 K, with particles being phase-~~-~~separated 68.3% of the time (55.8% SSPS, 12.5% LLPS). Predicted viscosities in this simulation were comparable to the *PhaseSep* simulation and ranged from 5.94·~~*~~10^{-3} Pa·s to 6.10^{11} Pa·s. Overall, biogenic SOA mass increased by an average of 14.19% at the surface level for this simulation relative to *PhaseSep* for the Continental United States. As shown in Figure 10B, the regions with the largest increases in biogenic SOA mass were located over boreal forests in Ontario and Quebec, Canada that correspond to the regions with highest reactive uptake (Figs. 7B and 7C) forming more homogenous SOA with increased H_{org}.

The removal of the assumption that all particles with a semisolid viscosity were phase-separated (*PhaseSep2*) decreased the overall phase separation frequency to 42.7~~29.0~~% from 68.5% in the *PhaseSep* simulation. The entirety of this reduction was from reductions in SSPS i.e. 29.0% from 54.8% in *PhaseSep*.~~-~~ Figure 10C gives the changes in biogenic SOA mass yields in the *PhaseSep2* case relative to the *PhaseSep* case, with largest increases in Canadian regions where SSPS regime is moving to either LLPS or homogenous liquid mixture. This causes SOA yield

increases explained by high reactive uptake in these regions (Figs. 7B and 7C). The phase separation frequency at the Centreville, Alabama site decreased to 65.4% from 79.3%, which is still in agreement with the values reported by Pye et al. (2017).~~%.~~ The average $T_{g,org}$~~T_{org}~~ increased by 2.3 K with a range of 137 K to 289 K and predicted viscosities were slightly higher but on a similar order of magnitude to the *PhaseSep* simulation and ranged from 5.93·~~*~~10^{-3} Pa·~~▲~~s- 9.99·~~*~~10^{11} Pa·~~▲~~s. Overall biogenic SOA mass yields increased by an average of 25.86% from the *PhaseSep* simulation for Continental United States. The initial assumption regarding phase separation at high viscosity seems to be similarly as important as the assumption regarding H_{org} in constraining the impact of phase state and morphology on reactive uptake of IEPOX. Table S1 shows a modest 4% improvement in model performance for total $PM_{2.5}$ OC mass, in the isoprene-abundant southeastern United States with *PhaseSep2*. The range of phase separation frequency in semi-solid particles is still wide when compared to other cases i.e. 29-55.8% SSPS. Increased frequency of bulk phase in semi-solid conditions in *PhaseSep2* relative to *PhaseSep* causes much less resistance to reactive uptake, closer to but still more than in *NonPhaseSep*. This is reflected in the similarity of γ_{IEPOX} between *PhaseSep2* and *NonPhaseSep* (Fig. 7C and Fig. S6). Hence, a very marginal difference in IEPOX SOA and biogenic SOA in *PhaseSep2* relative to *NonPhaseSep* occurs (Fig. S6), unlike much higher differences observed in *PhaseSep* (Fig. 8).

While modest improvement in model performance of $PM_{2.5}$ OC by aforementioned sensitivity simulations (*HighHorg* and *PhaseSep2*- see section 3.2.2.1) occurs, it does not addresses other major issues in the base CMAQ model performance. Firstly, these updates to phase state and phase separation considerations only translate to IEPOX SOA, the only explicit parametrization of multiphase reactive uptake in CMAQ. IEPOX SOA also just makes up approximately 12% of the

total $PM_{2.5}$ OC mass simulated by CMAQ on an average for SOAS 2013 period. There are other more important factors introducing major source of uncertainty in models across spatial scales including CMAQ. A very prominent uncertainty being missing representation of species like ONs reported as dominant in SOAS 2013 by new instrumentation providing higher molecular detail (Lee et al., 2016b; Massoli et al., 2018). Furthermore, field or laboratory studies on a wider suit of SOA are needed to explicitly parametrize their multiphase chemistry and are still missing in CMAQ. It is a challenge to implement these mechanistic representations of different SOA holistically, without increased computational cost in CMAQ.

4 Discussion and Atmospheric Implications

Current chemical transport models have not accurately accounted for the effects of aerosol composition on phase separation or viscosity. This work has updated the CMAQ model to include parameters to calculate the $T_{g,org}$~~T_{org}~~ based on the Gordon-Taylor equation for SOA. This implementation used molar mass and O:C ratio of the species, but other parameters could be used. For example, DeRieux et al., (2018) developed a calculation for $T_{g,i}$ based on the number of carbon-hydrogen and carbon-oxygen bonds in a molecule. DeRieux et al., (2018) showed their implementation to be in good agreement with implementation provided in this work (Eq. (4)) for species with molar masses in the range of those used by CMAQv5.2.1. This implementation also included parameters to determine whether SOA was phase-separated based on its viscosity, O:C ratio, sulfate concentrations, and the ambient RH. Our model predicted that 68.5% of the time particles would exhibit phase separation at the surface layer, which is in proximity with the 70% predicted by Pye et al. (2017). This implementation predicts that most of the SOA in the middle and upper troposphere over the United States is phase-separated with organics increasingly in a

semi-solid or even glassy state with increasing altitude. This is in agreement with previous fieldwork and modeling studies which has found that SOA in the upper troposphere tends to be in a glassy state (Lienhard et al., 2015; Shiraiwa et al., 2017). This work also shows LLPS to be more dominant in the eastern US, while semi-solid phase state being more prevalent in western US. This is in agreement with the predominant role of aerosol liquid water driving the liquid phase state and LLPS across the eastern United States, as observed in previous studies (Pye et al., 2017, 2018).

The model predicted that SOA dominated by anthropogenic constituents typically featured thick semi-solid organic coatings~~phases~~ surrounding aqueous cores, which caused the reactive uptake of IEPOX to become diffusion limited. Regions that were predicted to have larger fractions of biogenic SOA mass typically featured LLPS morphology that did not produce much of diffusion limitations. These aerosols also resulted in a smaller inorganic core volume increasing the concentrations of nucleophiles and acids, thus enhancing the rate of reaction in presence of abundant aerosol water over oceans, but exhibited reduction in SOA over land though not as much as solid-like particles exhibited. The phase separation parameters had the largest impact over the Ohio River valley, southern Canada (more pronounced near Great Lakes) and American southeast. These areas were also the most sensitive to future emission reductions of NO_x and SO_2.

Further experimental and modeling work is required to understand the effects of aerosol phase state on the viscosity of the inorganic core that cause variability in the value of D_a and can subsequently alter the reactive uptake of IEPOX. Combined effect of aerosol acidity and aforementioned higher core viscosity because of IEPOX SOA formation that has a self-limiting impact on IEPOX reactive uptake is also a caveat to be explored further (Zhang et al., 2019). The

Formatted: French (Canada)

Formatted: French (Canada)

Formatted: French (Canada)

Field Code Changed

Field Code Changed

conditions under which highly viscous SOA will separate from inorganics in a particle or if the particle will remain homogenously mixed should be further explored as well, given the differences in the frequency of predicted particle-phase separation between the *PhaseSep* and *PhaseSep2* simulations and the implications that this has for the reactive uptake of IEPOX (Table S1). Constraining the viscosity of SOA in low RH (< 30%) conditions is also an area that should be further explored to improve model performance. Furthermore, particle~~. Particle~~ morphology in case of phase-separated organic and inorganic species as 'core-shell' or 'partially engulfed' or 'emulsified' (smaller islands of organics in the aqueous inorganic core) is driven by the differences in the interfacial surface tensions (Gorkowski et al., 2017). However developing a computationally efficient method of modeling these alternative particle morphologies in CTMs is an area of ongoing research and needs further exploration. Recent studies have also shown that at very high RH ranges (95-100%), some particles will return to a core-shell morphology (Ham et al., 2019; Renbaum-Wolff et al., 2016). There is also little information on the criteria that drive a particle to adopt a~~drives this kind of~~ phase-separated morphology under these conditions~~ separation as well~~. Such variability in particle morphologies may modify the value of $k_{particle}$ by changing the core volume. It is imperative that these parameters be better constrained in models. Furthermore, there is much uncertainty in the organic shell~~phase~~ Henry's Law coefficient (H_{org}), where higher H_{org} increases the dissolution of IEPOX into the aerosol~~ phase~~. Some of the newly proposed reaction mechanisms leading to the formation of extremely-low volatile organic compounds (ELVOCs) and organosulfates may also increase the viscosity of the particle~~ phase~~, but have not been incorporated in this study.

This work paves the way for implementing a more accurate representation of multiphase chemistry of different complex systems on the lines of explicit representation of IEPOX SOA. Multiphase chemistry of other dominant SOA apart from IEPOX SOA, such as monoterpene-derived SOA and ONs derived from both isoprene and monoterpenes, are not incorporated in CMAQv5.2.1 (Pye et al., 2018; Slade et al., 2019), and should be a focus of future work. This work showed that organic water fraction is the biggest driver of viscosity, though the water abundance was set at a constant 10% of the inorganic water content to better reflect observed concentrations of organic water during daylight hours relevant to IEPOX SOA chemistry.~~.~~ Organic water uptake, even if higher than the amount assumed here~~increased~~, will still follow the diurnal trend of RH since it is diverted from the aqueous core that is derived from ISORRORPIA-based aerosol water in CMAQ v5.2.1. In this work, the O:C ratio of individual organic constituents as listed in Table 1 was used to calculate $T_{g,org}$ based on Shiraiwa et al. (2017). The O:C provides an indication of hygroscopocity of different organic species (Pye et al., 2017), but it is only a surrogate. Lack of explicitly representing ~~It does not, however, consider the~~ hydrophobicity or hygroscopic growth~~abundance~~ of various organic constituents is a limitation in the CMAQ modeling framework that was used. More recently, degree of diffusivity or ~~. Constraining abundance of organic water~~ uptake of semivolatile organic compounds (SVOCs) such as isoprene oxidation products and ONs in to more viscous or semi-solid particle-phase are found to differ. These changes in η_{org} profoundly impacts both aerosol growth kinetics and their size distribution dynamics (Vander Wall et al., 2020; Zaveri et al., 2020). To assess the actual impacts of aging and hygroscopic growth under varying conditions updates in the CMAQ model are required by adding explicit reactive uptake mechanisms~~in terms of its association with different organic species and~~

~~evaluating its reduction with future emission reductions of SO_x (SO_2 and sulfate) will be pertinent~~ for a wider range of non-IEPOX SOAs ~~future work~~.

Performing sensitivity simulations over the *PhaseSep* parametrization as part of this work also show that any assumptions made on determining phase separation or morphology (*PhaseSep2*) is as important as constraining the H_{org} ($High H_{org}$) factor in the regions with abundant IEPOX SOA such as, American and Canadian southeast. Incorporating explicit kinetics coupled with thermodynamic calculation of energies governing the mixing state of organic-inorganic aerosol mixtures under different aerosol phase states, as observed from recent and ongoing experimental findings, into atmospheric models such as CMAQ, would lead to more scientifically sound representations of the impact particle phase state and morphology have on SOA mass predictions.

Code availability

US EPA makes the source code of CMAQ version 5.2.1 model publicly available for download at: https://github.com/USEPA/CMAQ/tree/5.2.1 (last access: 6 November 2019). Corresponding author can make the modifications made to the CMAQ source code as part of this work available on request.

Data availability

The emissions and meteorological inputs along with other miscellaneous inputs to run CMAQ model for the SOAS 2013 episode (1 June 2013 to 15 July 2015) across continental United States can be downloaded from: https://drive.google.com/open?id=1XR6Xp3bZzrZIzNBx-

AgjcNCtC_HLlCkZ, made available by US EPA and University of North Carolina-Institute of Environment (last access: 6 November 2019).

Author contributions

RS and QZR lead the writing with WV. RS designed the new *PhaseSep* methodology along with sensitivity cases to run in consistent consultation with YZ, HOTP, YC, JDS, QZR and WV. QZR implemented the model code and performed the simulations in the regional scale model with reviews from HOTP. RS analyzed results of simulations with QZR, WV and HZ. BHL~~, CM~~, FDL-H, JAT, AHG and HZ analyzed the SOAS field data. RS and QZR prepared the paper with extensive reviews and edits from WV, YZ, YC, HOTP, HZ, and JDS.

Competing interests

The authors declare that they have no conflict of interest.

Disclaimer: The U.S. Environmental Protection Agency through its Office of Research and Development collaborated in the research described here. The research has been subjected to Agency administrative review and approved for publication but may not necessarily reflect official Agency policy. The views expressed in this article are those of the authors and do not necessarily represent the views or policies of the U.S. Environmental Protection Agency.

Acknowledgements

A National Science Foundation (NSF) Postdoctoral Fellowship under Atmospheric and Geospace Sciences (AGS-1524731) and the National Institute of Health (NIH) training grant supported YZ.

HZ and AHG were supported by NSF Grants AGS-1250569 and AGS-1644406. BHL, FDL, CM, and JAT were supported by a grant from the U.S. Department of Energy Atmospheric System Research Program (DE-SC0018221). JDS, YC, and YZ were supported by NSF-AGS grant 1703535. Claudia Mohr (Department of Atmospheric Sciences, University of Washington, Seattle, WA; Currently at: Department of Environmental Science and Analytical Chemistry, Stockholm University, SE-106 91 Stockholm, Sweden) and Anna Lutz (Department of Chemistry and Molecular Biology, University of Gothenberg, SE-41296 Gothenberg, Sweden) are acknowledged for providing the FIGAERO-CIMS measurements from the SOAS 2013 campaign.

References

Eyth, A., Zubrow, A., and Mason, R: Technical Support Document (TSD): Preparation of Emissions Inventories for the Version 6.1, 2011 Emissions Modeling Platform, [online] Available from: http://www.epa.gov/ttn/chief/emch/2011v6/2011v6.1_2018_2025_base_EmisMod_TSD_nov2014_v6.pdf (Accessed 20 November 2018), 2014.

Anttila, T., Kiendler-Scharr, A., Tillmann, R. and Mentel, T. F.: On the Reactive Uptake of Gaseous Compounds by Organic-Coated Aqueous Aerosols: Theoretical Analysis and Application to the Heterogeneous Hydrolysis of N2O5, J. Phys. Chem. A, 110(35), 10435–10443, doi:10.1021/jp062403c, 2006.

Appel, K. W., Napelenok, S. L., Foley, K. M., Pye, H. O. T., Hogrefe, C., Luecken, D. J., Bash, J. O., Roselle, S. J., Pleim, J. E., Foroutan, H., Hutzell, W. T., Pouliot, G. A., Sarwar, G., Fahey, K. M., Gantt, B., Gilliam, R. C., Heath, N. K., Kang, D., Mathur, R., Schwede, D. B., Spero, T. L., Wong, D. C. and Young, J. O.: Description and evaluation of the Community Multiscale Air Quality (CMAQ) modeling system version 5.1, Geosci Model Dev, 10(4), 1703–1732, doi:10.5194/gmd-10-1703-2017, 2017.

Bash, J. O., Baker, K. R. and Beaver, M. R.: Evaluation of improved land use and canopy representation in BEIS v3.61 with biogenic VOC measurements in California, Geoscientific Model Development, 9(6), 2191–2207, doi:https://doi.org/10.5194/gmd-9-2191-2016, 2016.

Bates, K. H., Crounse, J. D., St. Clair, J. M., Bennett, N. B., Nguyen, T. B., Seinfeld, J. H., Stoltz, B. M. and Wennberg, P. O.: Gas Phase Production and Loss of Isoprene Epoxydiols, J. Phys. Chem. A, 118(7), 1237–1246, doi:10.1021/jp4107958, 2014.

914 Bateman, A. P., Bertram, A. K., and Martin, S. T.: Hygroscopic Influence on the Semisolid-to-
915 Liquid Transition of Secondary Organic Materials, The Journal of Physical Chemistry A, 119,
916 4386-4395, 10.1021/jp508521c, 2015a.

917 Bateman, A. P., Gong, Z., Liu, P., Sato, B., Cirino, G., Zhang, Y., Artaxo, P., Bertram, A. K.,
918 Manzi, A. O., Rizzo, L. V., Souza, R. A. F., Zaveri, R. A., and Martin, S. T.: Sub-micrometre
919 particulate matter is primarily in liquid form over Amazon rainforest, Nature Geoscience, 9, 34,
920 10.1038/ngeo2599~~, 2015b.~~
921
922 ~~https://www.nature.com/articles/ngeo2599#supplementary-information, 2015b.~~

923 Bertram, A. K., Martin, S. T., Hanna, S. J., Smith, M. L., Bodsworth, A., Chen, Q., Kuwata, M.,
924 Liu, A., You, Y., and Zorn, S. R.: Predicting the relative humidities of liquid-liquid phase
925 separation, efflorescence, and deliquescence of mixed particles of ammonium sulfate, organic
926 material, and water using the organic-to-sulfate mass ratio of the particle and the oxygen-to-
927 carbon elemental ratio of the organic component, Atmos. Chem. Phys., 11, 10995-11006,
928 10.5194/acp-11-10995-2011, 2011.

929 Bondy, A. L., Craig, R. L., Zhang, Z., Gold, A., Surratt, J. D. and Ault, A. P.: Isoprene-Derived
930 Organosulfates: Vibrational Mode Analysis by Raman Spectroscopy, Acidity-Dependent
931 Spectral Modes, and Observation in Individual Atmospheric Particles, J Phys Chem A, 122(1),
932 303–315, doi:10.1021/acs.jpca.7b10587, 2018.

933 Budisulistiorini, S. H., Baumann, K., Edgerton, E. S., Bairai, S. T., Mueller, S., Shaw, S. L.,
934 Knipping, E. M., Gold, A. and Surratt, J. D.: Seasonal characterization of submicron aerosol
935 chemical composition and organic aerosol sources in the southeastern United States: Atlanta,
936 Georgia,and Look Rock, Tennessee, Atmospheric Chemistry and Physics, 16(8), 5171–5189,
937 doi:https://doi.org/10.5194/acp-16-5171-2016, 2016.

938 Budisulistiorini, S. H., Nenes, A., Carlton, A. G., Surratt, J. D., McNeill, V. F. and Pye, H. O. T.:
939 Simulating Aqueous-Phase Isoprene-Epoxydiol (IEPOX) Secondary Organic Aerosol Production
940 During the 2013 Southern Oxidant and Aerosol Study (SOAS), Environ. Sci. Technol., 51(9),
941 5026–5034, doi:10.1021/acs.est.6b05750, 2017.

942 Carlton, A. G. and Baker, K. R.: Photochemical Modeling of the Ozark Isoprene Volcano:
943 MEGAN, BEIS, and Their Impacts on Air Quality Predictions, Environ. Sci. Technol., 45(10),
944 4438–4445, doi:10.1021/es200050x, 2011.

945 Carslaw, K. S., Lee, L. A., Reddington, C. L., Pringle, K. J., Rap, A., Forster, P. M., Mann, G.
946 W., Spracklen, D. V., Woodhouse, M. T., Regayre, L. A. and Pierce, J. R.: Large contribution of
947 natural aerosols to uncertainty in indirect forcing, Nature, 503(7474), 67–71,
948 doi:10.1038/nature12674, 2013.

949 Chenyakin, Y.: Are diffusion coefficients calculated using the Stokes-Einstein equation
950 combined with viscosities consistent with measured diffusion coefficients of tracer organics
951 within organics-water mediums?, University of British Columbia., doi: 10.14288/1.0166352
952 2015.

Cui, T., Zeng, Z., dos Santos, E. O., Zhang, Z., Chen, Y., Zhang, Y., Rose, C. A., Budisulistiorini, S. H., Collins, L. B., Bodnar, W. M., de Souza, R. A. F., Martin, S. T., Machado, C. M. D., Turpin, B. J., Gold, A., Ault, A. P., and Surratt, J. D.: Development of a hydrophilic interaction liquid chromatography (HILIC) method for the chemical characterization of water-soluble isoprene epoxydiol (IEPOX)-derived secondary organic aerosol, Environmental Science: Processes & Impacts, 20, 1524-1536, 10.1039/C8EM00308D, 2018.

DeRieux, W.-S. W., Li, Y., Lin, P., Laskin, J., Laskin, A., Bertram, A. K., Nizkorodov, S. A. and Shiraiwa, M.: Predicting the glass transition temperature and viscosity of secondary organic material using molecular composition, Atmospheric Chemistry and Physics, 18(9), 6331–6351, doi: 0https://doi.org/10.5194/acp-18-6331-2018, 2018.

Docherty, K. S., Stone, E. A., Ulbrich, I. M., DeCarlo, P. F., Snyder, D. C., Schauer, J. J., Peltier, R. E., Weber, R. J., Murphy, S. M., Seinfeld, J. H., Grover, B. D., Eatough, D. J. and Jimenez, J. L.: Apportionment of primary and secondary organic aerosols in southern California during the 2005 study of organic aerosols in riverside (SOAR-1), Environ. Sci. Technol., 42(20), 7655–7662, doi: 10.1021/es8008166, 2008.

Eddingsaas, N. C., VanderVelde, D. G., and Wennberg, P. O.: Kinetics and products of the acid-catalyzed ring-opening of atmospherically relevant butyl epoxy alcohols, The Journal of Physical Chemistry A, 114, 8106-8113, doiDOI: 10.1021/jp103907c, 2010.

Edwards, P. M., Aikin, K. C., Dube, W. P., Fry, J. L., Gilman, J. B., de Gouw, J. A., Graus, M. G., Hanisco, T. F., Holloway, J., Hübler, G., Kaiser, J., Keutsch, F. N., Lerner, B. M., Neuman, J. A., Parrish, D. D., Peischl, J., Pollack, I. B., Ravishankara, A. R., Roberts, J. M., Ryerson, T. B., Trainer, M., Veres, P. R., Wolfe, G. M., Warneke, C., and Brown, S. S.: Transition from high- to low-NOx control of night-time oxidation in the southeastern US, Nature Geoscience, 10, 490, doi: 10.1038/ngeo2976 ,, https://www.nature.com/articles/ngeo2976#supplementary-information, 2017.

Emery, C., Jung, J., Koo, B. and Yarwood, G.: Improvements to CAMx Snow Cover Treatments and Carbon Bond Chemical Mechanism for Winter Ozone. Final report for Utah DAQ, Utah Department of Air Quality., 2015.

Evoy, E., Maclean, A. M., Rovelli, G., Li, Y., Tsimpidi, A. P., Karydis, V. A., Kamal, S., Lelieveld, J., Shiraiwa, M., Reid, J. P., and Bertram, A. K.: Predictions of diffusion rates of large organic molecules in secondary organic aerosols using the Stokes–Einstein and fractional Stokes–Einstein relations, Atmos. Chem. Phys., 19, 10073-10085, doi: 10.5194/acp-19-10073-2019, 2019.

Freedman, M. A.: Phase separation in organic aerosol, Chem. Soc. Rev., 46(24), 7694–7705, doi:10.1039/C6CS00783J, 2017.

Fulcher, G. S.: Analysis of recent measurements of viscosity of glasses, J. Amer. Ceram. Soc, 8, 339–355, doi: 10.1111/j.1151-2916.1925. ,1925.

Gaston, C. J., Riedel, T. P., Zhang, Z., Gold, A., Surratt, J. D. and Thornton, J. A.: Reactive Uptake of an Isoprene-Derived Epoxydiol to Submicron Aerosol Particles, Environmental Science & Technology, 48(19), 11178–11186, doi:10.1021/es5034266, 2014.

Gordon, M. and Taylor, J.: Ideal Copolymers and the Second-Order Transitions of Synthetic Rubbers. I. Non-Crystalline Copolymers, Journal of Applied Chemistry, 2(9), 493–500, doi:10.1002/jctb.5010020901, 1952.

Gorkowski, K., Donahue, N. M. and Sullivan, R. C.: Emulsified and liquid–liquid phase-separated states of α-pinene secondary organic aerosol determined using aerosol optical tweezers, Environmental Science & technology, 51(21), 12154-12163, doi:10.1021/acs.est.7b03250, 2017.

Grandey, B. S., Rothenberg, D., Avramov, A., Jin, Q., Lee, H.-H., Liu, X., Lu, Z., Albani, S. and Wang, C.: Effective radiative forcing in the aerosol–climate model CAM5.3-MARC-ARG, Atmospheric Chemistry and Physics, 18(21), 15783–15810, doi:10.5194/acp-18-15783-2018, 2018.

Grayson, J. W., Zhang, Y., Mutzel, A., Renbaum-Wolff, L., Böge, O., Kamal, S., Herrmann, H., Martin, S. T. and Bertram, A. K.: Effect of varying experimental conditions on the viscosity of <i>α</i>-pinene derived secondary organic material, Atmospheric Chemistry and Physics, 16(10), 6027–6040, doi:10.5194/acp-16-6027-2016, 2016.

Grayson, J. W., Evoy, E., Song, M., Chu, Y., Maclean, A., Nguyen, A., Upshur, M. A., Ebrahimi, M., Chan, C. K., Geiger, F. M., Thomson, R. J. and Bertram, A. K.: The effect of hydroxyl functional groups and molar mass on the viscosity of non-crystalline organic and organic-water particles, Atmospheric Chemistry and Physics, 17(13), 8509–8524, doi:10.5194/acp-17-8509-2017, 2017.

Guenther, A., Karl, T., Harley, P., Wiedinmyer, C., Palmer, P. I. and Geron, C.: Estimates of global terrestrial isoprene emissions using MEGAN (Model of Emissions of Gases and Aerosols from Nature), Atmospheric Chemistry and Physics, 6(11), 3181–3210, doi: ~~https://doi.org/~~10.5194/acp-6-3181-2006, 2006.

Guo, H., Xu, L., Bougiatioti, A., Cerully, K. M., Capps, S. L., Hite, J. R., Carlton, A. G., Lee, S.-H., Bergin, M. H., Ng, N. L., Nenes, A. and Weber, R. J.: Fine-particle water and pH in the southeastern United States, Atmospheric Chemistry and Physics, 15(9), 5211–5228, doi:10.5194/acp-15-5211-2015, 2015.

Ham, S., Babar, Z. B., Lee, J., Lim, H. and Song, M.: Liquid-liquid phase separation in secondary organic aerosol particles produced from α-pinene ozonolysis and α-pinene photo-oxidation with/without ammonia, Atmos. Chem. Phys. Discuss., 1–27, doi:10.5194/acp-2019-19, 2019.

Hansen, D. A., Edgerton, E. S., Hartsell, B. E., Jansen, J. J., Kandasamy, N., Hidy, G. M. and Blanchard, C. L.: The Southeastern Aerosol Research and Characterization Study: Part 1—

Overview, Journal of the Air & Waste Management Association, 53(12), 1460–1471, doi:10.1080/10473289.2003.10466318, 2003.

Heath, N. K., Pleim, J. E., Gilliam, R. C. and Kang, D.: A simple lightning assimilation technique for improving retrospective WRF simulations, Journal of Advances in Modeling Earth Systems, 8(4), 1806–1824, doi:10.1002/2016MS000735, 2016.

Hildebrant Ruiz, L. and Yarwood, G.: Interactions between Organic Aerosol and NOy: Influence on Oxidant Production., University of Texas at Austin. [online] Available from: http://aqrp.ceer.utexas.edu/projectinfoFY12_13/12-012/12-012%20Final%20Report.pdf, 2013.

Huang, W., Saathoff, H., Pajunoja, A., Shen, X., Naumann, K.-H., Wagner, R., Virtanen, A., Leisner, T. and Mohr, C.: α-Pinene secondary organic aerosol at low temperature: chemical composition and implications for particle viscosity, Atmospheric Chemistry and Physics, 18(4), 2883–2898, doi:~~https://doi.org/~~10.5194/acp-18-2883-2018, 2018.

Hwang, S.-H., Lee, J. Y., Yi, S.-M. and Kim, H.: Associations of particulate matter and its components with emergency room visits for cardiovascular and respiratory diseases, PLOS ONE, 12(8), e0183224, doi:10.1371/journal.pone.0183224, 2017.

Jacobs, M. I., Burke, W. J. and Elrod, M. J.: Kinetics of the reactions of isoprene-derived hydroxynitrates: gas phase epoxide formation and solution phase hydrolysis, Atmospheric Chemistry and Physics, 14(17), 8933–8946, doi: 0~~https://doi.org/10~~.5194/acp-14-8933-2014, 2014.

Jaques, P. A. and Kim, C. S.: Measurement of total lung deposition of inhaled ultrafine particles in healthy men and women, Inhal Toxicol, 12(8), 715–731, doi:10.1080/08958370050085156, 2000.

Koop, T., Bookhold, J., Shiraiwa, M. and Pöschl, U.: Glass transition and phase state of organic compounds: dependency on molecular properties and implications for secondary organic aerosols in the atmosphere, Phys. Chem. Chem. Phys., 13(43), 19238–19255, doi:10.1039/C1CP22617G, 2011.

Krechmer, J. E., Coggon, M. M., Massoli, P., Nguyen, T. B., Crounse, J. D., Hu, W., Day, D. A., Tyndall, G. S., Henze, D. K., Rivera-Rios, J. C., Nowak, J. B., Kimmel, J. R., Mauldin, R. L., Stark, H., Jayne, J. T., Sipilä, M., Junninen, H., Clair, J. M. S., Zhang, X., Feiner, P. A., Zhang, L., Miller, D. O., Brune, W. H., Keutsch, F. N., Wennberg, P. O., Seinfeld, J. H., Worsnop, D. R., Jimenez, J. L. and Canagaratna, M. R.: Formation of Low Volatility Organic Compounds and Secondary Organic Aerosol from Isoprene Hydroxyhydroperoxide Low-NO Oxidation, Environ. Sci. Technol., 49(17), 10330–10339, doi:10.1021/acs.est.5b02031, 2015.

Lee, L. A., Reddington, C. L. and Carslaw, K. S.: On the relationship between aerosol model uncertainty and radiative forcing uncertainty, PNAS, 113(21), 5820–5827, doi:10.1073/pnas.1507050113, 2016a~~2016~~.

Lee, B. H.; Mohr, C.; Lopez-Hilfiker, F. D.; Lutz, A.; Hallquist, M.; Lee, L.; Romer, P.; Cohen, R. C.; Iyer, S.; Kurtén, T.; Hu, W.; Day, D. A.; Campuzano-Jost, P.; Jimenez, J.-L.; Xu, L.; Ng,

N. L.; Guo, H.; Weber, R. J.; Wild, R. J.; Brown, S. S.; Koss, A.; de Gouw, J.; Olson, K.; Goldstein, A. H.; Seco, R.; Kim, S.; McAvey, K.; Shepson, P. B.; Starn, T.; Baumann, K.; Edgerton, E. S.; Liu, J.; Shilling, J. E.; Miller, D. O.; Brune, W. H.; Schobesberger, S.; D'Ambro, E. L.; Thornton, J. A.: Highly functionalized organic nitrates in the southeast United States: Contribution to secondary organic aerosol and reactive nitrogen budgets. *Proc. Natl. Acad. Sci. U. S. A.*, *113* (6), 1516– 1521, 2016b.

Liao, J., Froyd, K. D., Murphy, D. M., Keutsch, F. N., Yu, G., Wennberg, P. O., St Clair, J. M., Crounse, J. D., Wisthaler, A., Mikoviny, T., Jimenez, J. L., Campuzano-Jost, P., Day, D. A., Hu, W., Ryerson, T. B., Pollack, I. B., Peischl, J., Anderson, B. E., Ziemba, L. D., Blake, D. R., Meinardi, S. and Diskin, G.: Airborne measurements of organosulfates over the continental U.S, J Geophys Res Atmos, 120(7), 2990–3005, doi:10.1002/2014JD022378, 2015.

Lienhard, D. M., Huisman, A. J., Krieger, U. K., Rudich, Y., Marcolli, C., Luo, B. P., Bones, D. L., Reid, J. P., Lambe, A. T., Canagaratna, M. R., Davidovits, P., Onasch, T. B., Worsnop, D. R., Steimer, S. S., Koop, T. and Peter, T.: Viscous organic aerosol particles in the upper troposphere: diffusivity-controlled water uptake and ice nucleation?, Atmospheric Chemistry and Physics, 15(23), 13599–13613, doi:~~https://doi.org/~~10.5194/acp-15-13599-2015, 2015.

Lopez-Hilfiker, F. D., Mohr, C., D'Ambro, E. L., Lutz, A., Riedel, T. P., Gaston, C. J., Iyer, S., Zhang, Z., Gold, A., Surratt, J. D., Lee, B. H., Kurten, T., Hu, W. W., Jimenez, J., Hallquist, M., and Thornton, J. A.: Molecular Composition and Volatility of Organic Aerosol in the Southeastern U.S.: Implications for IEPOX Derived SOA, Environmental Science & Technology, 50, 2200-2209, 10.1021/acs.est.5b04769, 2016.

Maclean, A. M., Butenhoff, C. L., Grayson, J. W., Barsanti, K., Jimenez, J. L. and Bertram, A. K.: Mixing times of organic molecules within secondary organic aerosol particles: a global planetary boundary layer perspective, Atmospheric Chemistry and Physics, 17(21), 13037–13048, doi:10.5194/acp-17-13037-2017, 2017.

Marais, E. A., Jacob, D. J., Jimenez, J. L., Campuzano-Jost, P., Day, D. A., Hu, W., Krechmer, J., Zhu, L., Kim, P. S., Miller, C. C., Fisher, J. A., Travis, K., Yu, K., Hanisco, T. F., Wolfe, G. M., Arkinson, H. L., Pye, H. O. T., Froyd, K. D., Liao, J. and McNeill, V. F.: Aqueous-phase mechanism for secondary organic aerosol formation from isoprene: application to the southeast United States and co-benefit of SO_2 emission controls, Atmospheric Chemistry and Physics, 16(3), 1603–1618, doi:0~~https://doi.org/10~~.5194/acp-16-1603-2016, 2016.

Marcolli, C., Luo, B. and Peter, T.: Mixing of the Organic Aerosol Fractions: Liquids as the Thermodynamically Stable Phases, J. Phys. Chem. A, 108(12), 2216–2224, doi:10.1021/jp036080l, 2004.

Marsh, A., Petters, S. S., Rothfuss, N. E., Rovelli, G., Song, Y. C., Reid, J. P. and Petters, M. D.: Amorphous phase state diagrams and viscosity of ternary aqueous organic/organic and inorganic/organic mixtures, Physical Chemistry Chemical Physics, 20, 15086–15097, doi:10.1039/c8cp00760h, 2018.

Massoli, P., Stark, H., Canagaratna, M. R., Krechmer, J. E., Xu, L., Ng, N. L., Mauldin, R. L., Yan, C., Kimmel, J., Misztal, P. K., Jimenez, J. L., Jayne, J. T., and Worsnop, D. R.: Ambient

Measurements of Highly Oxidized Gas-Phase Molecules during the Southern Oxidant and Aerosol Study (SOAS) 2013, ACS Earth and Space Chemistry, 2, 653-672, 10.1021/acsearthspacechem.8b00028, 2018.

Martin, S. T.: Phase Transitions of Aqueous Atmospheric Particles, Chem. Rev., 100(9), 3403–3454, doi:10.1021/cr990034t, 2000.

Murphy, B. N., Woody, M. C., Jimenez, J. L., Carlton, A. M. G., Hayes, P. L., Liu, S., Ng, N. L., Russell, L. M., Setyan, A., Xu, L., Young, J., Zaveri, R. A., Zhang, Q., and Pye, H. O. T.: Semivolatile POA and parameterized total combustion SOA in CMAQv5.2: impacts on source strength and partitioning, Atmos. Chem. Phys., 17, 11107-11133, doi:10.5194/acp-17-11107-2017, 2017.

Nozière, B., Kalberer, M., Claeys, M., Allan, J., D'Anna, B., Decesari, S., Finessi, E., Glasius, M., Grgić, I., Hamilton, J. F., Hoffmann, T., Iinuma, Y., Jaoui, M., Kahnt, A., Kampf, C. J., Kourtchev, I., Maenhaut, W., Marsden, N., Saarikoski, S., Schnelle-Kreis, J., Surratt, J. D., Szidat, S., Szmigielski, R. and Wisthaler, A.: The molecular identification of organic compounds in the atmosphere: state of the art and challenges, Chem. Rev., 115(10), 3919–3983, doi:10.1021/cr5003485, 2015.

O'Brien, R. E., Wang, B., Kelly, S. T., Lundt, N., You, Y., Bertram, A. K., Leone, S. R., Laskin, A. and Gilles, M. K.: Liquid-liquid phase separation in aerosol particles: imaging at the nanometer scale, Environ. Sci. Technol., 49(8), 4995–5002, doi:10.1021/acs.est.5b00062, 2015.

Pajunoja, A., Malila, J., Hao, L., Joutsensaari, J., Lehtinen, K. E. J. and Virtanen, A.: Estimating the Viscosity Range of SOA Particles Based on Their Coalescence Time, Aerosol Science and Technology, 48(2), i–iv, doi:10.1080/02786826.2013.870325, 2014.

Paulot, F., Crounse, J. D., Kjaergaard, H. G., Kürten, A., St Clair, J. M., Seinfeld, J. H. and Wennberg, P. O.: Unexpected epoxide formation in the gas-phase photooxidation of isoprene, Science, 325(5941), 730–733, doi:10.1126/science.1172910, 2009.

Price, H. C., Mattsson, J., Zhang, Y., Bertram, A. K., Davies, J. F., Grayson, J. W., Martin, S. T., O'Sullivan, D., Reid, J. P., Rickards, A. M. J. and Murray, B. J.: Water diffusion in atmospherically relevant α-pinene secondary organic material †Electronic supplementary information (ESI) available. See DOI: 10.1039/c5sc00685f Click here for additional data file., Chem Sci, 6(8), 4876–4883, doi:10.1039/c5sc00685f, 2015.

Pye, H. O. T., Pinder, R. W., Piletic, I. R., Xie, Y., Capps, S. L., Lin, Y. H., Surratt, J. D., Zhang, Z., Gold, A., Luecken, D. J., Hutzell, W. T., Jaoui, M., Offenberg, J. H., Kleindienst, T. E., Lewandowski, M. and Edney, E. O.: Epoxide pathways improve model predictions of isoprene markers and reveal key role of acidity in aerosol formation, E and T Contents, 47(19), 11056–11064, doi:10.1021/es402106h, 2013.

Pye, H. O. T., Murphy, B. N., Xu, L., Ng, N. L., Carlton, A. G., Guo, H., Weber, R., Vasilakos, P., Appel, K. W., Budisulistiorini, S. H., Surratt, J. D., Nenes, A., Hu, W., Jimenez, J. L., Isaacman-VanWertz, G., Misztal, P. K. and Goldstein, A. H.: On the implications of aerosol

liquid water and phase separation for organic aerosol mass, Atmospheric Chemistry and Physics, 17(1), 343–369, doi:10.5194/acp-17-343-2017, 2017.

Pye, H. O. T., Zuend, A., Fry, J. L., Isaacman-VanWertz, G., Capps, S. L., Appel, K. W., Foroutan, H., Xu, L., Ng, N. L. and Goldstein, A. H.: Coupling of organic and inorganic aerosol systems and the effect on gas–particle partitioning in the southeastern US, Atmos Chem Phys, 18(1), 357–370, doi:10.5194/acp-18-357-2018, 2018.

Regayre, L. A., Pringle, K. J., Lee, L. A., Rap, A., Browse, J., Mann, G. W., Reddington, C. L., Carslaw, K. S., Booth, B. B. B. and Woodhouse, M. T.: The Climatic Importance of Uncertainties in Regional Aerosol–Cloud Radiative Forcings over Recent Decades, J. Climate, 28(17), 6589–6607, doi:10.1175/JCLI-D-15-0127.1, 2015.

Reid, J. P., Bertram, A. K., Topping, D. O., Laskin, A., Martin, S. T., Petters, M. D., Pope, F. D., and Rovelli, G.: The viscosity of atmospherically relevant organic particles, Nature Communications, 9, 956, doi:10.1038/s41467-018-03027-z, 2018.

Renbaum-Wolff, L., Grayson, J. W., Bateman, A. P., Kuwata, M., Sellier, M., Murray, B. J., Shilling, J. E., Martin, S. T., and Bertram, A. K.: Viscosity of α-pinene secondary organic material and implications for particle growth and reactivity, Proceedings of the National Academy of Sciences, 110, 8014-8019, doi:10.1073/pnas.1219548110, 2013.

Renbaum-Wolff, L., Song, M., Marcolli, C., Zhang, Y., Liu, P. F., Grayson, J. W., Geiger, F. M., Martin, S. T. and Bertram, A. K.: Observations and implications of liquid-liquid phase separation at high relative humidities in secondary organic material produced by α-pinene ozonolysis without inorganic salts, Atmospheric Chemistry and Physics, 16(12), 7969–7979, doi:10.5194/acp-16-7969-2016, 2016.

Riedel, T., Lin, Y.-H., Zhang, Z., Chu, K., Thornton, J., Vizuete, W., Gold, A., Surratt, J. D.: Constraining condensed-phase formation kinetics of secondary organic aerosol components from isoprene epoxydiols, Atmospheric Chemistry and Physics, 16, 1245-1254, doi: 10.5194/acp-16-1245-2016.

Riva, M., Chen, Y., Zhang, Y., Lei, Z., Olson, N. E., Boyer, H. C., Narayan, S., Yee, L. D., Green, H. S., Cui, T., Zhang, Z., Baumann, K., Fort, M., Edgerton, E., Budisulistiorini, S. H., Rose, C. A., Ribeiro, I. O., e Oliveira, R. L., dos Santos, E. O., Machado, C. M. D., Szopa, S., Zhao, Y., Alves, E. G., de Sá, S. S., Hu, W., Knipping, E. M., Shaw, S. L., Duvoisin Junior, S., de Souza, R. A. F., Palm, B. B., Jimenez, J.-L., Glasius, M., Goldstein, A. H., Pye, H. O. T., Gold, A., Turpin, B. J., Vizuete, W., Martin, S. T., Thornton, J. A., Dutcher, C. S., Ault, A. P., and Surratt, J. D.: Increasing Isoprene Epoxydiol-to-Inorganic Sulfate Aerosol Ratio Results in Extensive Conversion of Inorganic Sulfate to Organosulfur Forms: Implications for Aerosol Physicochemical Properties, Environmental Science & Technology, 53, 8682-8694, doi: 10.1021/acs.est.9b01019, 2019.

Ryder, O. S., Ault, A. P., Cahill, J. F., Guasco, T. L., Riedel, T. P., Cuadra-Rodriguez, L. A., Gaston, C. J., Fitzgerald, E., Lee, C., Prather, K. A. and Bertram, T. H.: On the role of particle

inorganic mixing state in the reactive uptake of N2O5 to ambient aerosol particles, Environ. Sci. Technol., 48(3), 1618–1627, doi:10.1021/es4042622, 2014.

Schmedding, R., Ma, M., Zhang, Y., Farrell, S., Pye, H. O. T., Chen, Y., Wang, C.-T., Rasool, Q. Z., Budisulistiorini, S., Ault, A. P., Surratt, J. and Vizuete, W.: α-Pinene-Derived organic coatings on acidic sulfate aerosol impacts secondary organic aerosol formation from isoprene in a box model, Atmos. Environ., 213, 456-462, ~~https://~~doi~~.org/~~10.1016/j.atmosenv.2019.06.005, 2019.

Shiraiwa, M., Li, Y., Tsimpidi, A. P., Karydis, V. A., Berkemeier, T., Pandis, S. N., Lelieveld, J., Koop, T. and Pöschl, U.: Global distribution of particle phase state in atmospheric secondary organic aerosols, Nature Communications; London, 8, 15002, doi: 10.1021/acs.est.9b01196 ~~http://dx.doi.org.libproxy.lib.unc.edu/10.1038/ncomms15002~~, 2017.

Slade, J. H., Ault, A. P., Bui, A., Ditto, J., Lei, Z., Bondy, A. L., Olson, N. E., Cook, R. D., Desrochers, S. J., Harvey, R.M., Erickson, M. H., Wallace, H. W., Alvarez, S. L., Flynn, J. H., Boor, B. E., Petrucci, G. A., Gentner, D. R., Griffin, R. J. and Shepson, P. B.: Bouncier particles at night: biogenic secondary organic aerosol chemistry and sulfate drive diel variations in the aerosol phase in a mixed forest, Environ. Sci. Technol., 53(9), 4977-4987, doi~~DOI~~: 10.1021/acs.est.8b07319, 2019.

Song, M., Liu, P. F., Hanna, S. J., Li, Y. J., Martin, S. T. and Bertram, A. K.: Relative humidity-dependent viscosities of isoprene-derived secondary organic material and atmospheric implications for isoprene-dominant forests, Atmospheric Chemistry and Physics, 15(9), 5145–5159, doi:10.5194/acp-15-5145-2015, 2015.

Song, M., Liu, P. F., Hanna, S. J., Zaveri, R. A., Potter, K., You, Y., Martin, S. T. and Bertram, A. K.: Relative humidity-dependent viscosity of secondary organic material from toluene photo-oxidation and possible implications for organic particulate matter over megacities, Atmospheric Chemistry and Physics, 16(14), 8817–8830, doi:10.5194/acp-16-8817-2016, 2016.

Song, M., Ham, S., Andrews, R. J., You, Y. and Bertram, A. K.: Liquid–liquid phase separation in organic particles containing one and two organic species: importance of the average O : C, Atmospheric Chemistry and Physics, 18(16), 12075–12084, doi:10.5194/acp-18-12075-2018, 2018.

Surratt, J. D., Murphy, S. M., Kroll, J. H., Ng, N. L., Hildebrandt, L., Sorooshian, A., Szmigielski, R., Vermeylen, R., Maenhaut, W., Claeys, M., Flagan, R. C. and Seinfeld, J. H.: Chemical composition of secondary organic aerosol formed from the photooxidation of isoprene, J Phys Chem A, 110(31), 9665–9690, doi:10.1021/jp061734m, 2006.

Surratt, J. D., Lewandowski, M., Offenberg, J. H., Jaoui, M., Kleindienst, T. E., Edney, E. O. and Seinfeld, J. H.: Effect of Acidity on Secondary Organic Aerosol Formation from Isoprene, Environmental Science & Technology, 41(15), 5363–5369, doi:10.1021/es0704176, 2007.

Surratt, J. D., Chan, A. W. H., Eddingsaas, N. C., Chan, M., Loza, C. L., Kwan, A. J., Hersey, S. P., Flagan, R. C., Wennberg, P. O. and Seinfeld, J. H.: Reactive intermediates revealed in

Formatted: Default Paragraph Font

secondary organic aerosol formation from isoprene, Proceedings of the National Academy of Sciences, 107(15), 6640–6645, doi:10.1073/pnas.0911114107, 2010.

Tamman, G. and Hesse, W.: The dependence of viscosity upon the temperature of supercooled liquids., Z. Anorg. Allg. Chem, 156, 245–257, 1926.

Ullmann, D. A., Hinks, M. L., Maclean, A. M., Butenhoff, C. L., Grayson, J. W., Barsanti, K., Jimenez, J. L., Nizkorodov, S. A., Kamal, S., and Bertram, A. K.: Viscosities, diffusion coefficients, and mixing times of intrinsic fluorescent organic molecules in brown limonene secondary organic aerosol and tests of the Stokes–Einstein equation, Atmos. Chem. Phys., 19, 1491-1503, doi:10.5194/acp-19-1491-2019, 2019.

Vander Wall, A. C., Perraud, V., Wingen, L. M., and Finlayson-Pitts, B. J.: Evidence for a kinetically controlled burying mechanism for growth of high viscosity secondary organic aerosol, Environmental Science: Processes & Impacts, 22, 66-83, 10.1039/C9EM00379G, 2020.

Virtanen, A., Joutsensaari, J., Koop, T., Kannosto, J., Yli-Pirilä, P., Leskinen, J., Mäkelä, J. M., Holopainen, J. K., Pöschl, U., Kulmala, M., Worsnop, D. R., and Laaksonen, A.: An amorphous solid state of biogenic secondary organic aerosol particles, Nature, 467, 824-827, doi:10.1038/nature09455, 2010.

Vogel, H.: The law of relation between the viscosity of liquids and the temperature., Phys. Z., 22, 645–646, 1921.

Xu, L., Suresh, S., Guo, H., Weber, R. J., and Ng, N. L.: Aerosol characterization over the southeastern United States using high-resolution aerosol mass spectrometry: spatial and seasonal variation of aerosol composition and sources with a focus on organic nitrates, Atmos. Chem. Phys., 15, 7307-7336, doi:10.5194/acp-15-7307-2015, 2015.

Xu, L., Middlebrook, A. M., Liao, J., de Gouw, J. A., Guo, H., Weber, R. J., Nenes, A., Lopez-Hilfiker, F. D., Lee, B. H., Thornton, J. A., Brock, C. A., Neuman, J. A., Nowak, J. B., Pollack, I. B., Welti, A., Graus, M., Warneke, C., and Ng, N. L.: Enhanced formation of isoprene-derived organic aerosol in sulfur-rich power plant plumes during Southeast Nexus, *Journal of Geophysical Research: Atmospheres*, 121, 11,137-111,153, 10.1002/2016jd025156, 2016.

Xu, L., Pye, H. O. T., He, J., Chen, Y., Murphy, B. N. and Ng, N. L.: Experimental and model estimates of the contributions from biogenic monoterpenes and sesquiterpenes to secondary organic aerosol in the southeastern United States, Atmospheric Chemistry and Physics, 18(17), 12613–12637, doi: ~~https://doi.org/~~10.5194/acp-18-12613-2018, 2018.

Yarwood, G., Whitten, G. Z., Jung, J., Heo, G. and Allen, D. T.: Development, evaluation and testing of version 6 of the Carbon Bond chemical mechanism (CB6), The University of Texas at Austin., 2010.

You, Y., Renbaum-Wolff, L., Carreras-Sospedra, M., Hanna, S. J., Hiranuma, N., Kamal, S., Smith, M. L., Zhang, X., Weber, R. J., Shilling, J. E., Dabdub, D., Martin, S. T. and Bertram, A. K.: Images reveal that atmospheric particles can undergo liquid-liquid phase separations, Proc. Natl. Acad. Sci. U.S.A., 109(33), 13188–13193, doi:10.1073/pnas.1206414109, 2012.

Yu, C. H., Zhu, X. and Fan, Z.: Spatial/Temporal Variations and Source Apportionment of VOCs Monitored at Community Scale in an Urban Area, edited by Y. Zhang, PLoS ONE, 9(4), e95734, doi:10.1371/journal.pone.0095734, 2014.

Zanobetti, A. and Schwartz, J.: The Effect of Fine and Coarse Particulate Air Pollution on Mortality: A National Analysis, Environmental Health Perspectives, 117(6), 898–903, doi:10.1289/ehp.0800108, 2009.

Zaveri, R. A., Shilling, J. E., Zelenyuk, A., Zawadowicz, M. A., Suski, K., China, S., Bell, D. M., Veghte, D., and Laskin, A.: Particle-Phase Diffusion Modulates Partitioning of Semivolatile Organic Compounds to Aged Secondary Organic Aerosol, Environmental Science & Technology, 10.1021/acs.est.9b05514, 2020.

Zhang, H., Surratt, J. D., Lin, Y. H., Bapat, J. and Kamens, R. M.: Effect of relative humidity on SOA formation from isoprene/NO photooxidation: enhancement of 2-methylglyceric acid and its corresponding oligoesters under dry conditions, Atmospheric Chemistry and Physics, 11(13), 6411–6424, doi: ~~https://doi.org/~~10.5194/acp-11-6411-2011, 2011.

Zhang, Q., Jimenez, J. L., Canagaratna, M. R., Allan, J. D., Coe, H., Ulbrich, I., Alfarra, M. R., Takami, A., Middlebrook, A. M., Sun, Y. L., Dzepina, K., Dunlea, E., Docherty, K., DeCarlo, P. F., Salcedo, D., Onasch, T., Jayne, J. T., Miyoshi, T., Shimono, A., Hatakeyama, S., Takegawa, N., Kondo, Y., Schneider, J., Drewnick, F., Borrmann, S., Weimer, S., Demerjian, K., Williams, P., Bower, K., Bahreini, R., Cottrell, L., Griffin, R. J., Rautiainen, J., Sun, J. Y., Zhang, Y. M. and Worsnop, D. R.: Ubiquity and dominance of oxygenated species in organic aerosols in anthropogenically-influenced Northern Hemisphere midlatitudes: UBIQUITY AND DOMINANCE OF OXYGENATED OA, Geophysical Research Letters, 34(13), n/a-n/a, doi:10.1029/2007GL029979, 2007.

Zhang, Y., ~~Chen, Y., Lei, Z., Olson, N. E., Zhang, Z., Gold, A., Jayne, J. T., Worsnop, D. R., Onasch, T. B., Ault, A. P. and Surratt, J. D.: Predicting the Viscosity and pH on Inorganic-Irganic Mixed Isoprene-Derived Epoxydiols (IEPOX) aerosols, In Prep.~~

Zhang, Y., Chen, Y., Lambe, A. T., Olson, N. E., Lei, Z., Craig, R. L., Zhang, Z., Gold, A., Onasch, T. B., Jayne, J. T., Worsnop, D. R., Gaston, C. J., Thornton, J. A., Vizuete, W., Ault, A. P. and Surratt, J. D.: Effect of the Aerosol-Phase State on Secondary Organic Aerosol Formation from the Reactive Uptake of Isoprene-Derived Epoxydiols (IEPOX), Environ. Sci. Technol. Lett., 5(3), 167–174, doi:10.1021/acs.estlett.8b00044, 2018a.

Zhang, H., Yee, L. D., Lee, B. H., Curtis, M. P., Worton, D. R., Isaacman-VanWertz, G., Offenberg, J. H., Lewandowski, M., Kleindienst, T. E., and Beaver, M. R.: Monoterpenes are the largest source of summertime organic aerosol in the southeastern United States, Proceedings of the National Academy of Sciences, 115, 2038-2043, doi: 10.1073/pnas.1717513115,~~2018b.~~ 2018b.

Zhang, Y., Chen, Y., Lei, Z., Olson, N. E., Riva, M., Koss, A. R., Zhang, Z., Gold, A., Jayne, J. T., Worsnop, D. R., Onasch, T. B., Kroll, J. H., Turpin, B. J., Ault, A. P., and Surratt, J. D.: Joint Impacts of Acidity and Viscosity on the Formation of Secondary Organic Aerosol from Isoprene

Epoxydiols (IEPOX) in Phase Separated Particles, ACS Earth and Space Chemistry, 3, 2646-2658, 10.1021/acsearthspacechem.9b00209, 2019.

Zuend, A. and Seinfeld, J. H.: Modeling the gas-particle partitioning of secondary organic aerosol: the importance of liquid-liquid phase separation, Atmospheric Chemistry and Physics, 12(9), 3857–3882, doi: https://doi.org/10.5194/acp-12-3857-2012, 2012.

Zuend, A., Marcolli, C., Luo, B. P. and Peter, T.: A thermodynamic model of mixed organic-inorganic aerosols to predict activity coefficients, Atmospheric Chemistry and Physics, 8(16), 4559–4593, doi: https://doi.org/10.5194/acp-8-4559-2008, 2008.

Tables

Table 1 - CMAQ defined aerosol phase species (Pye et al., 2017; Murphy et al., 2017) used in the calculation of the predicted organic phase parameter (overall SOA viscosity- η_{org}) and their respective organic-mass-to-organic-carbon ratio (*OM:OC*) (Pye et al., 2017), atomic oxygen-to-carbon ratio (*O:C*), molar weight (Pye et al., 2017), and predicted individual glass transition temperature (T_g) and viscosity at standard temperature.

Species Name	Description	Source	OM : OC ratio	O : C ratio	Molar weight (g/mole)	Predicted T_g (K)	Predicted η_{org} at T= 298K And ALW = 0 (Pa·s)
AALK1	SV alkane VOC SOA	ANTH	1.56	0.3153~~3146~~	225	256	$7.54 \cdot 10^{9}$
AALK2	SV alkane VOC SOA	ANTH	1.42	0.203~~2026~~	205.1	233	$5.34 \cdot 10^{7}$
ABNZ1	SV High NOx SOA product from benzene	ANTH	2.68	1.211~~2106~~	161	289	$1.67 \cdot 10^{14}$
ABNZ2	SV High NOx SOA product from benzene	ANTH	2.23	0.8518~~8506~~	134	234	$2.66 \cdot 10^{7}$
ABNZ3	LV low NOx SOA product from Benzene	ANTH	3.00	1.467~~4666~~	180	322	$1.00 \cdot 10^{12}$
AGLY	Glyoxal / methylglyoxal SOA	BIOG	2.13	0.771~~7706~~	66.4	160	$1.71 \cdot 10^{3}$
AISO1	SV SOA product from isoprene	BIOG	2.20	0.827~~8266~~	132.0	230	$1.20 \cdot 10^{7}$
AISO2	HV SOA product from isoprene	BIOG	2.23	0.8518~~8506~~	133.0	233	$2.26 \cdot 10^{7}$

AISO3	Acid-catalyzed isoprene SOA compounds (2-methyltetrols + IEPOX organosulfate)	BIOG	2.80	1.3073~~3066~~	168.2	301	1.00·~~*~~10^{12}
ALVOO1	LV Oxidized combustion organic compounds	ANTH	2.27	0.8838~~826~~	136	238	6.59·~~*~~10^{7}
ALVOO2	LV Oxidized combustion organic compounds	ANTH	2.06	0.7157~~146~~	136	222	3.97·~~*~~10^{6}
AOLGA	Oligomer products of anthropogenic SOA compounds	ANTH	2.50	1.0670~~666~~	206	303	1.00·~~*~~10^{12}
AOLGB	Oligomer products of biogenic SOA compounds	BIOG	2.10	0.7477~~466~~	248	300	1.00·~~*~~10^{12}
AORGC	Glyoxal and Methylglyoxal SOA	BIOG	2.00	0.6676~~666~~	177	251	1.33·~~*~~10^{9}
APAH1	SV High-NOx SOA product from PAHs	ANTH	1.63	0.3713~~706~~	195.6	239	1.58·~~*~~10^{8}
APAH2	SV High-NOx SOA product from PAHs	ANTH	1.49	0.2592~~586~~	178.7	216	2.80·~~*~~10^{6}
APAH3	LV low-NOx SOA product from PAHs	ANTH	1.77	0.4834~~826~~	212.2	260	1.97·~~*~~10^{10}
APCSO	Potential combustion SOA	ANTH	2.00	0.6676~~666~~	170	245	3.91·~~*~~10^{8}
ASQT	SV SOA from sesquiterpenes	BIOG	1.52	0.2832~~826~~	135	179	1.87·~~*~~10^{4}

ASVOO1	SV Oxidized combustion organic products	ANTH	1.88	0.5715~~5706~~	135	207	4.69·~~*~~10^{5}
ASVOO2	SV Oxidized combustion organic products	ANTH	1.73	0.4514~~4506~~	135	195	1.10·~~*~~10^{5}
ASVOO3	SV Oxidized Combustion organic compounds	ANTH	1.60	0.3473~~3466~~	134	184	3.19·~~*~~10^{4}
AIVPO1	Intermediate Volatility Primary organic compounds	ANTH	1.17	0.003~~0026~~	266	260	3.22·~~*~~10^{10}
ALVPO1	LV Primary organic compounds	ANTH	1.39	0.179~~1786~~	218	241	2.58·~~*~~10^{8}
ASVPO1	SV Primary organic compounds	ANTH	1.32	0.123~~1226~~	230	245	7.00·~~*~~10^{8}
ASVPO2	SV primary organic compounds	ANTH	1.26	0.075~~0746~~	241	249	1.86·~~*~~10^{9}
ASVPO3	SV primary organic compounds	ANTH	1.21	0.035~~0346~~	253	254	6.63·~~*~~10^{9}
ATOL1	SV high NOx Toluene SOA	ANTH	2.26	0.875~~8746~~	163	259	8.17·~~*~~10^{9}
ATOL2	SV High NOx Toluene SOA	ANTH	1.82	0.523~~5226~~	175	23	7.25·~~*~~10^{7}
ATOL3	LV low NOx Toluene SOA	ANTH	2.70	1.227~~2266~~	194	309	1.00·~~*~~10^{12}
ATRP1	SV SOA product from monoterpenes	BIOG	1.84	0.539~~5386~~	177	239	1.30·~~*~~10^{8}

ATRP2	HV SOA product from monoterpenes	BIOG	1.83	0.5315~~306~~	198	254	3.93·~~*~~10^{9}
AXYL1	SV High NOx SOA product from xylene	ANTH	2.42	1.003~~0026~~	174	278	3.16·~~*~~10^{12}
AXYL2	SV High NOx SOA product from xylene	ANTH	1.93	0.611~~6106~~	185	252	1.85·~~*~~10^{9}
AXYL3	LV low-NOx SOA product from xylene	ANTH	2.30	0.907~~9066~~	218	297	1.43·~~*~~10^{16}

Table 2 - Rate constants used to calculate the effective first order rate constant for aqueous phase IEPOX SOA formation catalyzed by H^+, HSO_4^- with water and SO_4^{2-} as nucleophiles

Rate Constant	Value ($M^{-2}\,s^{-1}$)	Reference
$k_{H^+,water}$	9.00x10^{-4}	Eddingsaas et al., 2010; Pye et al., 2013
$k_{HSO_4^-,water}$	1.31x10^{-5}	Eddingsaas et al., 2010
$k_{H^+,SO_4^{2-}}$	1.27x10^{-3}	Riedel et al. 2016; Budisulistiorini et al., 2017

Formatted: French (Canada)

Formatted: French (Canada)

Table 3 – Brief summary of different simulations conducted in this work in CMAQ v 5.2.1

Simulations	Details
NonPhaseSep	Base CMAQ v5.2.1 parameterization assuming homogeneous, internally mixed organic-inorganic fine aerosol, no phase separation (Pye et al., 2017)
PhaseSep	CMAQ parametrization with additional term in reactive uptake calculation to capture the impact of phase separation and organic coating described in sections 2.1-2.3 and 2.5
Emissions reduction	PhaseSep with EPA recommended emissions reductions of 34% and 48% for NO_x and SO_2 from 2013 to 2025 (See Section 2.6)
HighHorg	PhaseSep with higher organic phase Henry's law Coefficient (3 orders of magnitude higher than in PhaseSep) (See Section 2.6)
PhaseSep2	PhaseSep with the assumption that for solid or semi-solid phase Zuend and Seinfeld (2012) phase separation~~sepration~~ criteria is followed (See Section 2.6)

Formatted: Font: Italic

Formatted: Font: Italic

Formatted: Font: Italic

Formatted: Font: Italic

Formatted: Font: Italic

Figures

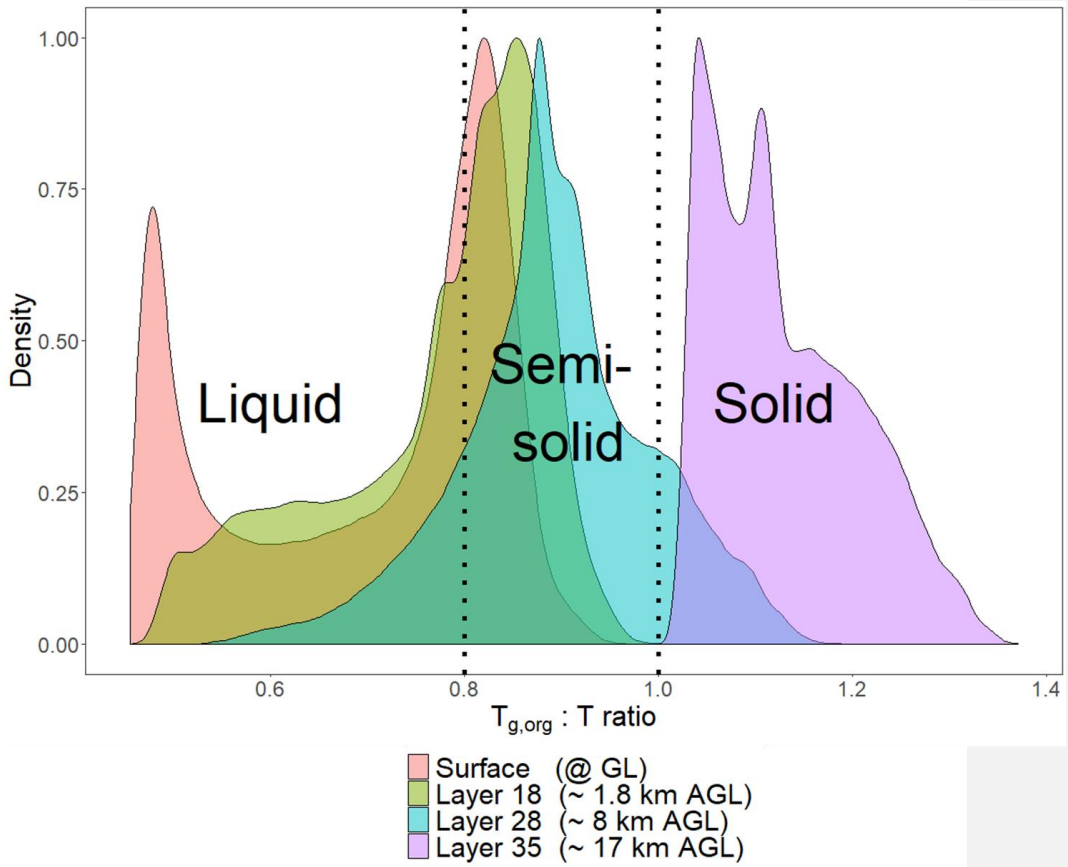

Figure 1- Probability density distribution of glass transition temperature to ambient temperature ratio ($T_{g,org}$~~T_{org}~~:T) for all grid cells and time steps at the surface layer (red), 1.8 km above Surface layer (green, layer 18-lower troposphere), 8 km above Surface layer (blue, layer 28-upper troposphere) and 17 km above Surface layer (purple, layer 35-stratosphere).

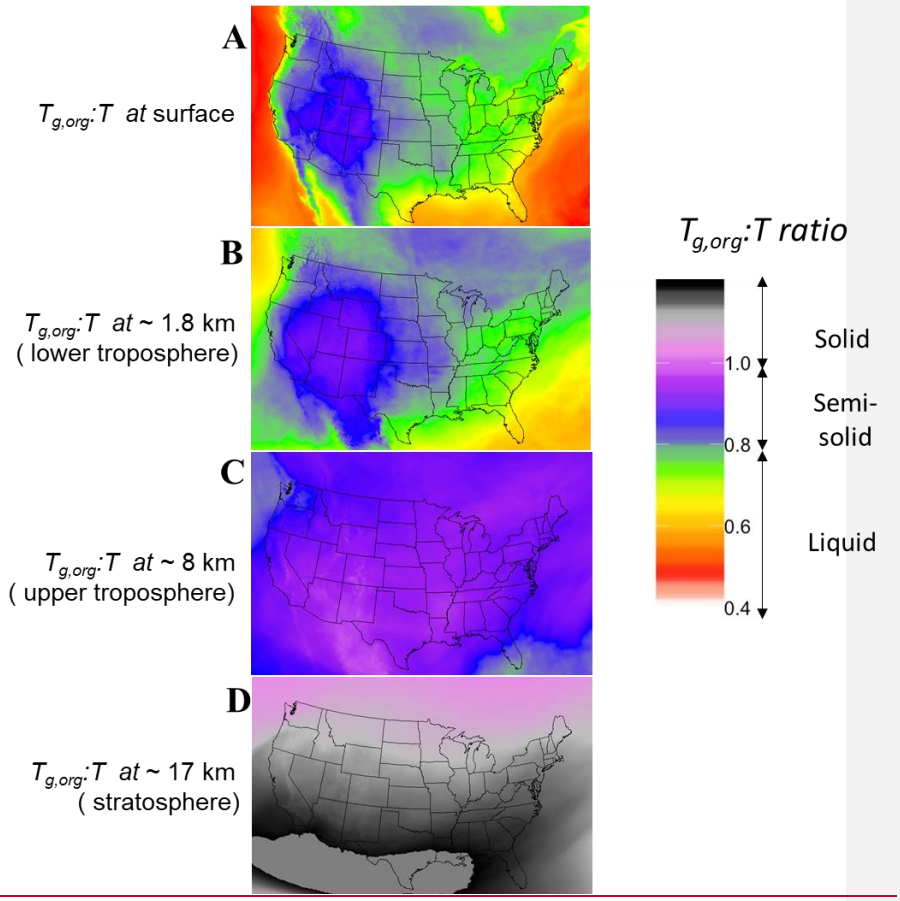

Figure 2- For all time steps and over the continental United States, the average glass transition temperature to ambient temperature ($T_{g,org}$~~T_{org}~~:T) ratio at the (**A)** surface level, **(B)** 1.8 km above Surface layer (lower troposphere), **(C)** 8 km (upper troposphere) and **(D)**17 km above Surface layer (stratosphere).

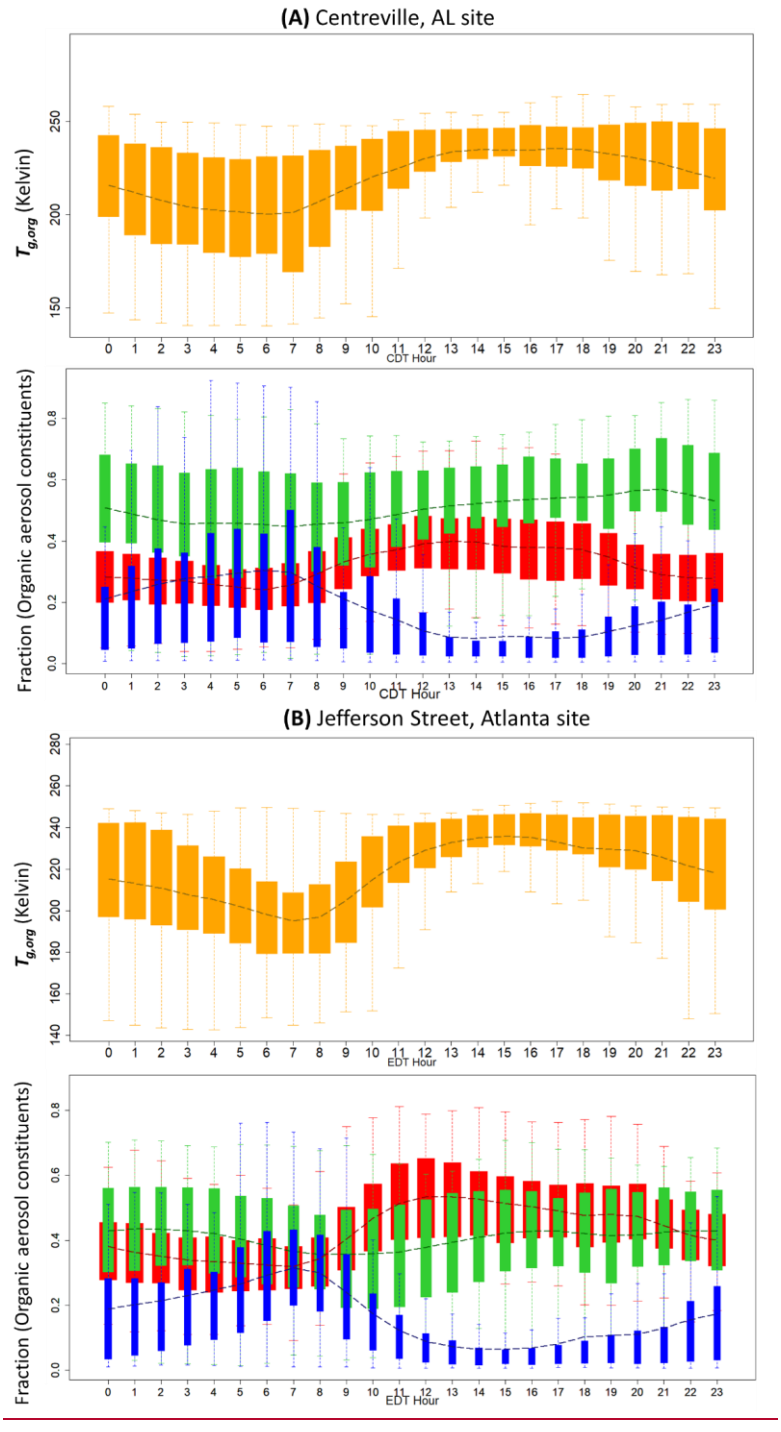
(A) Centreville, AL site
$T_{g,org}$ (Kelvin)
CDT Hour
Fraction (Organic aerosol constituents)
CDT Hour
(B) Jefferson Street, Atlanta site
$T_{g,org}$ (Kelvin)
EDT Hour
Fraction (Organic aerosol constituents)
EDT Hour

Figure 3 – Diurnal pattern for SOAS (~~From~~ June 1- July ~~to June~~ 15)~~,~~ 2013 of the contributions of ~~biogenic SOA (green),~~ anthropogenic OA~~SOA~~ (red), biogenic OA (green), and aerosol water associated with organics (blue) to organic glass transition temperature ($T_{g,org}$ -orange ~~T_{org}~~) at the (**A)** Centreville, AL site and the (**B)** Jefferson Street, Atlanta site. Bars/shaded boxes indicate 25th to 75th percentiles. Extreme bounds of whiskers indicate 5th to 95th percentiles (i.e. 95% confidence interval). Dashed lines indicate means.

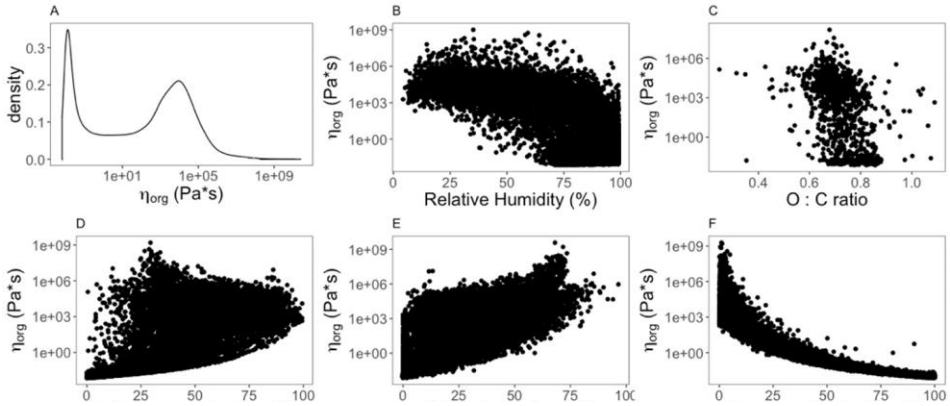

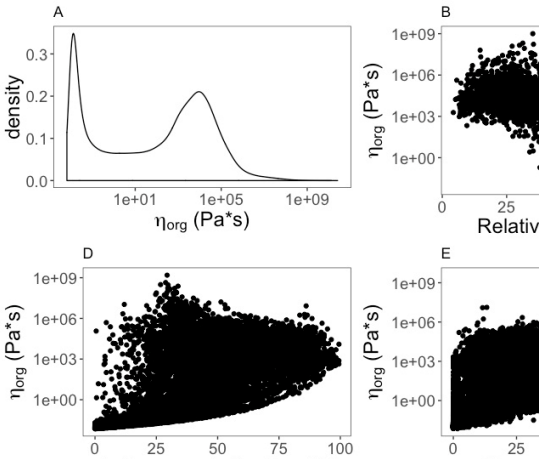

Figure 4- For all grid cells and time steps at the surface layer the (**A)** Probability distribution of the organic phase viscosity , and correlations of particle viscosity (η_{org}) with (**B)** relative humidity, (**C)** atomic oxygen-to-carbon (O:C) ratio, (**D)** anthropogenic SOA weight fraction, (**E)** biogenic SOA weight fraction and, (**F)** organic-phase water content (*ws*).

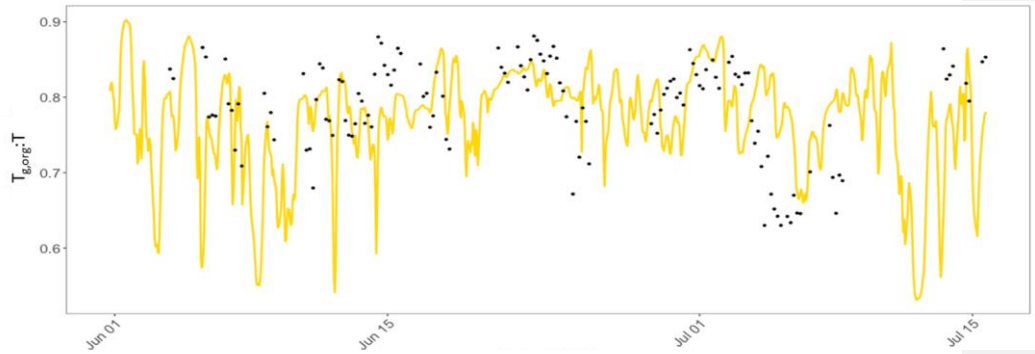

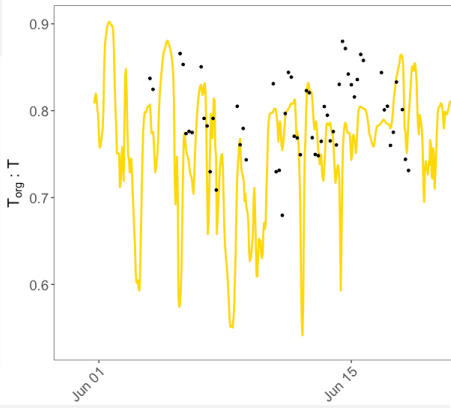

Figure 5 – Predicted glass transition temperature to ambient temperature ratio ($T_{g,org}$~~T_{org}~~:T) at the Centreville, Alabama during the 2013 SOAS campaign based on OA composition reported by Zhang et al. (2018b) (black). Predicted $T_{g,org}$~~T_{org}~~:T from this work is shown in yellow.

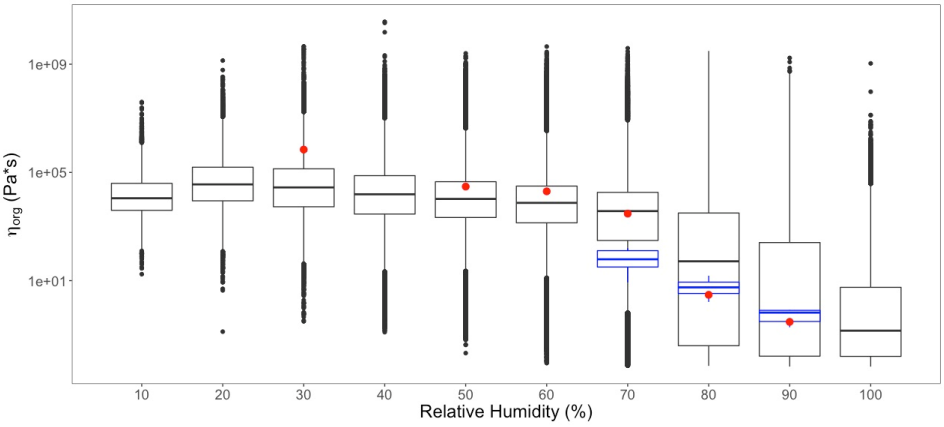

Figure 6 – Model predicted SOA viscosity (η_{org}) and experimental data for η_{org} from Zhang et al. (2018a) (red) and Song et al. (2016) (blue), at varying RH.

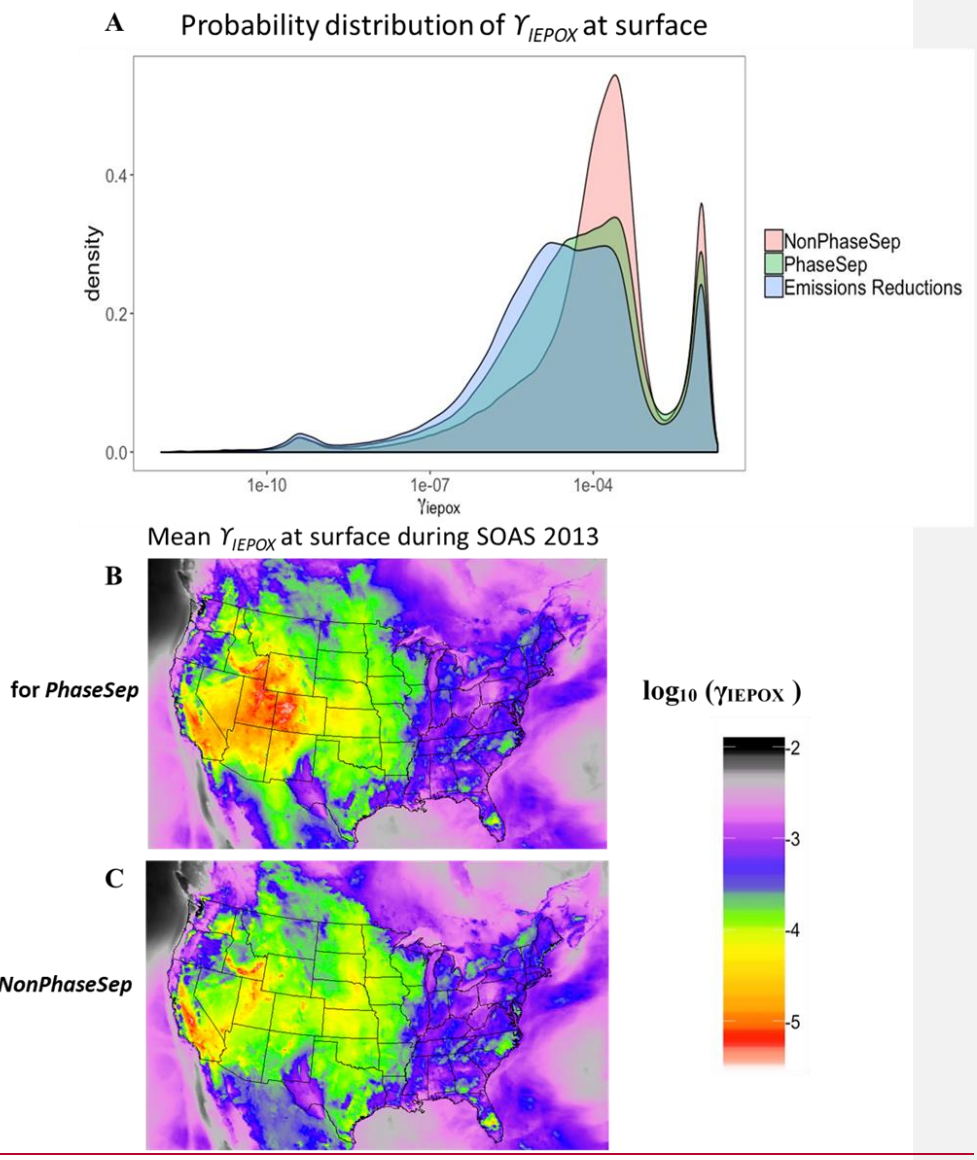
A
Probability distribution of γ_{IEPOX} at surface
density
0.0
0.2
0.4
1e-10
1e-07
1e-04
γiepox
NonPhaseSep
PhaseSep
Emissions Reductions
Mean γ_{IEPOX} at surface during SOAS 2013
B
for PhaseSep
C
for NonPhaseSep
log10 (γIEPOX)
-2
-3
-4
-5

1375

Figure 7 – For all grid cells and time steps the predicted **(A)** probability distribution of γ_{IEPOX} at the surface level for the *NonPhaseSep* (red), *PhaseSep* (green), and *Emission reductions* (blue) simulations. For each grid cell the mean value of γ_{IEPOX} for the (**B)** *PhaseSep* simulation and **(C)** *NonPhaseSep* simulation.

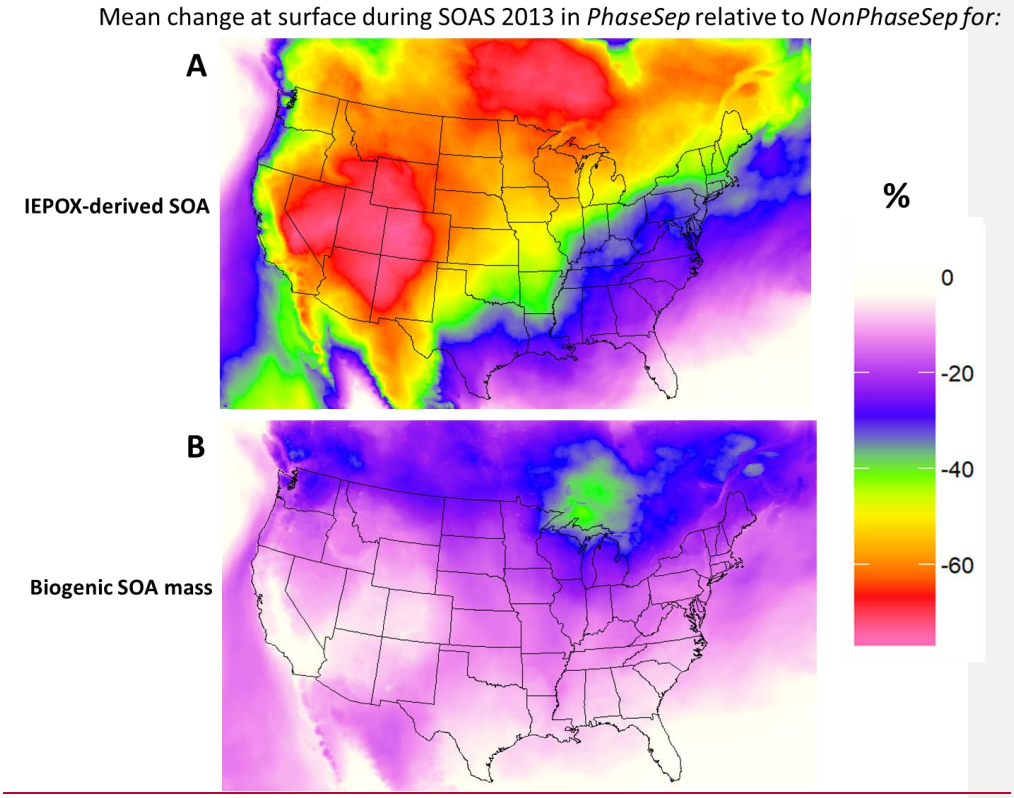

Figure 8 – Spatial map of the mean percent relative change of **(A)** IEPOX-derived SOA and **(B)** biogenic SOA mass ~~(primarily driven by IEPOX SOA)~~ in *PhaseSep* case relative to the *NonPhaseSep* Simulation.

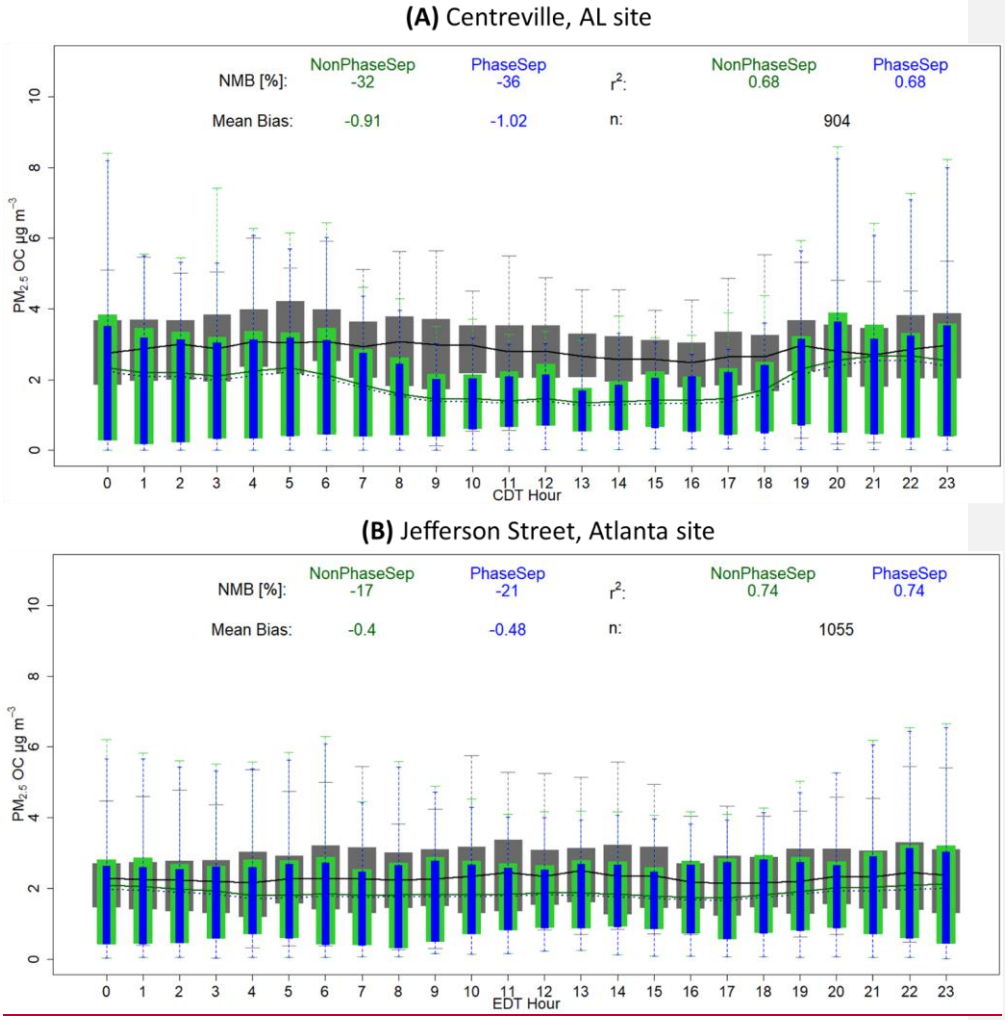

Figure 9 – $PM_{2.5}$ organic carbon (OC) mass ($\mu g/m^3$) as a function of hour of the day. Non-aggregated performance statistics- Mean Bias ($\mu g/m^3$), % Normalized Mean Bias (NMB) and Spearman's Correlation coefficient (r^2) of *NonPhaseSep* (green) and *PhaseSep* (blue) cases relative to observed (grey) $PM_{2.5}$ OC mass for (**A)** Rural Centreville, Alabama site and, (**B)** Urban

Jefferson Street, Atlanta, Georgia site. Bars/shading indicate 25th to 75th percentiles. Extreme bounds of whiskers~~Lines~~ indicate 5th to 95th percentiles (i.e. 95% confidence interval). Lines indicate means (dashed line = *PhaseSep*).~~means.~~ n= number of observation points.

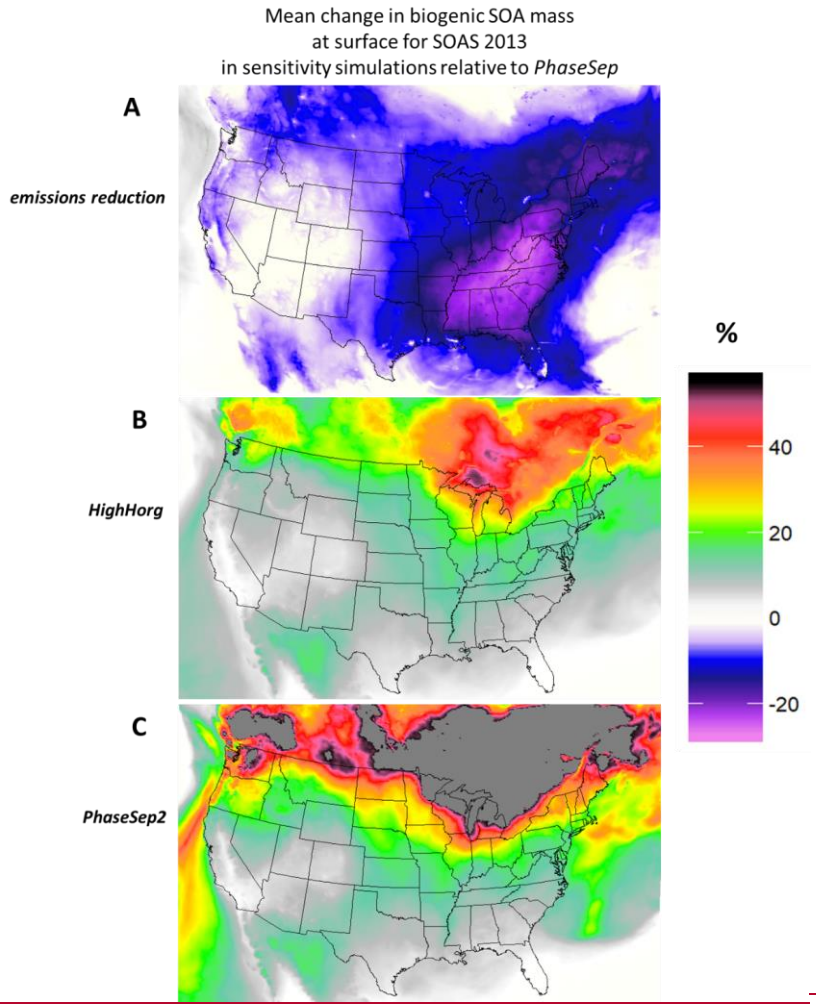

Figure 10 –Relative change (%) in biogenic SOA mass at the surface level from the PhaseSep parameterization for the (**A)** NO_x and SO_2 *emissions reduction* sensitivity simulation, (**B)** *HighHorg* sensitivity simulation, and (**C)** the *PhaseSep2* simulation that did not assume semi-solid particles were automatically phase–separated.